CYP2J2 Regulation in Adult Ventricular Myocytes: Cell-wide Consequences and Effects on Stress Responses

Eric Anthony Evangelista

A dissertation

submitted in partial fulfillment of the

requirements for the degree of

Doctor of Philosophy

University of Washington

2020

Reading Committee:

Rheem A. Totah, Chair

Libin Xu

Sina A. Gharib

Program Authorized to Offer Degree:

School of Pharmacy

University of Washington

Abstract

CYP2J2 Regulation in Adult Ventricular Myocytes: Cell-wide Consequences and Effects on Stress Responses

Eric A. Evangelista

Chair of the Supervisory Committee:

Dr. Rheem A. Totah

Department of Medicinal Chemistry

Cytochrome P450 2J2 (CYP2J2) is drug metabolizing member of the cytochrome P450 (CYP) superfamily. While CYPs involved in drug metabolism are generally highly expressed in "drug clearance" organs such as the small intestine, liver and kidneys, CYP2J2 is predominantly expressed in the heart. In ventricular myocytes, CYP2J2 is the primary arachidonic acid (AA) CYP epoxygenase and thus the primary source of the AA metabolites, the epoxyeicosatrienoic acids (EETs). EETs have been extensively investigated in disease settings and a large body of evidence suggests that EETs are cardioprotective against a wide array of cardiovascular conditions. While the exact mechanisms of this protection are largely unknown, EETs have been shown to act as signaling molecules, activating many pathways that prevent cellular damage. Given the critical functions of EETs in cardiac cells, CYP2J2 is an important enzyme to study, particularly in how various cellular and disease stressors affect the expression of this enzyme and ultimately, how these changes alter cardiomyocyte homeostasis.

The overall aim of this dissertation was to investigate the regulation of the CYP2J2 gene in adult human ventricular myocytes under various stressors caused by pathophysiological conditions. Quantifying CYP2J2 mRNA and protein in cardiomyopathic ventricular tissues suggests that CYP2J2 levels are decreased as a result of cardiac disease, specifically in ischemia and diabetes. *In vitro* studies with ventricular myocytes confirm that hypoxia and type 2 diabetes downregulate *CYP2J2* expression. Interestingly, increasing oxidative stress has the opposite effects, instead up-regulating *CYP2J2*. Focusing on the consequences of down-regulation, we inhibited CYP2J2 enzyme activity or silenced gene expression of *CYP2J2* and then subjected ventricular myocytes to oxidative stress, hypoxia and human type 2 diabetic serum. Findings indicate that when this gene is silenced, cardiomyocytes become more susceptible to toxicity and death associated with these stresses. This increased sensitivity could be mitigated and reversed with the addition of external EETs. The *in vitro* cell work provide support for CYP2J2 as a cardioprotective enzyme via its metabolism of AA and EETs formation.

Separately, the effects of *CYP2J2* silencing on the transcriptome of ventricular myocytes was investigated using RNA-sequencing. Viability assays suggest that silencing *CYP2J2* gene expression is not in of itself toxic to the cells. RNASeq results, however, indicate that there are cell-wide consequences to gene expression when downregulating *CYP2J2*. Many pathways are affected, including genes involved in maintaining and controlling ion channels and cell electrophysiology. These findings were further investigated and confirmed by patch clamp experiments. Pharmacological inhibition of CYP2J2 in ventricular myocytes have direct and immediate consequences on the action potential duration (APD). Further investigation suggests that the resulting aberrant APD is likely due to potassium channel current blockage or inhibition.

In summary, *CYP2J2* expression is adversely affected by cell stressors associated with disease states. The resulting downregulation limits the cardioprotection conferred by CYP2J2 to ventricular myocytes, likely through its bioactivation of AA to EETs, and makes cells more susceptible to toxicity by disease stressors. While the downregulation of *CYP2J2* in ventricular myocytes does not seem to outwardly affect cardiomyocyte health by itself, without a secondary external stressor, there are many alterations in the cells' internal signaling, with detrimental effects on cardiomyocyte health and function.

Table of Contents

List of Tables

List of Figures

Acknowledgments

Thank you to:

Rheem Totah for being an amazing mentor and giving me the freedom to explore on my own. I apologize for being a stubborn student and thank you for putting up with me over an entire decade.

Sina Gharib for your immense patience while I struggled learning how to work with big data and for being on my reading committee and reading through my dissertation and helping to make it better.

Libin Xu and William Atkins. Thank you for being a part of my committee and helping me become a better scientist with your helpful questions, suggestions, and insight.

Yvonne Lin. Thank you for being my GSR and serving on my committee despite having such a busy schedule of your own.

Rudiger Kaspera and Brianne Raccor. My early mentors. Thank you for you for providing a strong scientific foundation and for putting up with all of my questions and blunders along the way.

Theresa Aliwarga. Thank you for all of the laughter and help over the long years of our tenure in Rheem's lab.

Ben Maldonato, Christi Cho, and Drake Russel. You guys are the best labmates and I wish you guys all the best with your own graduate school journeys.

The Totah lab, past and present. For everything you've taught me over the years.

Ryan Seguin. You are reliably amusing. *taps shoulder*

Michelle Redhair, a great friend and mentor. Thank you for all of the adventures, laughter, advice and insight over the years. You are awesome!

Jenny Chang. What can I say, you're always there when I need you and I hope to be there to return the kindness you've shown over the years.

Dennis Goulet and David Baggett. BEST COHORT EVER!

David Wagner, Jenny Sager, Jenna Shope, and Becca Sager. The best bouldering group ever. See you in New Zealand!

Dr. Talus, Tanakazi, Bobnoxious, and One Green Bean. Thank you for being great friends and always being on my side (even when I'm wrong?)

Medicinal Chemistry staff: We'd all be lost without you.

Last but not least, my family, without whom I would not be where I am today!

Dedication

To my parents,

For always encouraging me to move forward and up,

And picking me up while encouraging me forward when I tripped and fell.

Chapter 1: Introduction

1.1 Cytochrome P450s: Background and Regulation

Cytochrome P450s (CYPs) are a superfamily of membrane-bound enzymes involved in the oxidation of numerous compounds, both endogenous and xenobiotics entering the body (Ortiz de Montellano, 2005; McDonnell and Dang, 2013; Manikandan and Nagini, 2018). In mammals, there are 18 distinct families, and in humans there are 57 CYP genes. Mammalian CYPs are arranged into families and subfamilies by sequence identity. CYPs with sequences that are over 40% identical are classified into the same family, designated by an Arabic numeral, and those that have greater than 55% sequence identity are further placed into the same subfamily, designated by a letter (Manikandan and Nagini, 2018). Nomenclature of these enzymes in mammals is determined chronologically by date of discovery.

Utilizing its co-enzyme partners, P450 Oxidoreductase (POR) and cytochrome b5 (CYPb5), electrons from NADPH are shuttled from the flavin adenine dinucleotide (FAD) through the flavin mononucleotide (FMN) domains of POR one at a time to the heme iron in the substrate bound active site of CYPs. This first electron results in the reduction of the ferric heme iron to ferrous heme iron allowing molecular oxygen to bind. Following oxygen binding, a second electron reduction (from POR or CYPb5) and addition of two protons occurs. Molecular oxygen is then split breaking the O-O bond. The first oxygen atom is inserted into the substrate while the other is reduced to water (Guengerich, 2001); hence, CYPs are also known as “mixed function oxygenases”. CYPs are involved in a wide range of physiological functions, including the mitochondrial electron transport chain, hormone synthesis and breakdown, fatty acid metabolism, and drug metabolism (Ortiz de Montellano, 2005).

Research involving cytochrome P450s is mostly centered on their role in drug metabolism and disposition. CYPs are extensively expressed in cells that make up the intestinal epithelium, liver and kidney; the primary organs involved in drugs metabolism and disposition (Shimada *et al.*, 1994; Zanger and Schwab, 2013). Most drugs on the market today are cleared, and sometimes bioactivated, by one or more CYPs belonging to families 1, 2 or 3, the major drug metabolizing families as extensively reviewed by Manikandan and Nagini (Manikandan and Nagini, 2018). With such important roles in the activity and clearance of pharmaceuticals, it is therefore important to consider the regulation of CYP enzymes, particularly in disease states when the patient is most likely taking several medications and there are greater risks for adverse events involving CYPs.

Cytochrome P450 expression and activity are regulated by a variety of mechanisms including genetic predisposition, epigenetic gene regulation, and non-genetic factors (Zanger and Schwab, 2013). Many CYPs have well known and well characterized genetic polymorphisms that affect the expression and activity of the resulting enzyme. CYP2D6 is a classic example, where some allelic variants (e.g. CYP2D6 *3 and *4) result in the production of truncated, and therefore nonfunctional, protein. In contrast, some individuals also carry multiple copies of the CYP2D6 gene, allowing them to express higher amounts of active enzyme, resulting in greater and faster clearance of drug substrates of CYP2D6.

In addition to genetic polymorphisms, CYP expression and activity can be modulated at the transcriptional level as well as post-transcriptionally. For example, *CYP2E1* expression is modulated by ethanol, a CYP2E1 substrate. On a transcriptional level, ethanol can induce expression. In addition, the presence of ethanol can also stabilize the protein, thus altering the half-life which can affect its apparent activity in the liver. Other P450s can be similarly

modulated by chemicals that are often substrates for these enzymes. Many exogenous compounds can also act as activators of a wide variety of transcriptional regulators that control CYP expression. *CYP3A4* expression, for example, is regulated by the pregnane X receptor (PXR), thus any ligands which activate PXR can potentially induce *CYP3A4* expression. Hence, there are a wide range of variables to consider when studying CYP expression and activity *in vivo*.

1.2 CYP2J2

Cytochrome P450 2J2 (CYP2J2) is a drug metabolism enzyme and the only human isoform in the CYP2J sub-family. It was first identified, isolated and cloned in 1996 from a human liver cDNA library (Wu *et al.*, 1996). Compared to other drug metabolizing CYPs, CYP2J2 protein expression in the liver and small intestine is low, comprising ~1-3% of total drug metabolism P450s (Zanger and Schwab, 2013). Instead, it is predominantly expressed in extrahepatic tissues, including the heart, skeletal muscle, placenta, small intestine, kidney, lung, pancreas, bladder and brain (Wu *et al.*, 1996; Zeldin *et al.*, 1997; Bièche *et al.*, 2007). Several studies, including our own, report robust expression and activity of CYP2J2 in the heart (Wu *et al.*, 1996; Delozier *et al.*, 2007; Michaud *et al.*, 2010; Evangelista *et al.*, 2013). Drug bioactivation, metabolism and clearance are not physiological roles typically attributed to the heart, thus leading to the hypothesis that CYP2J2 has a physiological role beyond detoxification of exogenous compounds, one that is central to cardiac health and function. As a drug metabolizing enzyme, however, CYP2J2 is subject to drug interactions like other members of the CYP2 family. It is, therefore, important to understand the role that CYP2J2 plays in cardiac

homeostasis, particularly how disease states and associated stresses to the cells affect its regulation and function in the heart.

While a crystal structure is not available yet for CYP2J2, molecular modeling suggests structural similarity to CYP3A4, the principal isoform involved in drug metabolism. It is not surprising that the two enzymes share a large number of substrates of diverse topography and therapeutic areas, such as the antihistamine drugs terfenadine, astemizole and ebastine (Matsumoto and Yamazoe, 2001; Hashizume *et al.*, 2002; Matsumoto *et al.*, 2002; Lafite *et al.*, 2007), anticancer drug tamoxifen, and drugs such as thioridazine or cyclosporine (Lee *et al.*, 2012). Notably, while CYP3A4 can often metabolize substrates at multiple sites on the molecule, CYP2J2 is more regioselective, preferring one or two sites for metabolism (examples provided in Figure 1.1). Lee et al. attributed this characteristic to the fact that while the active sites of the two enzymes are similar in volume, CYP3A4 is more cavernous, with large volume located above the heme, while CYP2J2 is more elongated and restrictive over the active heme iron (Lee *et al.*, 2012). The result is that small molecules can adopt multiple conformations in the CYP3A4 active site, allowing different sites to come within proximity of the heme iron. In contrast, molecules are often confined to a single or few conformations in the CYP2J2 active site, constraining sites on the molecule that are exposed for metabolism.

CYP2J2 has attracted attention for its ability to oxidize arachidonic acid regio-selectively to *cis*-5,6-, 8,9-, 11,12- or 14,15-epoxyeicosatrienoic acids (EETs) (Roman, 2002). These investigations greatly increased interest in CYP2J2 and its biochemical characterization, localized expression, and the need for model systems suitable to study its importance in maintaining cardiovascular homeostasis. In addition to arachidonic acid, other long chain polyunsaturated fatty acids (PUFAs) have been identified as substrates for this enzyme, many of

which have been identified as precursor signaling molecules within the body, providing further evidence that CYP2J2 has a physiological role beyond drug metabolism and detoxification (Fer *et al.*, 2008). To date, arachidonic acid remains the putative endogenous substrate for this enzyme. While other CYP isoforms are capable of bioactivating AA to EETs, most notably the CYP2C family, the robust expression of CYP2J2 in the heart combined with the cardioprotective effects demonstrated by EETs have identified CYP2J2 as a cardioprotective enzyme and the principal source of EETs in cardiomyocytes (Node *et al.*, 1999; Xiao *et al.*, 2010; Wei *et al.*, 2014; Yang *et al.*, 2015).

Studies demonstrating drug metabolism in cardiac tissue are scant in the literature. Our lab, along with a few others, have shown that drugs can be metabolized in the heart (Evangelista *et al.*, 2013; Arnold and Das, 2018), thus affecting overall tissue toxicity. The inhibitory or inductive effect by such drugs on arachidonic acid metabolism could have profound down-stream consequences by reducing EETs and their protective properties. However, a human heart model remains elusive and testing relies on animal models, cell systems or recombinant enzymes. Much of CYP2J2's activity has been assessed in such models as E.coli expressed or Baculovirus-infected insect cell expressed enzyme (Supersomes) (Lafite *et al.*, 2007), human liver microsomes (Lee *et al.*, 2012) or in humanized animal models that over-express the enzyme in cardiac tissue (Seubert *et al.*, 2004; Deng *et al.*, 2011).

Since CYP2J2 can metabolize a wide range of drugs from various therapeutic classes similar to CYP3A4, it is reasonable to expect drug-drug interactions to occur (Chen *et al.*, 2009; Lee, Neul, Clouser-roche, *et al.*, 2010; Lee, Neul, Clouser-Roche, *et al.*, 2010; Lee *et al.*, 2012). In the context of traditional drug metabolism that focuses on major drug metabolism organs (intestines, liver, and kidney), interactions with CYP2J2 are not of clinical significance. This is

because CYP2J2 expression and activity is often low in these organs in healthy individuals when compared to the expression and activity of other CYP isoforms, most notably CYP3A4/5, CYP2D6, the CYP2Cs, and CYP2E1 (Shimada *et al.*, 1994; Paine *et al.*, 2006; Zanger and Schwab, 2013; Michaels and Wang, 2014). In the context of cardiac drug-interactions, however, CYP2J2 may be more important to consider as it is the most abundantly expressed drug metabolizing CYP isoform in cardiomyocytes (Delozier *et al.*, 2007; Evangelista *et al.*, 2013). As a result, circulating drugs have the potential to cause drug interactions in the heart with detrimental side effects through inhibiting CYP2J2 activity.

CYP2J2 expression can be altered by several mechanisms. As a drug metabolizing CYP isoform, exogenous compounds such as drugs and toxins can potentially modulate *CYP2J2* gene expression. Previous studies by our lab indicate that *CYP2J2* gene expression is not affected by canonical CYP inducers in adult-derived ventricular myocytes (Evangelista *et al.*, 2013). This is not the case in other cell models, however, as the antioxidant BHT upregulates *CYP2J2* expression in HepG2 cells but not in cardiomyocytes (Lee and Murray, 2010). Others have observed increases in *CYP2J2* transcript and protein levels in response to bacterial lipopolysaccharides in peripheral blood mononuclear cells (Bystrom *et al.*, 2013). In addition to xenobiotic regulation, endogenous regulation has also been observed. Chen et al. reported an inverse relationship between *CYP2J2* transcript levels and let-7b miRNA levels in human squamous cell lung cancer (Chen *et al.*, 2012).

Finally, on a transcriptional level, CYP2J2 appears to be polymorphic like its other CYP2 family relatives. To date, however, only a single potentially clinically relevant single nucleotide polymorphism (SNP) of CYP2J2 has been identified and observed in different ethnic groups. The *CYP2J2*7* mutation (King *et al.*, 2002) is a G>T polymorphism present in the promoter

region of the gene (-50 bp) and results in decreased gene expression, but has no effect on protein activity (King *et al.*, 2002; Yamazaki *et al.*, 2006). There is a large body of evidence showing an association between *CYP2J2*7* and the incidence of adverse cardiac events such as myocardial infarction (Spiecker *et al.*, 2004; Liu *et al.*, 2007; Börgel *et al.*, 2008; Marciante *et al.*, 2008). Given the link between CYP2J2 and cardiac health, it is important to understand how varying physiological and pathological conditions regulate and affect *CYP2J2* expression in the heart in health and disease.

1.3 Arachidonic acid and EETs

Arachidonic acid (AA) is a 20-carbon omega-6 polyunsaturated fatty acid with four double bonds between carbons 5 and 6, 8 and 9, 11 and 12, and 14 and 15 (Oliw *et al.*, 1982). AA can be obtained through diet from food sources such as meat, including poultry, red meat, fish, and eggs (Piomelli, 1993; Tallima and El Ridi, 2017). Alternatively, animals can synthesize AA from linoleic acid (LA), an 18-carbon polyunsaturated fatty acid with two double bonds. In the cell, LA is enzymatically lengthened and desaturated into AA. In the cell, free AA levels are highly controlled, and it is stored in the membrane, specifically esterified to the *sn*-2 position of glycerophospholipids via an acyl-CoA dependent enzyme. Stored AA is released through signaling cascades that culminate in the activation of phospholipase A_2 (PLA2), which cleaves AA from the membrane and releases it into the cytosol (Oliw *et al.*, 1982; Thomas *et al.*, 1984; Oliw, 1994). Once released free AA can undergo metabolism via several pathways to produce eicosanoids with distinct downstream effects (Figure 1.2). The cyclooxygenase (COX) pathway of AA produces prostaglandin H_2, a precursor to prostacyclins, prostaglandins and thromboxanes

(Otto and Smith, 1995) and the lipoxygenase (LOX) pathway produces leukotrienes and mid-chain AA-hydroxymetabolites (Brash, 1999). AA is also a substrate for various cytochrome P450 (CYP) isoforms, leading to the formation of two distinct classes of eicosanoids; the epoxyeicosatrienoic acids (EETs) and the hydroxyeicosatetraenoic acids (HETEs) (Capdevila *et al.*, 1981; Proctor *et al.*, 1987). Of particular interest to the studies presented here are that the EET products of AA oxidation which are important signaling molecules that exert a wide range of physiological effects.

EETs are oxidative AA metabolites enzymatically produced by CYPs, particularly the CYP2 families. The CYP2C and CYP2J families are putatively identified as the principal AA epoxygenases in cardiac tissue (Roman, 2002). Other drug metabolism CYPs such as CYP3A4 can produce EETs from AA, however most oxidations performed by these isoforms typically result in a monohydroxylation of AA, leading to the production of HETEs. Lastly, CYPs identified to have primarily endogenous substrates, particularly the CYP4 family, can also oxidize AA but as hydroxylases rather than epoxygenases.

As epoxide metabolites, EETs are inherently unstable and have a short half-life. Non-enzymatically, they can be hydrolyzed by the aqueous environment of the cell cytoplasm. In addition, they are light and air-sensitive (Aliwarga *et al.*, 2017). Biologically, the signaling cascade can also be turned off by the ubiquitous cytoplasmic enzyme soluble epoxide hydrolase (sEH), hydrolyzing EETs to the less biologically active dihydroxyeicosatrienoic acids (DHETs). Combined, the nonenzymatic and enzymatic pathways of EET degradation serve as regulators of EET actions in the cell. Additionally, like its precursor AA, EETs have been shown to be stored in the lipid bilayers of cell membranes, also at the *sn*-2 positions of glycerophospholipids and

PLA2 activity will also release any stored EETs from the cell membrane in the same manner as AA.

EETs have many biological functions including, but not limited to, angiogenesis, regulation of vasodilation, inhibition of cytokine-induced endothelial cell adhesion molecule expression, inhibition of vascular smooth muscle cell migration, protection of endothelial cells against hypoxia-re-oxygenation injury, up-regulation of endothelial nitric oxide biosynthesis, and protection of doxorubicin-induced cardiotoxicity (Node *et al.*, 1999; Pozzi *et al.*, 2005; Larsen *et al.*, 2007; Spector and Norris, 2007; Campbell and Fleming, 2010; Pfister *et al.*, 2010). All these events are involved in cardiac electrophysiology and protect the heart from ischemic-reperfusion injury (Spiecker and Liao, 2006). Taken together, there is a large body of evidence suggesting critical and protective functions for EETs in cardiovascular homeostasis.

1.4 Dissertation Purpose and Organization

The primary purpose of this dissertation is to examine how CYP2J2 gene expression is regulated in adult human ventricular myocytes under various stressors caused by pathophysiological conditions. We also examine how the cell responds to external stressors when CYP2J2 is pharmacologically inhibited or its expression is silenced. The impact due to loss of gene expression in human cardiomyocytes are largely unknown, although, studies conducted have reported overwhelming evidence of CYP2J2 cardioprotection in multiple disease models (Ke *et al.*, 2007; Li *et al.*, 2012; Ma *et al.*, 2013; Zhu *et al.*, 2020). Previous studies have suggested that CYP2J2 may be downregulated in some cell models under specific stressors,

however, this has not been confirmed in human cardiac models (Marden *et al.*, 2003; Bystrom *et al.*, 2013).

This chapter, Chapter 1, provides a brief background on the superfamily of CYP enzymes, of which CYP2J2 is a member. This topic has been extensively reviewed elsewhere and here we only provide background that is central to the thesis project. In addition to the general background into CYPs, CYP2J2 is discussed in detail, including its role as a drug metabolism enzyme and its endogenous functions. Finally, a brief background of one of CYP2J2's endogenous substrates arachidonic acid (AA) and resulting metabolites, the epoxyeicosatrienoic acids (EETs) are provided along with what is known about their physiological functions, with emphasis on cardiovascular context.

In Chapter 2, the effects of silencing *CYP2J2* gene expression in adult ventricular myocytes is explored. Gene expression of *CYP2J2* was silenced in adult ventricular myocytes by external siRNA. Following silencing, RNA sequencing (RNASeq) provides a global examination of the effects of *CYP2J2* gene downregulation on the transcriptome. The findings are validated by a series of *in vitro* experiments to further confirm some of the observations provided by RNASeq.

In Chapter 3, adult cardiomyocytes are subjected to reactive oxygen species (ROS), a hallmark of many disease conditions. External ROS are added in the form of hydrogen peroxide at varying concentrations. Additionally, internal ROS production was induced through treatment with the chemotherapeutic doxorubicin, a drug known to adversely affect mitochondria by increasing cellular ROS levels (Gorini *et al.*, 2018). Through these stresses, the effects of ROS on *CYP2J2* expression is examined. Finally, the consequences due to loss of CYP2J2 protein on cardiomyocyte survival against ROS toxicity are investigated.

Chapter 4 delves into the effects of hypoxia on *CYP2J2* expression in cardiomyocytes, and basal CYP2J2 levels affect cell viability in hypoxic environments. Similar to ROS stress, we explored two methods of inducing a hypoxic response in cardiomyocytes; low oxygen tension and a chemical hypoxia mimetic, $CoCl_2$, allowing for insights into how CYP2J2 might be involved in the hypoxic response in ventricular myocytes.

The final research chapter, Chapter 5 investigates changes in *CYP2J2* response in cardiomyocytes cultured in human type 2 diabetic serum. Diabetes is a multifactorial disease with multiple characteristics that exert various stresses, including hyperglycemia, inflammatory factors, hypoxia, and elevated ROS. In this chapter, the effects of type 2 diabetes stressors on ventricular myocytes are examined. In doing so, the cellular effects of type 2 diabetes serum on adult cardiomyocytes were examined and a potential role for CYP2J2 protection investigated.

Finally, Chapter 6 provides some conclusions and discussion from studies presented in the preceding chapters and offers some guidance to future directions that could be examined in light of the information gleaned from the investigations presented.

Figures

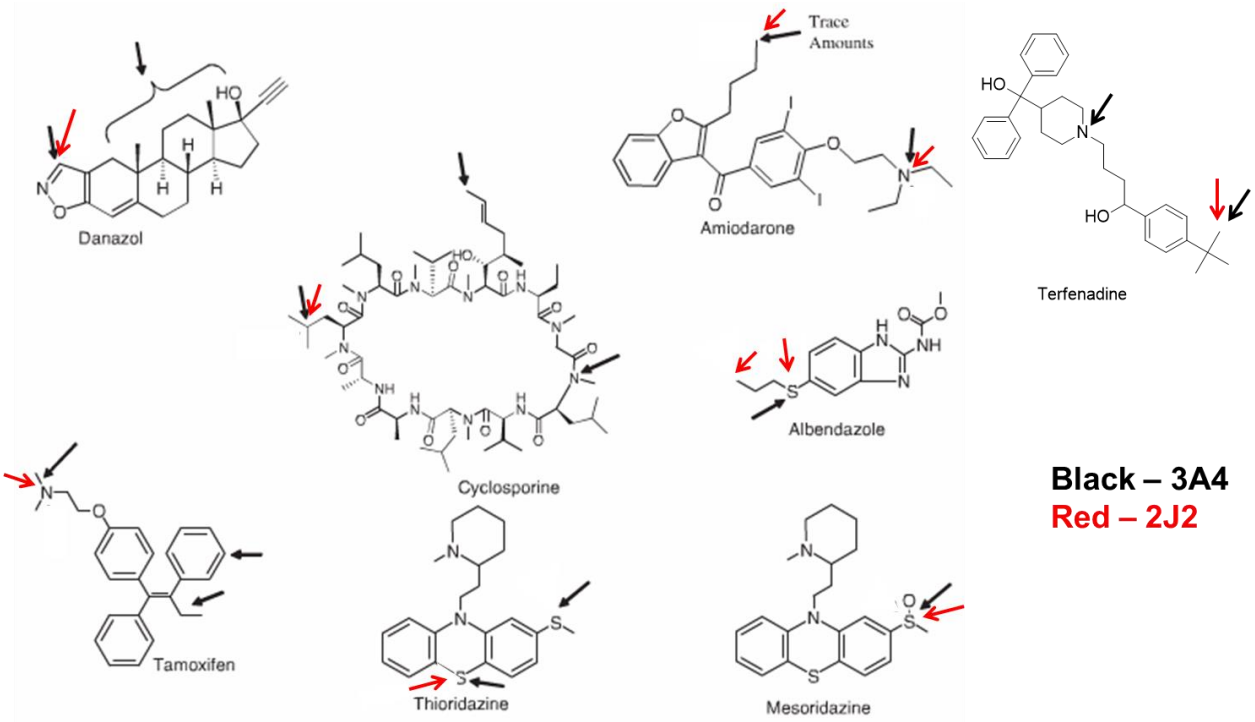

Figure 1.1. Cytochrome P450 metabolic sites for representative chemical entities. Sites denoted by black arrows are sites metabolized by CYP3A4 while sites denoted by red arrows are sites oxidized by CYP2J2. While there is significant overlap between the two, CYP3A4 typically oxidizes multiple sites on a given molecule and CYP2J2 has one or two preferred sites on any molecule. This figure is adapted from Lee et al. (Lee *et al.*, 2012).

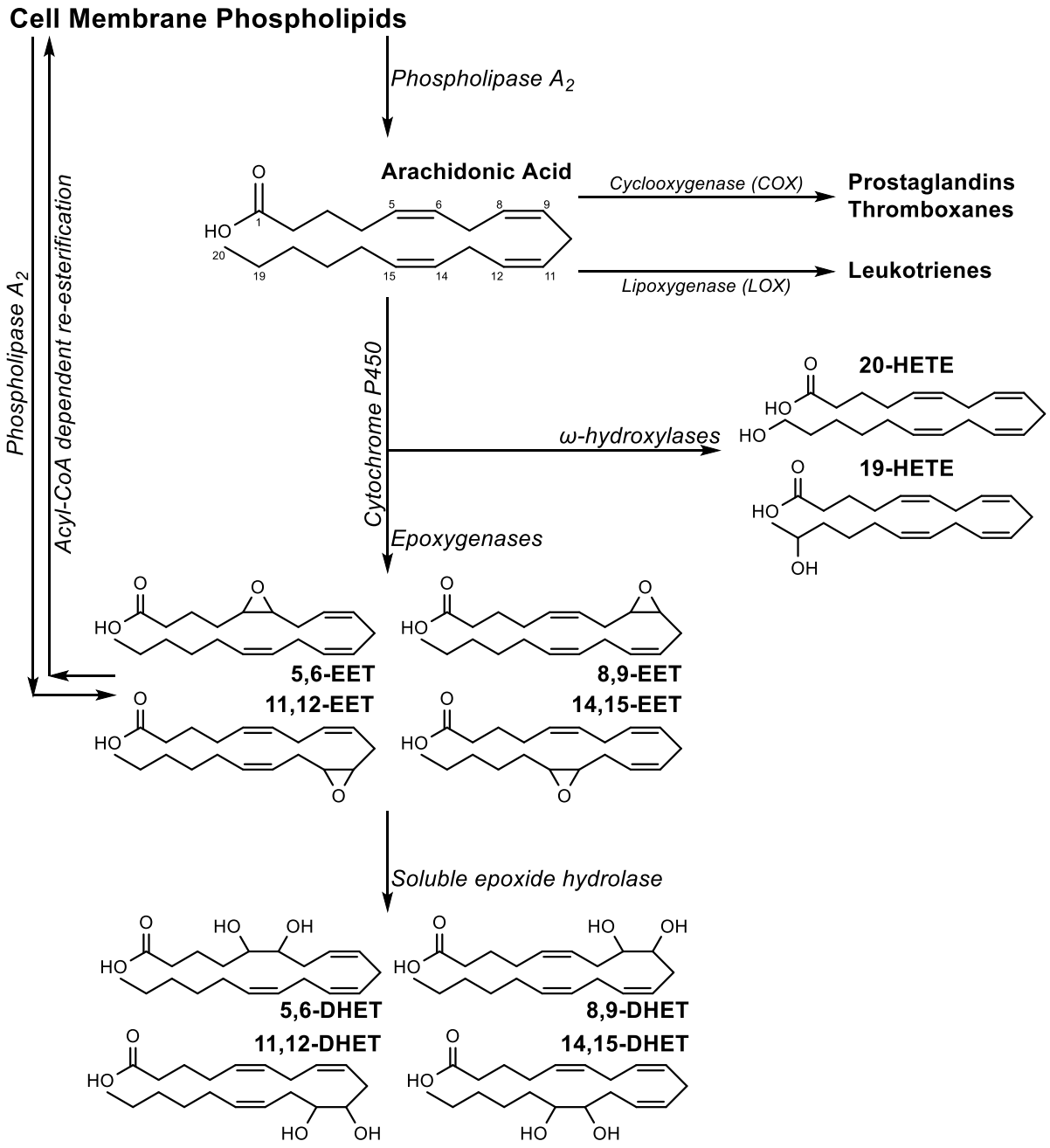

Figure 1.2. Scheme depicting the route of endogenous AA metabolism. AA acts as a precursor to multiple endogenous signaling molecules, including prostaglandins, thromboxanes, leukotrienes, HETEs and EETs. It is stored in the membrane and released by the enzyme PLA2. Additionally, EETs can also be re-esterified to the membrane for storage. EET signaling is inactivated by hydrolysis catalyzed by soluble epoxide hydrolase into DHETs.

References

Aliwarga T, Raccor BS, Lemaitre RN, Sotoodehnia N, Gharib SA, Xu L, and Totah RA (2017) Enzymatic and free radical formation of cis- and trans- epoxyeicosatrienoic acids in vitro and in vivo. *Free Radic Biol Med* **112**:131–140.

Arnold WR, and Das A (2018) An Emerging Pathway of Doxorubicin Cardiotoxicity Mediated through CYP2J2. *Biochemistry* **57**:2294–2296, NIH Public Access.

Bièche I, Narjoz C, Asselah T, Vacher S, Marcellin P, Lidereau R, Beaune P, and de Waziers I (2007) Reverse transcriptase-PCR quantification of mRNA levels from cytochrome (CYP)1, CYP2 and CYP3 families in 22 different human tissues. *Pharmacogenet Genomics* **17**:731–742.

Börgel J, Bulut D, Hanefeld C, Neubauer H, Mügge A, Epplen JT, Holland-Letz T, and Spiecker M (2008) The CYP2J2 G-50T polymorphism and myocardial infarction in patients with cardiovascular risk profile. *BMC Cardiovasc Disord* **8**:41.

Brash AR (1999) Lipoxygenases: occurrence, functions, catalysis, and acquisition of substrate. *J Biol Chem* **274**:23679–82.

Bystrom J, Thomson SJ, Johansson J, Edin ML, Zeldin DC, Gilroy DW, Smith AM, and Bishop-Bailey D (2013) Inducible CYP2J2 and Its Product 11,12-EET Promotes Bacterial Phagocytosis: A Role for CYP2J2 Deficiency in the Pathogenesis of Crohn's Disease? *PLoS One* **8**.

Campbell WB, and Fleming I (2010) Epoxyeicosatrienoic acids and endothelium-dependent responses. *Pflugers Arch* **459**:881–95.

Capdevila J, Parkhill L, Chacos N, Okita R, Masters BS, and Estabrook RW (1981) The oxidative metabolism of arachidonic acid by purified cytochromes P-450. *Biochem Biophys*

Res Commun **101**:1357–63.

Chen C, Li G, Liao W, Wu J, Liu L, Ma D, Zhou J, Elbekai RH, Edin ML, Zeldin DC, and Wang DW (2009) Selective inhibitors of CYP2J2 related to terfenadine exhibit strong activity against human cancers in vitro and in vivo. *J Pharmacol Exp Ther* **329**:908–18.

Chen F, Chen C, Yang S, Gong W, Wang Y, Cianflone K, Tang J, and Wang DW (2012) Let-7b inhibits human cancer phenotype by targeting cytochrome P450 epoxygenase 2J2. *PLoS One* **7**:e39197.

Delozier TC, Kissling GE, Coulter SJ, Dai D, Foley JF, Bradbury JA, Murphy E, Steenbergen C, Zeldin DC, and Goldstein JA (2007) Detection of human CYP2C8, CYP2C9, and CYP2J2 in cardiovascular tissues. *Drug Metab Dispos* **35**:682–688.

Deng P, You T, Chen X, Yuan T, Huang H, and Zhong D (2011) Identification of Amiodarone Metabolites in Human Bile by Ultraperformance Liquid Chromatography / Quadrupole Time-of- Flight Mass Spectrometry ABSTRACT : **39**:1058–1069.

Evangelista EA, Kaspera R, Mokadam NA, Jones III JP, and Totah RA (2013) Activity, inhibition, and induction of cytochrome P450 2J2 in adult human primary cardiomyocytes. *Drug Metab Dispos* **41**.

Fer M, Dréano Y, Lucas D, Corcos L, Salaün JP, Berthou F, and Amet Y (2008) Metabolism of eicosapentaenoic and docosahexaenoic acids by recombinant human cytochromes P450. *Arch Biochem Biophys* **471**:116–125.

Gorini S, De Angelis A, Berrino L, Malara N, Rosano G, and Ferraro E (2018) Chemotherapeutic Drugs and Mitochondrial Dysfunction: Focus on Doxorubicin, Trastuzumab, and Sunitinib. *Oxid Med Cell Longev* **2018**:7582730.

Guengerich FP (2001) Common and uncommon cytochrome P450 reactions related to

metabolism and chemical toxicity. *Chem Res Toxicol* **14**:611–650, American Chemical Society.

Hashizume T, Imaoka S, Mise M, Terauchi Y, Fujii T, Miyazaki H, Kamataki T, and Funae Y (2002) Involvement of CYP2J2 and CYP4F12 in the Metabolism of Ebastine in Human Intestinal Microsomes. *J Pharmacol Exp Ther* **300**:298–304.

Ke Q, Xiao YF, Bradbury JAA, Graves JP, Degraff LM, Seubert JM, and Zeldin DC (2007) Electrophysiological Properties of Cardiomyocytes Isolated from CYP2J2 Transgenic Mice. *Mol Pharmacol* **72**:mol.

King LM, Ma J, Srettabunjong S, Graves J, Bradbury JA, Li L, Spiecker M, Liao JK, Mohrenweiser H, and Zeldin DC (2002) Cloning of CYP2J2 gene and identification of functional polymorphisms. *Mol Pharmacol* **61**:840–52.

Lafite P, Dijols S, Zeldin DC, Dansette PM, and Mansuy D (2007) Selective, competitive and mechanism-based inhibitors of human cytochrome P450 2J2. **464**:155–168.

Larsen BT, Campbell WB, and Gutterman DD (2007) Beyond vasodilatation: non-vasomotor roles of epoxyeicosatrienoic acids in the cardiovascular system. *Trends Pharmacol Sci* **28**:32–38.

Lee AC, and Murray M (2010) Up-Regulation of Human CYP2J2 in HepG2 Cells by Butylated Hydroxyanisole Is Mediated by c-Jun and Nrf2. *Mol Pharmacol* **77**:987–994.

Lee CA, Iii JPJ, Katayama J, Jiang Y, Freiwald S, Smith E, Walker GS, Totah RA, Al LEEET, Jones JP, Katayama J, Kaspera R, Jiang Y, Freiwald S, Smith E, Walker GS, Totah RA, Iii JPJ, Katayama J, Jiang Y, Freiwald S, Smith E, Walker GS, Totah RA, and Al LEEET (2012) Identifying a selective substrate and inhibitor pair for the evaluation of CYP2J2 activity. *Drug Metab Dispos* **40**:943–951.

Lee CA, Neul D, Clouser-roche A, Dalvie D, Wester MR, Jiang Y, Iii JPJ, Freiwald S, Zientek M, Totah RA, and Al LEEET (2010) Identification of Novel Substrates for Human Cytochrome P450 2J2 ABSTRACT : **38**:347–356.

Lee CA, Neul D, Clouser-Roche A, Dalvie D, Wester MR, Jiang Y, Jones III JP, Freiwald S, Zientek M, Totah RA, Laboratories DJ, Diego S, California C a L, and Al LEEET (2010) Identification of Novel Substrates for Human Cytochrome. *Drug Metab Dispos* **38**:347–356.

Li R, Xu X, Chen C, Yu X, Edin ML, Degraff LM, Lee CR, Zeldin DC, and Wang DW (2012) Cytochrome P450 2J2 is protective against global cerebral ischemia in transgenic mice. *Prostaglandins Other Lipid Mediat* **99**:68–78, Elsevier Inc.

Liu P-Y, Li Y-H, Chao T-H, Wu H-L, Lin L-J, Tsai L-M, and Chen J-H (2007) Synergistic effect of cytochrome P450 epoxygenase CYP2J2*7 polymorphism with smoking on the onset of premature myocardial infarction. *Atherosclerosis* **195**:199–206.

Ma B, Xiong X, Chen C, Li H, Xu X, Li X, Li R, Chen G, Dackor RT, Zeldin DC, and Wang DW (2013) Cardiac-specific overexpression of CYP2J2 attenuates diabetic cardiomyopathy in male streptozotocin-induced diabetic mice. *Endocrinology* **154**:2843–56.

Manikandan P, and Nagini S (2018) Cytochrome P450 Structure, Function and Clinical Significance: A Review. *Curr Drug Targets* **19**:38–54.

Marciante KD, Totah RA, Heckbert SR, Smith NL, Lemaitre RN, Lumley T, Rice KM, Hindorff LA, Bis JC, Hartman B, and Psaty BM (2008) Common variation in cytochrome P450 epoxygenase genes and the risk of incident nonfatal myocardial infarction and ischemic stroke. *Pharmacogenet Genomics* **18**:535–43.

Marden NY, Fiala-Beer E, Xiang S, and Murray M (2003) Role of activator protein-1 in the

down-regulation of the human CYP2J2 gene in hypoxia. *Biochem J* **373**:669–80.

Matsumoto S, Hirama T, Matsubara T, Nagata K, and Yamazoe Y (2002) Involvement of CYP2J2 on the intestinal first-pass metabolism of antihistamine drug, astemizole. *Drug Metab Dispos* **30**:1240–45.

Matsumoto S, and Yamazoe Y (2001) Involvement of multiple human cytochromes P450 in the liver microsomal metabolism of astemizole and a comparison with terfenadine. *Br J Clin Pharmacol* **51**:133–142.

McDonnell AM, and Dang CH (2013) Basic review of the cytochrome p450 system. *J Adv Pract Oncol* **4**:263–8, Harborside Press.

Michaels S, and Wang MZ (2014) The Revised Human Liver Cytochrome P450 "Pie": Absolute Protein Quantification of CYP4F and CYP3A Enzymes Using Targeted Quantitative Proteomics. *Drug Metab Dispos* **42**:1241, American Society for Pharmacology and Experimental Therapeutics.

Michaud V, Frappier M, Dumas M, and Turgeon J (2010) Metabolic Activity and mRNA Levels of Human Cardiac CYP450s Involved in Drug Metabolism. *PLoS One* **5**.

Node K, Huo Y, Ruan X, Yang B, Spiecker M, Ley K, Zeldin DC, and Liao JK (1999) Anti-inflammatory properties of cytochrome P450 epoxygenase-derived eicosanoids. *Science (80-)* **285**:1276–1279.

Oliw EH (1994) Oxygenation of polyunsaturated fatty acids by cytochrome P450 monooxygenases. *Prog Lipid Res* **33**:329–54.

Oliw EH, Guengerich FP, and Oates JA (1982) Oxygenation of arachidonic acid by hepatic monooxygenases. Isolation and metabolism of four epoxide intermediates. *J Biol Chem* **257**:3771–81.

Ortiz de Montellano PR (2005) *Cytochrome P450 : structure, mechanism, and biochemistry*, Kluwer Academic/Plenum Publishers.

Otto JC, and Smith WL (1995) Prostaglandin endoperoxide synthases-1 and -2. *J Lipid Mediat Cell Signal* **12**:139–56.

Paine MF, Hart HL, Ludington SS, Haining RL, Rettie AE, and Zeldin DC (2006) The Human Intestinal Cytochrome P450 " Pie ." *Methods* **34**:880–886.

Pfister SL, Gauthier KM, and Campbell WB (2010) Vascular Pharmacology of Epoxyeicosatrienoic Acids, in *Advances in Pharmacology* pp 27–59.

Piomelli D (1993) Arachidonic acid in cell signaling. *Curr Opin Cell Biol* **5**:274–280.

Pozzi A, Macias-Perez I, Abair T, Wei S, Su Y, Zent R, Falck JR, and Capdevila JH (2005) Characterization of 5,6-and 8,9-Epoxyeicosatrienoic Acids (5,6-and 8,9-EET) as Potent in Vivo Angiogenic Lipids*. , doi: 10.1074/jbc.M501730200.

Proctor KG, Falck JR, and Capdevila J (1987) Intestinal vasodilation by epoxyeicosatrienoic acids: arachidonic acid metabolites produced by a cytochrome P450 monooxygenase. *Circ Res* **60**:50–9.

Roman RJ (2002) P -450 Metabolites of Arachidonic Acid in the Control of Cardiovascular Function. *Physiol Rev* **82**:131–185.

Seubert J, Yang B, Bradbury JA, Graves J, Degraff LM, Gabel S, Gooch R, Foley J, Newman J, Mao L, Rockman HA, Hammock BD, Murphy E, and Zeldin DC (2004) Enhanced postischemic functional recovery in CYP2J2 transgenic hearts involves mitochondrial ATP-sensitive K+ channels and p42/p44 MAPK pathway. *Circ Res* **95**:506–14.

Shimada T, Yamazaki H, Mimura M, Inui Y, and Guengerich FP (1994) Interindividual Variations in Human Liver Cytochrome P-450 Enzymes Involved in the Oxidation of

Drugs, Carcinogens and Toxic Chemicals : Studies with Liver Microsomes of 30 Japanese. *J Pharmacol Exp Ther* **270**:414–423.

Spector AA, and Norris AW (2007) Action of epoxyeicosatrienoic acids on cellular function. *Am J Physiol Cell Physiol* **292**:C996–C1012.

Spiecker M, Darius H, Hankeln T, Soufi M, Sattler AM, Schaefer JR, Node K, Börgel J, Mügge A, Lindpaintner K, Huesing A, Maisch B, Zeldin DC, and Liao JK (2004) Risk of coronary artery disease associated with polymorphism of the cytochrome P450 epoxygenase CYP2J2. *Circulation* **110**:2132–6.

Spiecker M, and Liao JK (2006) Cytochrome P450 Epoxygenase CYP2J2 and the Risk of Coronary Artery Disease. **16**:204–208.

Tallima H, and El Ridi R (2017) Arachidonic acid: Physiological roles and potential health benefits - A review. *J Adv Res* **11**:33–41, Elsevier B.V.

Thomas JM, Hullin F, Chap H, and Douste-Blazy L (1984) Phosphatidylcholine is the major phospholipid providing arachidonic acid for prostacyclin synthesis in thrombin-stimulated human endothelial cells. *Thromb Res* **34**:117–23.

Wei X, Zhang D, Dou X, Niu N, Huang W, Bai J, and Zhang G (2014) Elevated 14,15-epoxyeicosatrienoic acid by increasing of cytochrome P450 2C8, 2C9 and 2J2 and decreasing of soluble epoxide hydrolase associated with aggressiveness of human breast cancer. *BMC Cancer* **14**:841.

Wu S, Moomaw CR, Tomer KB, Falck JR, and Zeldin DC (1996) Molecular cloning and expression of CYP2J2, a human cytochrome P450 arachidonic acid epoxygenase highly expressed in heart. *J Biol Chem* **271**:3460–8.

Xiao B, Li X, Yan J, Yu X, Yang G, Xiao X, Voltz JW, Zeldin DC, and Wang DW (2010)

Overexpression of cytochrome P450 epoxygenases prevents development of hypertension in spontaneously hypertensive rats by enhancing atrial natriuretic peptide. *J Pharmacol Exp Ther* **334**:784–94.

Yamazaki H, Okayama A, Imai N, Guengerich FP, and Shimizu M (2006) Inter-individual variation of cytochrome P4502J2 expression and catalytic activities in liver microsomes from Japanese and Caucasian populations. *Xenobiotica* **36**:1201–9.

Yang L, Ni L, Duan Q, Wang X, Chen C, Chen S, Chaugai S, Zeldin DC, Tang JR, and Wang DW (2015) CYP epoxygenase 2J2 prevents cardiac fibrosis by suppression of transmission of pro-inflammation from cardiomyocytes to macrophages. *Prostaglandins Other Lipid Mediat* **116**–**117**:64–75.

Zanger UM, and Schwab M (2013) Cytochrome P450 enzymes in drug metabolism: Regulation of gene expression, enzyme activities, and impact of genetic variation. *Pharmacol Ther* **138**:103–141.

Zeldin DC, Foley J, Boyle JE, Moomaw CR, Tomer KB, Parker C, Steenbergen C, and Wu S (1997) Predominant Expression of an Arachidonate Epoxygenase in Islets of Langerhans Cells in Human and Rat Pancreas. *Endocrinology* **138**:1338–1346.

Zhu Y, Ding A, Yang D, Cui T, Yang H, Zhang H, and Wang C (2020) CYP2J2-produced epoxyeicosatrienoic acids attenuate ischemia/reperfusion-induced acute kidney injury by activating the SIRT1-FoxO3a pathway. *Life Sci* **246**:117327.

Chapter 2: RNA Sequencing of *CYP2J2* silenced adult ventricular myocytes

Parts of this chapter have been published, with credits to Dr. Sina Gharib for data analysis and figure generation for RNASeq data, and to Dr. L. Fernando Santana for patch-clamp experimental data.

2.1 Introduction

Cytochrome P450s (CYPs) are a superfamily of enzymes involved in a wide range of physiological processes. These heme-containing monooxygenases have been extensively studied with the aim of understanding their role in the biotransformation and clearance of drugs and toxins (Ortiz de Montellano, 2005; McDonnell and Dang, 2013; Manikandan and Nagini, 2018). More recently, however, there is a growing interest in a subset of cytochrome P450s involved in the bioactivation of endogenous fatty acids into signaling molecules, with an emphasis on the CYP2 family (Fer *et al.*, 2008; Kaspera and Totah, 2009). Members of CYP2 family oxidize several polyunsaturated fatty acids (PUFAs), to metabolites that have important roles in various cell response and signal transduction pathways (Fer *et al.*, 2008). Delineating how these enzymes affect and interact with other molecules in cellular response cascades could be critical in understanding the mechanisms by which cells respond to external stresses and may identify new therapeutic targets. Among the human CYP2 enzymes, CYP2J2 is of particular interest because it is the only epoxygenase expressed in the heart with the highest presence in ventricular cardiomyocytes (Michaud *et al.*, 2010; Evangelista *et al.*, 2013).

Our understanding of the role and impact of CYP2J2 and arachidonic acid epoxide metabolites (epoxyeicosatrienoic acids, EETs) on cardiovascular health is rapidly advancing

(Aliwarga *et al.*, 2018). Several studies have reported on the protective effects of EETs in various disease states, particularly for their role in diabetes and related cardiovascular disorders. Interest in CYP2J2 is focused mainly on its role in bioactivating arachidonic acid to EETs, specifically in the heart. In addition to arachidonic acid, CYP2J2 has a wide range of substrates including several drugs, such as terfenadine and astemizole. CYP2J2 can metabolize other endogenous compounds, specifically other polyunsaturated fatty acids (PUFAs) such as docosahexaenoic acid (DHA) and eicosapentaenoic acid (EPA) (Fer *et al.*, 2008). Importantly, CYP2J2's PUFA substrates and resulting metabolites are involved in various and distinct signaling pathways. EETs, which are produced intracellularly, may act as secondary messengers, although a definitive receptor in the cardiomyocyte has yet to be identified. EETs have been shown to promote angiogenesis, regulate vascular tone, protect against hypoxia re-oxygenation injury, and regulate nitric oxide synthesis (Larsen *et al.*, 2007; Spector and Norris, 2007; Yang *et al.*, 2009). Importantly for the cardiomyocyte health, EETs are potent activators of several ion channels including ATP sensitive K channels (K_{ATP})(Lu *et al.*, 2001; Ke *et al.*, 2007; Kefaloyianni *et al.*, 2012) and L-type Ca channels (Xiao *et al.*, 2004; Parks *et al.*, 2014). CYP2J2-associated EETs can also act through the activation of a wide range of intracellular signaling pathways such as the MAPK/ERK and Akt pathways (Spector and Norris, 2007; Yang *et al.*, 2007; Skepner *et al.*, 2010).

The role of EETs in cardiovascular health further highlights the importance of CYP2J2 expression in the heart. Overexpression studies have shown that increased *CYP2J2* levels lead to increased EET levels and ultimately improves protection against arrhythmogenic susceptibility in animal models following cardiac hypertrophy (Westphal *et al.*, 2013). We have recently shown that *CYP2J2* gene expression in cardiomyocytes is altered in response to oxidative stress

(Evangelista *et al.*, 2018). We found that increased reactive oxygen species prompted cardiomyocytes to up-regulate *CYP2J2* expression—a response mitigated by the presence of antioxidants.

Given the multifaceted function of CYP2J2, we initially determined CYP2J2 protein levels in cardiac tissue obtained from patients with cardiomyopathy and control subjects. We then undertook an unbiased approach to systematically delineate pathways modulated by this gene in adult-derived cardiomyocytes. We used siRNA to effectively silence *CYP2J2* expression and performed RNA-sequencing (RNA-seq) and bioinformatics analyses to identify *CYP2J2*-regulated transcriptional programs in human cardiomyocytes and putative targets for future mechanistic and therapeutic studies. Finally, we looked at the effects of EET antagonism and CYP2J2 inhibition on K^+ ion channel currents in fresh isolated cardiomyocytes from a human *CYP2J2* expressing transgenic mouse model.

2.2 Methods

Materials and Reagents

Unless otherwise specified, solvents and materials were purchased from Fisher Scientific (Waltham, MA, USA) and used without further purification. Sodium pentobarbital was provided in solution by the Santana lab and used under their DEA license. Solid chemicals, unless otherwise specified, were obtained from Sigma Aldrich (St. Louis, MO) and used without further purification.

Adult cardiac ventricular tissue

Throughout the dissertation, data derived from human ventricular cardiac tissue will be presented. These tissues have two sources. Control tissues (n=17) were obtained commercially from BioIVT (Westbury, NY). These tissues were collected from individuals with no known cardiomyopathies. Case tissues (n=27) were obtained from the UW Medical Center through collaboration with Dr. Nahush Mokkadam. These tissues were surgical residues from patients undergoing left ventricular assist device (LVAD) or heart transplant procedures. Only discarded residual tissues were obtained and no patient identifiers were used; therefore, the Institutional Review Board at the University of Washington determined that it was non-human research (NHR) and waived the need for ethical review and informed consent. This policy was in accordance with Office for Human Research Protections guidelines (www.hhs.gov/ohrp/policy/cdebiol.html). Some demographics for tissue sources are provided in Table 2.1. An extensive list of medications that were taken by patients at the UWMC can be found with the Totah Lab and available upon request.

Chapter 2 presents data from nine individuals (N = 9: 8 males, 1 female) with non-ischemic cardiomyopathy. Ventricular tissue was immediately flash-frozen in liquid nitrogen upon receipt and stored at -80 °C until thawed for processing. Upon thawing, the tissue was washed with phosphate buffered saline and immediately processed. Ventricular tissue from seventeen individuals (N = 17: 10 males, 7 females) with no known cardiac or cardiovascular health issues were used as the control group. These tissues were obtained from BioIVT (Westbury, NY). The samples were shipped under dry ice and upon receipt, were stored at -80 °C until further processing.

Cardiac tissue processing

Frozen tissue was homogenized following the protocol by Aliwarga et al. for proteomic analyses (Aliwarga *et al.*, 2017). Briefly, heart tissues were homogenized in an ice-cold 1x DPBS using Precellys24 (Bertin Instruments, Rockville, MD) at 6,800 rpm for 6 x 30 s with 60 s delay between cycles. In order to prevent further proteolysis, 1 × EDTA-free Halt cocktail protease inhibitor was added promptly to the heart homogenates. Total protein content of heart homogenates was determined using a BCA method (Smith *et al.*, 1985). After dilution of heart homogenates to 2 mg/mL total protein content, solubilization, enrichment, and extraction of membrane-bound proteins were performed using Thermo Fisher Mem-PER^{TM} Plus membrane protein extraction kit (Thermo Fisher Scientific, Waltham, MA). Further sample preparation followed the published protocol by Xu et al (Xu *et al.*, 2017). Briefly, 0.7 mg/mL human serum albumin and 2.7 μg/mL bovine serum albumin were added into membrane-bound or cytosolic

fractions followed by protein denaturation and reduction step by adding 20 mM ammonium bicarbonate buffer, pH 7.8 and 17 mM dithiothreitol at 95^{o}C for 10 minutes with gentle shaking. Once the denatured protein mixtures reached room temperature, they were alkylated by adding 59 mM of iodoacetamide and incubating the samples at room temperature in the dark for 30 min. The proteins were then extracted and pelleted using ice cold 5:1:4 of methanol:chloroform:water. After mixing and centrifugation, the upper and lower layers were removed, and the remaining pellets were dried at room temperature for 10 min. The pellets were washed with ice cold methanol followed by centrifugation and drying at room temperature for 30 min. To initiate trypsin digestion, 0.04 μg of trypsin was added into each pellet that was resuspended in 50 mM ammonium bicarbonate, pH 7.8, and incubated at 37^{o}C for 18 hours. The reaction was terminated by flash freezing the samples on dry ice. Finally, a cold cocktail of stable labelled peptide internal standard and 80% acetonitrile containing 0.5% formic acid were added to the samples. After mixing and centrifuging, the supernatants were collected and analyzed by mass spectrometry.

Mass spectrometric assay for protein quantification

Quantification of CYP2J2 in cardiac tissues were carried out using a validated mass spectrometric proteomics method as published in Xu et. al (Xu *et al.*, 2017). Stable labelled CYP2J2 peptides with [$^{13}C_6$, $^{15}N_4$]- arginine or [$^{13}C_6$, $^{15}N_2$]- lysine residues on the C-terminus and at least one surrogate peptide was used as an internal standard and for protein quantitation, respectively. The peptides used for CYP2J2 quantitation were VIGQGQQPSTAAR, EVTVDTTLAGYHLPK, and LLDEVTYLEASK. The mass spectrometry parameters for both the light and heavy peptides used are provided in Table 2.2. Detailed mass spectrometric assay

was described by Xu et al (Xu *et al.*, 2017). Briefly, samples were analyzed on an AB SCIEX Triple Quadrupole 6500 (PE SCIEX, Concord, ON, Canada) with a Waters Acquity UPLC, I-class (Waters Technologies, Milford, MA) interface in ESI positive ionization mode. Chromatographic separation of peptides was achieved using a Waters Acquity UPLC HSS T3, 1.8 μm, C18, 100 Å, 2.1 x100 mm column preceded by a Phenomenex C18, 2 x 4 mm guard column. The mobile phase for this assay consisted of water containing 0.1% acetic acid and acetonitrile containing 0.1% acetic acid.

Adult cardiomyocyte culture protocol and *CYP2J2 and* scramble siRNA experiments

Cell culture materials including adult derived primary human cardiomyocytes (cat #36044-15), media (complete growth media, cat #M36044-15S), and extracellular matrix pre-coated flasks and plates (cat #E36044-15) were obtained from Celprogen Inc. (San Pedro, CA, USA). Media were further sterile filtered using a vacuum filter through a 0.22 μm polyethersulfone (PES) filter. Culturing and passage of cells followed previously published studies (Evangelista *et al.*, 2013, 2018).

CYP2J2 gene expression was silenced following previously published protocols (Evangelista *et al.*, 2018) using the RNAiMAX lipofectamine (Thermo Fisher Scientific, Waltham MA) and the CYP2J2 Trilencer siRNA or scrambled siRNA (Origene, Rockville, MD), closely following the manufacturer's suggested protocols. *HPRT1* silencing using Origene siRNA served as positive control. Lipofectamine was delivered using a reverse transfection protocol. siRNA was reconstituted to a stock concentration of 20 μM per the manufacturer protocols and prepared with lipofectamine using OptiMEM reduced serum media (Thermo

Fisher Scientific, Waltham, MA) by diluting the mixture to a concentration of 50 nM. The lipofectamine/siRNA mixture was incubated at room temperature for at least 10 minutes, during which time cells were washed, trypsinized, pelleted, resuspended and diluted to a concentration of 200,000 cells/mL in complete media. The lipofectamine/siRNA stocks were added to individual wells a 12-well plate to a final concentration of 10 nM siRNA (250 μL volume of 50 nM siRNA/lipofectamine in OptiMEM), followed by the cells (1 mL of cell suspension) for a final volume of 1250 μL in each well. The cells were incubated with lipofectamine/siRNA for 72 hours. Following gene silencing, cells were harvested and stored until total RNA isolation.

We performed two independent sets of experiments on human cardiomyocyte cultures treated with *CYP2J2* siRNA (n = 3) or scrambled siRNA (n = 3). The first set of studies were used for genome-wide RNA-seq analysis (n = 6 total), and the second set of experiments were performed for qPCR validation purposes (n = 6 total).

Terfenadine activity assay

CYP2J2 enzymatic activity following gene silencing was determined using previously published protocols (Evangelista *et al.*, 2013). Briefly, cells were treated with lipofectamine and either scramble or CYP2J2 siRNA as described above for 72 hours. After 72 hours, the cells were washed and treated with 1.5 μM terfenadine in serum free media. Mass spectrometry was used to determine relative levels of hydroxy-terfenadine using previously published parameters (Evangelista *et al.*, 2013), using midazolam (50 nM final concentration) as an internal standard for relative quantification and 10 mM ammonium acetate in water and acetonitrile as the mobile phase (aqueous and organic, respectively).

Total RNA Isolation and qPCR

Total RNA was extracted using the MagMax 96 Total RNA Isolation kit (Thermo Fisher Scientific, Waltham MA). Initial RNA quality (A260/A280) and quantity was determined using a Synergy HTX Multi-Mode Reader (BioTek, Winooski VT). In order to determine CYP2J2 siRNA knockdown efficiency, total RNA was used to synthesize cDNA using the High Capacity RNA-to-cDNA kit (Thermo Fisher Scientific, Waltham MA). RT-PCR was then carried out using TaqMan (Thermo Fisher Scientific, Waltham MA) FAM reporter primers for *CYP2J2* as well as a housekeeping gene, *GUSB*. Additionally, a select subset of genes were quantified using RT-PCR to validate RNA-seq findings in a separate experiment. Specifically, we used TaqMan primers for *HMOX1, SCN1B, PSAT1, KCNA2*, and *GLTP* to assay for the expression levels of these genes by RT-PCR following *CYP2J2* knockdown. Cycle threshold (C_T) values and the ΔC_T method followed by the $2^{\Delta CT}$calculation were used to determine the relative quantity of CYP2J2 (and other genes) mRNA present relative to the *GUSB*. The mRNA levels were first normalized to the housekeeping gene using the ΔC_T method and then expression levels in treated cells were compared to levels in untreated cells using the $\Delta\Delta C_T$ calculation. Relative gene expression levels were reported using the $2^{-\Delta\Delta CT}$ calculation (Livak and Schmittgen, 2001).

RNA-sequencing

Total RNA from adult cardiomyocytes treated with *CYP2J2* siRNA or scrambled siRNA (n = 3 per group) was isolated using methods described above. RNA-seq was performed at University of Washington's Northwest Genomics Center (http://nwgc.gs.washington.edu/). Briefly, library generation was performed using TruSeq Stranded mRNA library prep kit

(Illumina, San Diego, CA) using 1 μg total RNA. Sequencing was performed using an Illumina HiSeq 4000 instrument using paired end 75 bp lanes. Base calls were generated in real-time on the HiSeq instrument, and RTA-generated BCL files were converted to FASTQ files. Sequence read and base quality were checked using the FASTX-toolkit (http://hannonlab.cshl.edu/fastx_toolkit/) and FastQC (http://www.bioinformatics.babraham.ac.uk/projects/fastqc/), and adaptor and low-quality bases were trimmed. Sequences were aligned to GRCh38 with reference transcriptome Gencode release 26 (GRCh38.p10) using STAR (v2.5.3a). Transcript abundances were quantified using Kallisto (v0.43.1)(Bray *et al.*, 2016). All RNA-seq data meeting MINSEQE (Minimum Information About a Next-generation Sequencing Experiment) have been deposited at Gene Expression Omnibus repository (https://www.ncbi.nlm.nih.gov/geo/, GSE136957).

Validation of adult ventricular myocytes

RNA sequencing raw counts data were used to validate the ventricular myocyte cell model used in these studies. Specifically, we looked at the expression of Connexin 1 and 5 (*GJA1* and *GJA5*), Desmin (*DES*), heart-type fatty acid binding protein (*FABP3*), GATA-4 (*GATA4*), myocyte specific enhancer factor 2C (*MEF2C*), myosin heavy chain 6 and 7 (*MYH6* and *MYH7*), homeobox protein NKx-2.5 (*NKX2.5*), troponin I (*TNNI3*), tropomyosin alpha-1 chain (*TPM1*) and hERG (*KCNH2*).

Gene Expression Analysis

Initially, we applied correspondence analysis (Fellenberg *et al.*, 2001), a method for reducing high dimensional data, to all measured transcripts across experimental conditions after regularized log transformation of the raw counts(Love *et al.*, 2014). Next, we identified differentially expressed genes between *CYP2J2* knockdown vs. scrambled siRNA cardiomyocytes using DESeq2 (Love *et al.*, 2014) in the R statistical environment. Multiple hypothesis testing was addressed using Benjamini-Hochberg's false discovery rate (FDR) analysis with an FDR < 0.01 designating significant differential gene expression (Love *et al.*, 2014).

Bioinformatics and Pathway Analyses

To identify transcriptional programs altered by selective siRNA knockdown of *CYP2J2* in human cardiomyocytes, we applied Gene Set Enrichment Analysis (GSEA) (Subramanian *et al.*, 2005) using approximately 7,000 well-curated gene sets comprised of canonical biological pathways (e.g., Hallmark, KEGG, Reactome, Biocarta) and Gene Ontology (GO) annotations to all identified unique transcripts rank ordered based on DESeq2's test statistic. An FDR < 0.05 threshold for significant enrichment was used from possibly anti-conservative *P*-values computed based on 1000 random gene set selections. (Subramanian *et al.*, 2005) Network visualization of GSEA results was performed using Enrichment Map (Isserlin *et al.*, 2014), a plug-in application within the bioinformatics software platform, Cytoscape (Cline *et al.*, 2007). To generate the pathway enrichment network, all identified significant gene sets (FDR < 0.05) were used as nodes. Edges were drawn between pathways if at least 50% of their gene members

overlapped. Distinct biological modules emerged based on the network topology and consisted of aggregates of highly connected gene sets. We performed leading edge analysis (Subramanian *et al.*, 2007) on the gene sets that mapped to the "Ion Channel Signaling" GSEA module in order to identify transcripts with the largest contribution to pathway enrichment, and further refined these genes to those differentially expressed at FDR < 0.01. We next performed gene product interaction analysis using Ingenuity (IPA, Qiagen Bioinformatics, Redwood City, CA) on these "Ion Channel Signaling" associated genes, limiting relationships among nodes to those based on high confidence direct interactions. Upstream regulator and causal network analysis (IPA) were performed on all differentially expressed genes (FDR < 0.01). In this approach, critical orchestrators of the transcriptional response are identified by comparing the direction of change observed among differentially expressed genes following *CYP2J2* silencing and expected effects based on prior knowledge (i.e., published literature, canonical pathways) (Krämer *et al.*, 2014; Parimon *et al.*, 2019).

CYP2J2 Overexpressing mice

Transgenic mice overexpressing human CYP2J2 in cardiomyocytes under the αMHC promoter were obtained courtesy of Dr. Darryl Zeldin at the NIEHS. The mice were housed in a specific pathogen free vivarium under 12-hour light/dark cycles and had free access to food and water at all times. All experiments involving transgenic mice were reviewed and approved by the UW IACUC (protocol #4207-01).

Primary cardiomyocyte isolation

Primary ventricular cardiomyocytes were isolated from mice using collagen perfusion and heart digestion. Mice were terminally sedated via IP injection of sodium pentobarbital solution (0.25 mL), until the mouse was unconscious and unresponsive to pain via "toe-pinch" or "tail-pinch". Once sedated, the thoracic cavity was carefully cut along the thoracic margin along the diaphragm. The ribcage was then reflected via upward cut into the cavity. The heart was then drawn into a plastic transfer pipette cut to size and cut out of the thoracic cavity by severing the aorta. The heart was then rinsed in ice cold buffer (DE buffer) consisting of NaCl (130 mM), KCl (5 mM), pyruvic acid (3 nM), HEPES (25 mM), $MgCl_2$ (0.5 mM), NaH_2PO_4 (0.33 mM), dextrose (22 mM) and EGTA (150 μM). The heart, while in ice cold DE buffer as cannulated by fitting the aorta over a cannula tip, ligated in place by sutures.

Blood was then washed from the cardiac chambers via gravity driven perfusion of warmed (37 °C) De buffer through the cannula and through the chambers of the heart. Once the blood was rinsed, "DCP" buffer (consisting of NaCl (130 mM), KCl (5 mM), pyruvic acid (3 nM), HEPES (25 mM), $MgCl_2$ (0.5 mM), NaH_2PO_4 (0.33 mM), dextrose (22 mM), $CaCl_2$ (50 μM), 1 mg protease from *S. griseus* Type XIV (Sigma Aldrich, St Louis, MO), and 15-20 mg collagenase IV/25 mL buffer, optimized for the batch being used) was perfused through the heart to digest the extracellular matrix. Once the heart has lost its shape and the perfusion speed has increased slightly due to the loss of integrity, the ventricles were cut from the heart and placed in warm (37°C) collection buffer containing NaCl (130 mM), KCl (5 mM), pyruvic acid (3 nM), HEPES (25 mM), $MgCl_2$ (0.5 mM), NaH_2PO_4 (0.33 mM), dextrose (22 mM), $CaCl_2$ (500 μM), 0.5 mg protease from *S. griseus* Type XIV, BSA (5% w/v), and 10-15 mg collagenase IV/2.5 mL buffer (as optimized for the collagenase batch). The ventricles were gently agitated,

mechanically separating the cells from each other. The cells were then allowed to pellet by gravity over 10 minutes at room temperature. The supernatant was then removed and the pellet was washed with neutralization buffer containing NaCl (130 mM), KCl (5 mM), pyruvic acid (3 nM), HEPES (25 mM), $MgCl_2$ (0.5 mM), NaH_2PO_4 (0.33 mM), dextrose (22 mM), $CaCl_2$ (250 μM), and BSA (1 % w/v). The cells were then pelleted by gravity filtration and the neutralization buffer removed and replaced with the appropriate patch-clamp buffer.

Action potential duration in mouse ventricular myocytes.

Action potential duration (APD) were measured in isolated mouse ventricular myocytes by evoking at frequencies that ranged from 1-10 Hz through the injection of 1-4 nA of current via the patch-clamp pipette. Cells were then exposed to the epoxygenase inhibitor MS-PPOH (25 μM) and APD measured again.

Patch-Clamp experiments

Whole-cell K^+ currents were recorded in freshly isolated ventricular myocytes using an Axopatch 200B integrating amplifier (Axon Instruments, Union City, CA, USA), filtered at 2 kHz and digitized at 50 kHz. K^+ currents were elicited at test potentials (TP) from -120 mV to +40 mV at 10 mV increments from a holding potential (HP) of 0 mV to inactivate Na^+ and Ca^{2+} channels. The bath solution used included NaCl (20 mM), KCl (4.5 mM), choline chloride (130 mM), $CaCl_2$ (1 mM), $CoCl_2$ (2 mM), $MgCl_2$ (2 mM), HEPES (10 mM), and glucose (5.5 mM) at pH 7.4. Pipette solutions for whole-cell experiments included KCl (140 mM), $CaCl_2$ (465 μM), $MgCl_2$ (500 μM), Na_2ATP (5 mM), Na_2GTP (500 μM), HEPES (1 mM), and EGTA (1 mM) at

pH 7.3. Currents obtained were inhibited using glyburide (5 μM) and activated using pinacidil (5 μM).

2.3 Results

CYP2J2 protein levels are lower in individuals with cardiac disease

We utilized quantitative mass spectrometry to assess whether CYP2J2 protein content differed between individuals without cardiac disease and patients with non-ischemic cardiomyopathy. We observed significantly lower mean CYP2J2 protein levels in ventricular tissues of individuals with non-ischemic cardiomyopathy compared to ventricular tissue of subjects with no known heart disease as shown in Figure 2.1.

CYP2J2 expression knockdown results in decreased enzymatic activity

To determine whether the siRNA knockdown was effective at reducing protein levels and thus activity, we assessed CYP2J2 activity using terfenadine as a probe substrate. A significant decrease in terfenadine metabolism (>90 %) was observed between cells treated with CYP2J2 siRNA compared to cells treated with scramble as summarized in Figure 2.2. Our results also demonstrate that in the presence of a known CYP2J2 inhibitor, danazol (DAN), there is a significant drop in terfenadine hydroxylation in cells treated with siRNA, indicating that the observed changes in metabolism during siRNA treatment is due to reduction in CYP2J2 protein level and activity.

Validation of human adult derived ventricular myocytes

The panel of genes screened (gene in parentheses) included Connexin 1 and 5 (*GJA1* and *GJA5*), Desmin (*DES*), heart-type fatty acid binding protein (*FABP3*), GATA-4 (*GATA4*), myocyte specific enhancer factor 2C (*MEF2C*), myosin heavy chain 6 and 7 (*MYH6* and *MYH7*), homeobox protein NKx-2.5 (*NKX2.5*), troponin I (*TNNI3*), tropomyosin alpha-1 chain (*TPM1*) and hERG (*KCNH2*). Results demonstrate that the cells express several cardiac markers such as GJA1, GATA4, NKX2.5, MEF2C, TPM1, and KCNH2. Markers specific to ventricular myocytes were robustly expressed while those more specific to atrial myocytes were detected at very low levels (Figure 2.3).

CYP2J2 knockdown elicits widespread changes in human cardiomyocyte transcriptome

To assess the global effects of suppressing *CYP2J2* expression, we applied correspondence analysis to the entire cardiomyocyte transcriptome across the two experimental conditions. As depicted in Figure 2.4, we observed clear segregation between cardiomyocytes whose *CYP2J2* was knocked down by siRNA compared to cells treated with scramble siRNA, indicating that modulating *CYP2J2* expression results in large-scale alterations in cardiomyocyte gene expression profiles. Next, by applying a strict statistical threshold (FDR < 0.01) we identified over 1,100 transcripts that were differentially expressed between *CYP2J2*-silenced cardiomyocytes vs. controls treated with scramble siRNA. Figure 2.5 represents these differentially expressed genes as a hierarchically clustered heatmap with the top 25 up- and down-regulated genes displayed (Table 2.3). In order to validate transcriptional changes observed from the RNA-seq study, we repeated an independent set of experiments and used RT-

PCR to measure the expression of a subset of genes that were altered in response to *CYP2J2* knockdown. Figure 2.6 depicts the changes in the expression of *HMOX1, SCN1B, PSAT1, KCNA2, SCN5A,* and *GLTP* as assessed by qPCR. The first five genes had been identified as being up-regulated whereas GLTP was down-regulated based on the RNA-seq experiment and these changes were verified independently by qPCR.

Highly distinct transcriptional programs are activated in cardiomyocytes following CYP2J2 silencing

To better elucidate the transcriptional consequences of suppressing *CYP2J2* in human cardiomyocytes, we applied gene set enrichment analysis (GSEA) in order to systematically identify up and down-regulated pathways. Interrogating a large repertoire of canonical pathways and Gene Ontology categories, we observed that the predominant enrichment pattern was comprised of up-regulated processes (n = 360 gene sets, FDR < 0.05) with only one down-regulated pathway ("peptide chain elongation", FDR = 0.005) (complete list provided in Table 2.4). This finding suggests that silencing of *CYP2J2* promotes activation of a diverse set of compensatory programs. A network-based summary of the GSEA results is shown in Figure 2.7, in which enriched gene sets with significant overlap of members are connected to each other, revealing larger, functionally coherent biological modules. The most prominent modules thus identified were those populated by pathways involved in "Ion Channel Signaling", "Development", "Extracellular Matrix", and "Metabolism".

Inhibition of CYP2J2 expression modulates ion channel genes in cardiomyocytes

"Ion Channel Signaling" was the largest biological module identified in our network-based gene set analysis. We further investigated this module by focusing on the subset of its genes known as the "leading edge" that includes the most significant contributors to pathway enrichment based on differential expression. We limited the leading-edge genes to those differentially expressed at FDR < 0.01. We then performed network analysis to link these significantly expressed "leading edge" genes to one another based on their known direct interactions (Figure 2.8, details provided in Table 2.5). A number of key modulators of arrhythmogenesis and heart function were members of this network, including those associated with inherited cardiac conduction disorders such as SCN5A (Wang *et al.*, 1995), SCN1B (Watanabe *et al.*, 2008), KCND3 (Giudicessi *et al.*, 2011), FGF12 (Hennessey *et al.*, 2013), as well as genes linked to electrophysiological abnormalities and cardiac dysfunction such as KCNA1 (Si *et al.*, 2019), KCNA2 (Long *et al.*, 2017), CACNA1B (Yamada *et al.*, 2014), NOS2 (Zhang *et al.*, 2007), HSPA5 (Chen *et al.*, 2017), RHOA (Lauriol *et al.*, 2014), and CAMKK2(Watanabe *et al.*, 2014).

Upstream regulator analysis identifies key drivers of cardiomyocyte transcriptional response to CYP2J2 silencing

We next leveraged the unbiased nature of RNA-seq approach to identify upstream regulators by comparing the concordance between the direction of differential expression following *CYP*2J2 silencing with expected alterations in gene expression using curated knowledge bases. This analysis predicted that several master regulators of canonical pathways

were activated in response to inhibition of *CYP2J2* gene expression, with the most significant being HIF1-α, Sonic Hedgehog (SHH), TGF-β, Endothelin-1 (EDN1), and β-Catenin (CTNNB1) (*P*-value range: $1.2–7.9 \times 10^{-6}$, Table 2.6). Each of these upstream regulators has been implicated in cardiac development and remodeling, heart failure, myocyte injury and repair, consistent with our findings that developmental and extracellular matrix pathways are altered after *CYP2J2* suppression (Figure 2.7), and reduced protein expression of CYP2J2 in heart tissue of patients with cardiomyopathy (Figure 2.1).

Collectively, our results indicate that targeting *CYP2J2* profoundly alters diverse transcriptional programs and regulatory networks in human cardiomyocytes, and that many of these molecular effects are associated with deleterious cardiovascular consequences in animal models and human-based studies.

Action potential duration is prolonged in ventricular myocytes in the presence of MSPPOH

In the presence of the epoxygenase inhibitor MS-PPOH, we found that the APD of ventricular myocytes isolated from transgenic mice overexpressing cardiac CYP2J2 were prolonged. This prolongation specifically occurred during the later repolarization phase, approximately doubling the repolarization time of the cell (Figure 2.9).

K^+ ion channels are sensitive to EET antagonism or CYP2J2 inhibition

Finally, focusing on the "ion signaling" findings mentioned above, we looked at how CYP2J2 expression might affect potassium ion current in the ventricular cardiomyocytes of

human-CYP2J2 overexpressing transgenic mice. Following the baseline readings, ion density could be increased by treating the cells with pinacidil, an established K^+ channel activator. Following activation of these channels, ion current density was then decreased by concurrent treatment of the patched cells with either the CYP epoxygenase inhibitor MSPPOH or the CYP2J2 inhibitor grepafloxacin that ion current density decreased (Figure 2.10 and Figure 2.11).

2.4 Discussion

In this study, we first investigated CYP2J2 protein levels using quantitative proteomic mass spectrometry in ventricular tissue obtained from a cohort of individuals without heart disease (controls) and patients with cardiomyopathy. Subjects with cardiac disease had lower CYP2J2 protein content than controls. This observation is consistent with emerging evidence implicating CYP2J2 as a protective enzyme in cardiac homeostasis (Seubert *et al.*, 2004; Xiao *et al.*, 2004; Spiecker and Liao, 2006; Ke *et al.*, 2007; Zhang *et al.*, 2012; El-Serafi *et al.*, 2015). We therefore sought to determine the global effects of *CYP2J2* downregulation on adult human derived ventricular myocytes using siRNA to suppress expression, after confirming the ventricular identity of these cells using our RNASeq data. We found markers specific to ventricular myocytes robustly expressed while those more specific to atrial myocytes were detected only at very low levels. *GJA1* expression, for example was detected, but *GJA5*¸was not. Previous work using RT-PCR had also shown that *MYH7* was expressed, whereas *MYH6* could not be detected. Both *GJA1* and *MYH7* are ventricular forms of connexin and myosin heavy chain, respectively, while *GJA5* and *MYH6* expression are specific to atrial myocytes. We demonstrated that silencing *CYP2J2* expression profoundly decreased its enzymatic activity, and

by utilizing this model system, we further investigated the consequences of targeting the putative cardioprotective properties of CYP2J2 in the human heart.

We performed whole genome transcriptional profiling to elucidate the global effects of *CYP2J2* gene silencing in human adult-derived ventricular myocytes. A key finding of this study was the striking number of differentially altered genes and pathways following *CYP2J2* silencing, implying that this gene plays a central role in regulating cardiomyocyte homeostasis. *CYP2J2* has been demonstrated to have an important role in cardiovascular conditions, specifically as a protective enzyme against adverse cardiac events due to EET formation from arachidonic acid. However, our findings provide evidence for added multidimensional functions of *CYP2J2* in cardiac health beyond EET formation.

By leveraging pathway-based analyses, we identified a wide repertoire of processes influenced by *CYP2J2,* including those involved in "Ion Channel Signaling", "Development", "Extracellular Matrix", and "Metabolism". In the context of heart function and disease, changes in these broad categories are significant. Cardiac rhythmogenesis, for example, is due to sodium, potassium and calcium ion flow through specific ion channels. We found that knockdown of *CYP2J2* affected the expression of multiple sodium, potassium and calcium ion channels, several of which have been associated with the pathogenesis of cardiac dysrhythmias. The effects of chemical inhibition of CYP2J2 on potassium ion channel currents in transgenic mice overexpressing human CYP2J2 in cardiac tissue further support these findings. Independently, we were able to confirm detrimental effects of CYP2J2 inhibition on the action potential duration and the potassium currents using specific inhibitors of CYP2J2. Specifically, our findings show inhibition of CYP2J2 results in prolonged repolarization of ventricular action potential duration, likely due to decreased current flow through K^+ channels. One potential mechanism for this

observation may be through *CYP2J2*'s regulation of EET biosynthesis. Previous studies have demonstrated that EETs may act directly on ion channels, specifically L-type calcium channels and various potassium channels such as the K_{ATP} channel (Xiao *et al.*, 2004; Ke *et al.*, 2007). However, our interaction network analysis suggests that *CYP2J2* may also regulate other channel-associated proteins such as NOS2, HSPA5, RHOA, and CAMKK2 either through the formation of EETs or other undiscovered signaling molecules. Two other differentially up-regulated biological modules following CYP2J2 silencing were "Development" and "Extracellular Matrix". Alteration of programs involved in heart structure and remodeling represents a critical mechanism leading to many types of cardiac disorders such as cardiomyopathies, dysrhythmias, and congenital heart disease. Our gene set enrichment analysis identified multiple such pathways including "heart valve formation", "Glycosaminoglycan binding", "Integrin-1 pathway", "Syndecan-1 pathway", "Embryonic morphogenesis", and "Endocardial cushion development". Furthermore, when we performed upstream regulator and causal network analysis to identify the drivers of cardiomyocyte response to *CYP2J2* silencing, we identified several well-known orchestrators of tissue remodeling and development such as HIF1-α, SHH, TGF-β, EDN1, and CTNNB1 (β-Catenin). These master regulators have been implicated in cardiac dysfunction, development, and repair (Sakai *et al.*, 1996; Goddeeris *et al.*, 2007; Eckle *et al.*, 2008; Koitabashi *et al.*, 2011; Zhao *et al.*, 2018). Taken together, our findings highlight the widespread transcriptional landscape regulated by *CYP2J2* in human heart.

Despite its multifaceted role, it is important to note that when *CYP2J2* is knocked down, we do not observe increased cell death unless cardiomyocytes are exposed to external stressors such as reactive oxygen species, drug treatment or hypoxia (Evangelista *et al.*, 2018). It is

therefore likely that the deleterious functional consequences of *CYP2J2* suppression in cardiac cells require a second pathophysiological "hit" to manifest its protective effect.

Our study has several limitations. Most importantly, this study utilized an *in vitro* model to study the transcriptional consequences of silencing *CYP2J2*. While we utilized a well-characterized adult human cardiomyocyte system, extrapolating our findings to the intact heart remains to be demonstrated. While the main known function of *CYP2J2* is to form EETs from AA, there may likely be other unknown endogenous substrates that mediate the widespread effects we observed in the transcriptome of cardiac cells. Potential off-target effects of gene silencing are also a concern. The siRNAs used in these studies were validated to specifically knock down the target gene, however, there is a remote possibility that they may interact with other genes with downstream effects. Currently, the standard for ensuring specific target effects is to BLAST (https://blast.ncbi.nlm.nih.gov/Blast.cgi) the siRNA sequences to ensure specific alignment, all of which have been done by Origene as part of their internal validation and quality control (Origene, Rockville, MD).

We demonstrated that silencing of *CYP2J2* correlates with reduced protein expression, and thus reduced enzymatic activity. Changes in gene expression do not always correlate well with protein levels, and our reliance on transcriptomics in this study may not translate into functional effects in cardiomyocytes. However, the unbiased and comprehensive nature of RNA-seq provided a unique overview of cardiomyocyte programs regulated by CYP2J2 and allowed us to apply multi-level bioinformatics analyses that yielded several novel findings.

In summary, we demonstrated a central role played by *CYP2J2* in maintaining human cardiomyocyte homeostasis by regulating diverse transcriptional programs, particularly those

involved in rhythmogenesis and tissue remodeling. These altered pathways and their drivers can potentially serve as future druggable targets to restore health in cardiovascular diseases.

Tables

Table 2.1. Demographic data on ventricular tissue bank.

Tissue type	Source	Total (n)	Age Range (yrs.)	Mean Age (yrs.)	Male (n)	Female (n)
Control	BioIVT	17	65-78	70.8	10	7
Cases (all)	UWMC	27	20-70	54.6	19	8
Cases (Ischemic)	UWMC	16	34-64	51.6	12	4
Cases (Non-Ischemic)	UWMC	11	20-70	51.9	7	4
Cases (Diabetic)	UWMC	10	20-69	46.3	6	4
Cases (Non-Diabetic)	UWMC	17	29-70	58.4	13	4

Table 2.2. Mass spectrometric parameters for peptides used in CYP2J2 quantification in human cardiac tissue.

Protein	Peptide sequence	Light/Heavy	Parent ion	Product ion	Retention time (min)	CE (eV)	DP (V)
CYP2J2	VIGQGQQPSTAAR	Light	656.85	915.46	8.3	32.5	69
				730.38			
				602.33			
		Heavy	661.86	925.47			
				740.39			
				612.33			81.1
	EVTVDTTLAGYHLPK	Light	548.63	785.43	14.2	22.4	61.1
				714.39			
				608.32			
		Heavy	551.3	793.44			
				722.41			
				612.33			71.5
	LLDEVTYLEASK	Light	690.87	910.49	14.8	33.7	71.5
				811.42			
				710.37			
		Heavy	694.87	918.5			
				819.43			
				718.39			70.9

Table 2.3. List of top 25 differentially up- and down-regulated genes in CYP2J2-silenced cardiomyocytes.

Up-regulated				
Gene Symbol	**Gene Name**	**log_2[FoldChange]**	**P-value**	**FDR**
PSAT1	phosphoserine aminotransferase 1	1.828	3.67E-77	6.96E-73
PGAM1	phosphoglycerate mutase 1	1.575	4.62E-67	4.37E-63
CBX1	chromobox 1	1.157	6.65E-65	4.20E-61
SATB2	SATB homeobox 2	0.942	1.54E-60	7.27E-57
SHISA2	shisa family member 2	2.320	4.27E-60	1.62E-56
ZDHHC9	zinc finger DHHC-type containing 9	0.941	1.32E-59	4.17E-56
LIX1L	limb and CNS expressed 1 like	1.150	8.76E-58	2.37E-54
FUBP3	far upstream element binding protein 3	0.814	1.32E-49	3.13E-46
UBE3C	ubiquitin protein ligase E3C	0.953	1.23E-47	2.60E-44
HMOX1	heme oxygenase 1	1.828	7.48E-45	1.42E-41
MAPRE1	microtubule associated protein RP/EB family member 1	1.131	1.81E-42	3.12E-39
ST13	suppression of tumorigenicity 13	0.696	3.67E-40	5.79E-37
SLC13A4	solute carrier family 13 member 4	1.266	3.62E-38	5.27E-35
ENOPH1	enolase-phosphatase 1	0.957	1.61E-33	2.17E-30
ADCYAP1R1	ADCYAP receptor type I	1.948	1.53E-27	1.38E-24
DNAJB6	DnaJ heat shock protein family	0.605	2.75E-27	2.37E-24
EZR	ezrin	0.955	2.31E-24	1.83E-21
KCNA2	potassium voltage-gated channel subfamily A member 2	1.939	2.83E-24	2.10E-21
COL14A1	collagen type XIV alpha 1 chain	0.959	1.69E-23	1.19E-20
TNFRSF10B	TNF receptor superfamily member 10b	0.516	2.43E-23	1.64E-20
CRIM1	cysteine rich transmembrane BMP regulator 1	0.780	2.19E-22	1.43E-19
SYT2	synaptotagmin 2	1.254	4.69E-22	2.77E-19
MAF	MAF bZIP transcription factor	0.797	5.46E-21	3.04E-18
ABAT	4-aminobutyrate aminotransferase	0.766	6.84E-21	3.70E-18
IGF2BP1	insulin like growth factor 2 mRNA binding protein 1	0.408	8.42E-21	4.31E-18

Down-regulated				
Gene Symbol	**Gene Name**	**log_2[FoldChange]**	**P-value**	**FDR**
NEK9	NIMA related kinase 9	-0.492	1.31E-29	1.66E-26
GLTP	glycolipid transfer protein	-1.109	1.89E-29	2.24E-26
ZCCHC14	zinc finger CCHC-type containing 14	-0.576	2.76E-29	3.07E-26
DNAJC1	DnaJ heat shock protein family	-0.972	1.43E-28	1.50E-25
ARPC2	actin related protein 2/3 complex subunit 2	-0.797	6.28E-28	6.26E-25
PTPN21	protein tyrosine phosphatase, non-receptor type 21	-0.746	1.31E-27	1.24E-24
HMGN2	high mobility group nucleosomal binding domain 2	-0.625	1.28E-24	1.06E-21
HOXA10	homeobox A10	-0.557	2.89E-24	2.10E-21
CORO1C	coronin 1C	-0.685	2.49E-22	1.57E-19
ANXA1	annexin A1	-0.917	3.07E-22	1.87E-19
SIK2	salt inducible kinase 2	-0.536	2.96E-21	1.70E-18
RBM47	RNA binding motif protein 47	-0.831	7.83E-21	4.12E-18
ARL4C	ADP ribosylation factor like GTPase 4C	-0.790	2.59E-20	1.26E-17
DPY30	dpy-30, histone methyltransferase complex regulatory subunit	-0.861	4.00E-20	1.90E-17
ULK2	unc-51 like autophagy activating kinase 2	-0.649	4.87E-20	2.25E-17
DUSP16	dual specificity phosphatase 16	-0.684	1.82E-18	7.33E-16
STX3	syntaxin 3	-0.639	5.88E-18	2.23E-15
TGFBR2	transforming growth factor beta receptor 2	-0.874	9.71E-18	3.61E-15
SMIM10L1	small integral membrane protein 10 like 1	-0.754	4.70E-17	1.65E-14
TFDP1	transcription factor Dp-1	-0.414	9.21E-17	3.01E-14
BSPRY	B-box and SPRY domain containing	-1.529	1.41E-16	4.45E-14
CYP2J2	cytochrome P450 family 2 subfamily J member 2	-1.084	1.82E-16	5.67E-14
ACLY	ATP citrate lyase	-0.811	2.11E-16	6.45E-14
GTF2H1	general transcription factor IIH subunit 1	-0.907	1.40E-15	4.04E-13
SSH1	slingshot protein phosphatase 1	-0.520	1.41E-15	4.04E-13

Table 2.4. List of differentially up-regulated gene sets in *CYP2J2*-silenced cardiomyocytes (FDR < 0.05).

Gene Set Name	Number of members	FDR
GO_CATION_CHANNEL_COMPLEX	100	0
GO_PROTEINACEOUS_EXTRACELLULAR_MATRIX	241	0
GO_EXTRACELLULAR_MATRIX	286	0
GO_COLLAGEN_BINDING	48	0
GO_ENDOCARDIAL_CUSHION_DEVELOPMENT	30	0
GO_ENDOCARDIAL_CUSHION_MORPHOGENESIS	22	0
GO_CALCIUM_ION_BINDING	439	0
GO_CELL_FATE_COMMITMENT	173	0
NABA_CORE_MATRISOME	182	0
GO_EXOCYTIC_VESICLE_MEMBRANE	44	0
GO_VOLTAGE_GATED_CATION_CHANNEL_ACTIVITY	75	0
KEGG_NEUROACTIVE_LIGAND_RECEPTOR_INTERACTION	124	0
GO_TRANSPORTER_COMPLEX	190	7.01E-05
GO_MULTICELLULAR_ORGANISMAL_SIGNALING	83	7.51E-05
GO_VOLTAGE_GATED_ION_CHANNEL_ACTIVITY	113	8.09E-05
GO_POSITIVE_REGULATION_OF_KIDNEY_DEVELOPMENT	32	1.24E-04
GO_NEURON_FATE_COMMITMENT	54	1.32E-04
GO_CELL_FATE_SPECIFICATION	53	4.13E-04
NABA_MATRISOME_ASSOCIATED	370	5.03E-04
GO_VOLTAGE_GATED_POTASSIUM_CHANNEL_ACTIVITY	49	6.37E-04
GO_MESONEPHRIC_TUBULE_MORPHOGENESIS	46	6.76E-04
GO_TRANSMISSION_OF_NERVE_IMPULSE	33	7.08E-04
GO_REGULATION_OF_MORPHOGENESIS_OF_A_BRANCHING_STRUCTURE	41	8.42E-04
REACTOME_POTASSIUM_CHANNELS	61	8.79E-04
GO_POTASSIUM_CHANNEL_ACTIVITY	67	9.01E-04
GO_BRANCHING_INVOLVED_IN_URETERIC_BUD_MORPHOGENESIS	39	9.37E-04
GO_EXTRACELLULAR_STRUCTURE_ORGANIZATION	229	9.86E-04
GO_GATED_CHANNEL_ACTIVITY	188	1.22E-03
NABA_ECM_GLYCOPROTEINS	131	1.35E-03
GO_EXTRACELLULAR_MATRIX_STRUCTURAL_CONSTITUENT	50	1.36E-03
GO_EMBRYONIC_SKELETAL_SYSTEM_DEVELOPMENT	108	1.37E-03
REACTOME_GPCR_LIGAND_BINDING	165	1.38E-03
GO_ENDOCARDIAL_CUSHION_FORMATION	15	1.41E-03
HALLMARK_KRAS_SIGNALING_DN	116	1.45E-03
GO_POSITIVE_REGULATION_OF_VACUOLAR_TRANSPORT	14	1.50E-03
NABA_SECRETED_FACTORS	158	1.86E-03
GO_MYELIN_SHEATH	150	1.99E-03
GO_POTASSIUM_CHANNEL_COMPLEX	55	2.03E-03
GO_VOCALIZATION_BEHAVIOR	11	2.05E-03
GO_EPITHELIAL_TO_MESENCHYMAL_TRANSITION	50	2.11E-03
KEGG_ANTIGEN_PROCESSING_AND_PRESENTATION	46	2.11E-03
GO_DELAYED_RECTIFIER_POTASSIUM_CHANNEL_ACTIVITY	21	2.11E-03

GO_GLYCOSAMINOGLYCAN_BINDING	113	2.13E-03
REACTOME_VOLTAGE_GATED_POTASSIUM_CHANNELS	26	2.48E-03
GO_ANATOMICAL_STRUCTURE_MATURATION	31	2.49E-03
GO_MESONEPHROS_DEVELOPMENT	79	2.50E-03
GO_MESENCHYME_MORPHOGENESIS	37	2.53E-03
GO_REGULATION_OF_VACUOLAR_TRANSPORT	28	2.56E-03
GO_MAIN_AXON	42	2.56E-03
GO_G_PROTEIN_COUPLED_RECEPTOR_ACTIVITY	189	2.57E-03
GO_SKELETAL_SYSTEM_DEVELOPMENT	371	2.61E-03
GO_METALLOENDOPEPTIDASE_ACTIVITY	80	2.73E-03
GO_CARDIAC_CONDUCTION	58	2.84E-03
GO_COLLAGEN_TRIMER	54	2.86E-03
KEGG_ECM_RECEPTOR_INTERACTION	65	3.01E-03
NABA_ECM_REGULATORS	133	3.01E-03
GO_RESPONSE_TO_BMP	73	3.42E-03
GO_REGULATION_OF_POSTSYNAPTIC_MEMBRANE_POTENTIAL	37	4.13E-03
GO_REGULATION_OF_AMINE_TRANSPORT	39	4.16E-03
GO_PEPTIDYL_CYSTEINE_MODIFICATION	17	4.16E-03
GO_T_TUBULE	37	4.18E-03
GO_REGULATION_OF_CHONDROCYTE_DIFFERENTIATION	38	4.19E-03
GO_KIDNEY_MORPHOGENESIS	67	4.21E-03
GO_SARCOLEMMA	100	4.28E-03
GO_BRANCHING_MORPHOGENESIS_OF_AN_EPITHELIAL_TUBE	118	5.06E-03
REACTOME_EXTRACELLULAR_MATRIX_ORGANIZATION	63	5.07E-03
GO_CARDIAC_EPITHELIAL_TO_MESENCHYMAL_TRANSITION	22	5.11E-03
GO_CALCIUM_ION_REGULATED_EXOCYTOSIS_OF_NEUROTRANSMITTER	23	5.15E-03
GO_FEMALE_SEX_DIFFERENTIATION	90	5.26E-03
GO_SMOOTH_MUSCLE_CONTRACTION	33	5.30E-03
GO_GLIAL_CELL_FATE_COMMITMENT	10	5.55E-03
GO_HYALURONIC_ACID_BINDING	15	5.57E-03
GO_SPINAL_CORD_DEVELOPMENT	85	5.59E-03
GO_NEGATIVE_REGULATION_OF_CARTILAGE_DEVELOPMENT	18	5.74E-03
GO_REGULATION_OF_MESONEPHROS_DEVELOPMENT	20	6.15E-03
GO_POSITIVE_REGULATION_OF_TRANSMEMBRANE_RECEPTOR_PROTEIN_SERINE_THREONINE_KINASE_SIGNALING_PATHWAY	81	6.15E-03
GO_OSSIFICATION	205	6.19E-03
GO_EMBRYONIC_ORGAN_MORPHOGENESIS	238	6.23E-03
GO_HEART_VALVE_FORMATION	10	6.25E-03
HALLMARK_HEDGEHOG_SIGNALING	33	6.29E-03
GO_EXOCYTIC_VESICLE	115	6.32E-03
GO_EAR_DEVELOPMENT	156	6.32E-03
GO_HOMOPHILIC_CELL_ADHESION_VIA_PLASMA_MEMBRANE_ADHESION_MOLECULES	72	6.33E-03
GO_MORPHOGENESIS_OF_A_BRANCHING_STRUCTURE	143	6.36E-03
GO_EXTRACELLULAR_MATRIX_BINDING	39	6.43E-03
GO_NEURON_PROJECTION_GUIDANCE	176	6.46E-03
GO_POST_EMBRYONIC_MORPHOGENESIS	11	7.17E-03
GO_POTASSIUM_ION_TRANSPORT	91	7.21E-03

GO_RENAL_TUBULE_DEVELOPMENT	65	7.70E-03
GO_NODE_OF_RANVIER	11	7.74E-03
GO_SYNAPSE_PART	463	7.82E-03
GO_MHC_CLASS_II_PROTEIN_COMPLEX_BINDING	12	7.91E-03
GO_METAL_ION_TRANSMEMBRANE_TRANSPORTER_ACTIVITY	263	7.99E-03
GO_POSITIVE_REGULATION_OF_AMINE_TRANSPORT	19	8.07E-03
GO_REGULATION_OF_TRANSMEMBRANE_RECEPTOR_PROTEIN_SERINE_THREONINE_KINASE_SIGNALING_PATHWAY	164	8.31E-03
GO_CATION_CHANNEL_ACTIVITY	172	9.16E-03
GO_SKELETAL_SYSTEM_MORPHOGENESIS	170	9.94E-03
GO_RETINA_MORPHOGENESIS_IN_CAMERA_TYPE_EYE	32	9.99E-03
GO_SYNAPTIC_SIGNALING	268	1.00E-02
REACTOME_G_ALPHA_S_SIGNALLING_EVENTS	62	1.01E-02
GO_METANEPHROS_DEVELOPMENT	65	1.01E-02
GO_POSITIVE_REGULATION_OF_ION_TRANSPORT	158	1.01E-02
GO_REGULATION_OF_KIDNEY_DEVELOPMENT	44	1.01E-02
GO_NEPHRON_EPITHELIUM_DEVELOPMENT	77	1.01E-02
GO_CELL_CELL_ADHESION_VIA_PLASMA_MEMBRANE_ADHESION_MOLECULES	94	1.04E-02
GO_SODIUM_ION_TRANSMEMBRANE_TRANSPORT	56	1.07E-02
GO_RESPONSE_TO_IRON_ION	30	1.09E-02
REACTOME_COLLAGEN_FORMATION	48	1.09E-02
PID_INTEGRIN1_PATHWAY	56	1.12E-02
GO_SENSORY_ORGAN_MORPHOGENESIS	187	1.13E-02
GO_LOCOMOTORY_BEHAVIOR	130	1.14E-02
GO_MHC_PROTEIN_COMPLEX_BINDING	12	1.14E-02
KEGG_GLYCOLYSIS_GLUCONEOGENESIS	41	1.15E-02
GO_CELL_MORPHOGENESIS_INVOLVED_IN_DIFFERENTIATION	421	1.16E-02
GO_SEMAPHORIN_RECEPTOR_COMPLEX	11	1.16E-02
GO_POSITIVE_REGULATION_OF_MESONEPHROS_DEVELOPMENT	18	1.18E-02
GO_MUSCLE_SYSTEM_PROCESS	204	1.18E-02
GO_REGULATION_OF_BLOOD_PRESSURE	105	1.19E-02
GO_FEMALE_GENITALIA_DEVELOPMENT	11	1.19E-02
GO_REGULATION_OF_NEUROTRANSMITTER_LEVELS	138	1.20E-02
GO_DORSAL_SPINAL_CORD_DEVELOPMENT	13	1.21E-02
GO_MEMBRANE_DEPOLARIZATION_DURING_CARDIAC_MUSCLE_CELL_ACTION_POTENTIAL	12	1.22E-02
GO_NEGATIVE_REGULATION_OF_PLATELET_ACTIVATION	15	1.23E-02
GO_EXTRACELLULAR_MATRIX_COMPONENT	99	1.26E-02
GO_REGULATION_OF_EARLY_ENDOSOME_TO_LATE_ENDOSOME_TRANSPORT	16	1.31E-02
GO_REGULATION_OF_HEART_CONTRACTION	151	1.31E-02
GO_CELL_DIFFERENTIATION_IN_SPINAL_CORD	42	1.33E-02
GO_REGULATION_OF_CARTILAGE_DEVELOPMENT	51	1.40E-02
GO_FOREBRAIN_REGIONALIZATION	20	1.45E-02
GO_MESENCHYME_DEVELOPMENT	153	1.45E-02
GO_GLYCOPROTEIN_COMPLEX	14	1.46E-02
REACTOME_AMINE_LIGAND_BINDING_RECEPTORS	15	1.47E-02

GO_POST_ANAL_TAIL_MORPHOGENESIS	14	1.47E-02
GO_PEPTIDE_RECEPTOR_ACTIVITY	56	1.47E-02
GO_REGULATION_OF_BLOOD_CIRCULATION	198	1.47E-02
GO_METANEPHRIC_NEPHRON_MORPHOGENESIS	17	1.48E-02
GO_DORSAL_VENTRAL_PATTERN_FORMATION	74	1.49E-02
GO_ORGAN_MATURATION	15	1.49E-02
GO_SULFATION	11	1.50E-02
GO_KIDNEY_EPITHELIUM_DEVELOPMENT	108	1.50E-02
REACTOME_CLASS_B_2_SECRETIN_FAMILY_RECEPTORS	55	1.50E-02
GO_PASSIVE_TRANSMEMBRANE_TRANSPORTER_ACTIVITY	271	1.50E-02
GO_REGULATION_OF_SYSTEM_PROCESS	337	1.52E-02
GO_ANATOMICAL_STRUCTURE_ARRANGEMENT	16	1.52E-02
GO_TRANSFERASE_ACTIVITY_TRANSFERRING_NITROGENOUS_GROUPS	14	1.53E-02
GO_HEPARIN_BINDING	87	1.53E-02
REACTOME_GPCR_DOWNSTREAM_SIGNALING	251	1.53E-02
GO_OSTEOBLAST_DIFFERENTIATION	109	1.56E-02
HALLMARK_EPITHELIAL_MESENCHYMAL_TRANSITION	159	1.56E-02
GO_REGULATION_OF_CATECHOLAMINE_SECRETION	22	1.56E-02
GO_AXON	323	1.57E-02
GO_REGIONALIZATION	257	1.57E-02
GO_VOLTAGE_GATED_CALCIUM_CHANNEL_COMPLEX	23	1.61E-02
GO_EMBRYONIC_SKELETAL_SYSTEM_MORPHOGENESIS	83	1.61E-02
NABA_COLLAGENS	38	1.62E-02
GO_HEART_VALVE_DEVELOPMENT	28	1.63E-02
GO_METANEPHRIC_NEPHRON_DEVELOPMENT	22	1.65E-02
GO_METANEPHRIC_RENAL_VESICLE_MORPHOGENESIS	9	1.65E-02
GO_MEMBRANE_DEPOLARIZATION_DURING_ACTION_POTENTIAL	26	1.66E-02
GO_G_PROTEIN_COUPLED_RECEPTOR_SIGNALING_PATHWAY	359	1.66E-02
GO_PRESYNAPSE	214	1.66E-02
GO_PRESYNAPTIC_MEMBRANE	40	1.66E-02
GO_SYNAPTIC_MEMBRANE	185	1.67E-02
GO_LAMININ_BINDING	26	1.67E-02
GO_VENTRAL_SPINAL_CORD_DEVELOPMENT	38	1.77E-02
KEGG_GLYCINE_SERINE_AND_THREONINE_METABOLISM	23	1.77E-02
GO_NEPHRON_DEVELOPMENT	95	1.80E-02
GO_CELL_CELL_SIGNALING	451	1.81E-02
GO_PYRUVATE_METABOLIC_PROCESS	48	1.83E-02
GO_CARTILAGE_DEVELOPMENT	122	1.83E-02
REACTOME_CLASS_A1_RHODOPSIN_LIKE_RECEPTORS	103	1.98E-02
NABA_PROTEOGLYCANS	13	1.98E-02
GO_REGULATION_OF_PATHWAY_RESTRICTED_SMAD_PROTEIN_PHOSPHORYLATION	46	1.98E-02
GO_TAXIS	310	1.99E-02
GO_TELENCEPHALON_REGIONALIZATION	11	1.99E-02
GO_BONE_DEVELOPMENT	129	1.99E-02
KEGG_CALCIUM_SIGNALING_PATHWAY	125	1.99E-02
GO_MUSCLE_CONTRACTION	166	2.00E-02
GO_CALCIUM_CHANNEL_COMPLEX	38	2.05E-02

BIOCARTA_UCALPAIN_PATHWAY	17	2.06E-02
GO_CELL_FATE_DETERMINATION	33	2.06E-02
GO_NEURONAL_CELL_BODY_MEMBRANE	14	2.07E-02
GO_POTASSIUM_ION_HOMEOSTASIS	12	2.08E-02
GO_ADULT_BEHAVIOR	98	2.17E-02
REACTOME_SIGNALING_BY_GPCR	327	2.18E-02
GO_DIENCEPHALON_DEVELOPMENT	57	2.19E-02
GO_CARDIAC_MUSCLE_CELL_ACTION_POTENTIAL	28	2.23E-02
GO_MODULATION_OF_SYNAPTIC_TRANSMISSION	217	2.24E-02
GO_POSITIVE_REGULATION_OF_ASTROCYTE_DIFFERENTIATION	10	2.25E-02
GO_SODIUM_CHANNEL_COMPLEX	10	2.25E-02
GO_NEURON_FATE_SPECIFICATION	24	2.25E-02
GO_AUTONOMIC_NERVOUS_SYSTEM_DEVELOPMENT	32	2.26E-02
GO_POSITIVE_REGULATION_OF_PATHWAY_RESTRICTED_SMAD_PROTEIN_PHOSPHORYLATION	36	2.26E-02
REACTOME_PLATELET_HOMEOSTASIS	59	2.28E-02
GO_RENAL_VESICLE_DEVELOPMENT	12	2.33E-02
GO_SMOOTH_MUSCLE_CELL_DIFFERENTIATION	27	2.34E-02
GO_EAR_MORPHOGENESIS	94	2.35E-02
GO_VOLTAGE_GATED_SODIUM_CHANNEL_ACTIVITY	13	2.39E-02
GO_POSITIVE_REGULATION_OF_SKELETAL_MUSCLE_TISSUE_DEVELOPMENT	22	2.41E-02
GO_REGULATION_OF_CELL_PROJECTION_SIZE	8	2.43E-02
GO_REGULATION_OF_ION_TRANSPORT	386	2.46E-02
GO_NEUROTRANSMITTER_TRANSPORT	105	2.51E-02
GO_EMBRYONIC_ORGAN_DEVELOPMENT	345	2.54E-02
GO_AXON_PART	164	2.58E-02
GO_BEHAVIOR	369	2.58E-02
GO_VOLTAGE_GATED_SODIUM_CHANNEL_COMPLEX	9	2.59E-02
REACTOME_INTERACTION_BETWEEN_L1_AND_ANKYRINS	17	2.59E-02
GO_PRESYNAPTIC_PROCESS_INVOLVED_IN_SYNAPTIC_TRANSMISSION	83	2.59E-02
GO_NEPHRON_TUBULE_FORMATION	12	2.59E-02
GO_MHC_PROTEIN_COMPLEX	17	2.60E-02
KEGG_GRAFT_VERSUS_HOST_DISEASE	16	2.60E-02
GO_REGULATION_OF_HEART_RATE_BY_CARDIAC_CONDUCTION	23	2.60E-02
GO_CARDIAC_SEPTUM_MORPHOGENESIS	45	2.60E-02
REACTOME_GLUCAGON_TYPE_LIGAND_RECEPTORS	18	2.60E-02
GO_NERVE_DEVELOPMENT	57	2.60E-02
GO_CELLULAR_POTASSIUM_ION_HOMEOSTASIS	10	2.61E-02
GO_REPLACEMENT_OSSIFICATION	23	2.61E-02
GO_BONE_MORPHOGENESIS	67	2.61E-02
GO_OXIDOREDUCTASE_ACTIVITY_ACTING_ON_THE_CH_NH2_GROUP_OF_DONORS	13	2.68E-02
GO_SEX_DIFFERENTIATION	199	2.69E-02
GO_SYNAPSE_ORGANIZATION	111	2.69E-02
GO_ADENYLATE_CYCLASE_MODULATING_G_PROTEIN_COUPLED_RECEPTOR_SIGNALING_PATHWAY	76	2.71E-02
GO_REGULATION_OF_ENDOTHELIAL_CELL_DIFFERENTIATION	20	2.71E-02

GO_ACTION_POTENTIAL	63	2.71E-02
GO_SENSORY_PERCEPTION_OF_PAIN	46	2.74E-02
PID_SYNDECAN_1_PATHWAY	37	2.74E-02
GO_CELL_FATE_COMMITMENT_INVOLVED_IN_FORMATION_OF_PRIMARY_GERM_LAYER	21	2.74E-02
GO_PATTERN_SPECIFICATION_PROCESS	346	2.75E-02
GO_NEGATIVE_REGULATION_OF_CHONDROCYTE_DIFFERENTIATION	13	2.75E-02
GO_EYE_MORPHOGENESIS	103	2.76E-02
GO_EPITHELIAL_TO_MESENCHYMAL_TRANSITION_INVOLVED_IN_ENDOCARDIAL_CUSHION_FORMATION	11	2.79E-02
REACTOME_CYTOSOLIC_SULFONATION_OF_SMALL_MOLECULES	9	2.81E-02
GO_PERIKARYON	67	2.81E-02
GO_G_PROTEIN_COUPLED_AMINE_RECEPTOR_ACTIVITY	20	2.82E-02
REACTOME_OTHER_SEMAPHORIN_INTERACTIONS	12	2.86E-02
GO_POSITIVE_REGULATION_OF_ENDOTHELIAL_CELL_DIFFERENTIATION	10	2.87E-02
GO_SINGLE_ORGANISM_BEHAVIOR	279	2.87E-02
GO_CELL_MORPHOGENESIS_INVOLVED_IN_NEURON_DIFFERENTIATION	299	2.87E-02
GO_SODIUM_ION_TRANSMEMBRANE_TRANSPORTER_ACTIVITY	78	2.91E-02
GO_NEGATIVE_REGULATION_OF_AMINE_TRANSPORT	16	2.93E-02
GO_SPHINGOLIPID_MEDIATED_SIGNALING_PATHWAY	9	2.98E-02
KEGG_DILATED_CARDIOMYOPATHY	67	3.04E-02
GO_NEGATIVE_REGULATION_OF_COAGULATION	29	3.12E-02
GO_POSITIVE_REGULATION_OF_NEURAL_PRECURSOR_CELL_PROLIFERATION	33	3.12E-02
GO_POSITIVE_REGULATION_OF_NERVOUS_SYSTEM_DEVELOPMENT	347	3.13E-02
GO_TRABECULA_FORMATION	18	3.13E-02
GO_LIPOPROTEIN_PARTICLE_RECEPTOR_ACTIVITY	12	3.14E-02
GO_ENDOCRINE_SYSTEM_DEVELOPMENT	98	3.14E-02
GO_CONNECTIVE_TISSUE_DEVELOPMENT	157	3.14E-02
GO_VOLTAGE_GATED_CALCIUM_CHANNEL_ACTIVITY	24	3.14E-02
GO_POSITIVE_REGULATION_OF_EPITHELIAL_CELL_PROLIFERATION	119	3.14E-02
GO_NEURAL_RETINA_DEVELOPMENT	36	3.15E-02
GO_SULFUR_COMPOUND_BINDING	152	3.18E-02
GO_MULTICELLULAR_ORGANISMAL_RESPONSE_TO_STRESS	44	3.23E-02
GO_GLUTAMATE_RECEPTOR_SIGNALING_PATHWAY	27	3.23E-02
GO_CAMERA_TYPE_EYE_MORPHOGENESIS	78	3.25E-02
GO_GROWTH_FACTOR_ACTIVITY	99	3.25E-02
GO_NEURON_PROJECTION_MORPHOGENESIS	328	3.26E-02
GO_REGULATION_OF_CALCIUM_ION_DEPENDENT_EXOCYTOSIS	62	3.26E-02
GO_CENTRAL_NERVOUS_SYSTEM_NEURON_DIFFERENTIATION	133	3.27E-02
GO_FORELIMB_MORPHOGENESIS	34	3.29E-02
GO_DEVELOPMENTAL_INDUCTION	23	3.31E-02
GO_CRANIAL_NERVE_DEVELOPMENT	35	3.34E-02
GO_MESENCHYMAL_CELL_DIFFERENTIATION	113	3.35E-02
GO_SEMAPHORIN_PLEXIN_SIGNALING_PATHWAY_INVOLVED_IN_NEURON_PROJECTION_GUIDANCE	13	3.36E-02
GO_ATRIOVENTRICULAR_VALVE_DEVELOPMENT	17	3.36E-02

GO_POSITIVE_REGULATION_OF_METANEPHROS_DEVELOPMENT	10	3.36E-02
GO_POSITIVE_REGULATION_OF_SODIUM_ION_TRANSPORT	30	3.36E-02
GO_REGULATION_OF_DOPAMINE_SECRETION	12	3.36E-02
GO_EMBRYONIC_FORELIMB_MORPHOGENESIS	28	3.37E-02
GO_LYMPHOCYTE_MIGRATION	17	3.38E-02
GO_LUNG_ALVEOLUS_DEVELOPMENT	35	3.42E-02
GO_PLASMA_MEMBRANE_PROTEIN_COMPLEX	336	3.43E-02
GO_REGULATION_OF_TRANSMEMBRANE_TRANSPORT	281	3.43E-02
GO_POSITIVE_REGULATION_OF_PROTEIN_BINDING	67	3.44E-02
REACTOME_GLYCOLYSIS	24	3.44E-02
GO_POSITIVE_REGULATION_OF_NEURON_DIFFERENTIATION	258	3.50E-02
GO_BASEMENT_MEMBRANE	78	3.50E-02
GO_RESPONSE_TO_NICOTINE	32	3.51E-02
GO_NAD_METABOLIC_PROCESS	41	3.51E-02
GO_MIDGUT_DEVELOPMENT	12	3.52E-02
GO_REGULATION_OF_TRANSCRIPTION_INVOLVED_IN_CELL_FATE_COMMITMENT	16	3.52E-02
GO_ODONTOGENESIS	85	3.53E-02
GO_LOW_DENSITY_LIPOPROTEIN_RECEPTOR_ACTIVITY	10	3.54E-02
PID_INTEGRIN_A9B1_PATHWAY	17	3.56E-02
GO_SECRETORY_GRANULE_LUMEN	42	3.56E-02
GO_POSTSYNAPSE	289	3.57E-02
GO_CELL_SURFACE_RECEPTOR_SIGNALING_PATHWAY_INVOLVED_IN_CELL_CELL_SIGNALING	45	3.64E-02
GO_CIRCULATORY_SYSTEM_PROCESS	242	3.67E-02
GO_RESPONSE_TO_PROSTAGLANDIN	23	3.73E-02
GO_PHASIC_SMOOTH_MUSCLE_CONTRACTION	10	3.73E-02
GO_CELLULAR_RESPONSE_TO_CADMIUM_ION	7	3.73E-02
GO_POSITIVE_REGULATION_OF_STEROL_TRANSPORT	15	3.73E-02
GO_ADENYLATE_CYCLASE_ACTIVATING_G_PROTEIN_COUPLED_RECEPTOR_SIGNALING_PATHWAY	36	3.74E-02
GO_DEVELOPMENTAL_MATURATION	142	3.74E-02
GO_NEUROPEPTIDE_BINDING	10	3.74E-02
GO_PANCREAS_DEVELOPMENT	59	3.80E-02
GO_CARDIAC_MUSCLE_CELL_CONTRACTION	22	3.84E-02
GO_POSITIVE_REGULATION_OF_AMINO_ACID_TRANSPORT	10	3.86E-02
GO_POSITIVE_REGULATION_OF_NEURON_PROJECTION_DEVELOPMENT	207	3.86E-02
GO_AMIDE_TRANSMEMBRANE_TRANSPORTER_ACTIVITY	10	3.87E-02
GO_SYNAPTIC_VESICLE_RECYCLING	22	3.89E-02
GO_SODIUM_CHANNEL_ACTIVITY	21	3.89E-02
GO_EMBRYONIC_MORPHOGENESIS	458	3.98E-02
GO_ENDOCHONDRAL_BONE_MORPHOGENESIS	41	3.98E-02
GO_ADRENAL_GLAND_DEVELOPMENT	18	3.98E-02
GO_ATRIOVENTRICULAR_VALVE_MORPHOGENESIS	15	3.99E-02
GO_CELLULAR_RESPONSE_TO_VASCULAR_ENDOTHELIAL_GROWTH_FACTOR_STIMULUS	27	4.00E-02
GO_CELL_SUBSTRATE_ADHESION	136	4.02E-02
GO_POSITIVE_REGULATION_OF_PROTEIN_TYROSINE_KINASE_ACTIVITY	27	4.03E-02

GO_CELL_SURFACE	458	4.04E-02
REACTOME_FACILITATIVE_NA_INDEPENDENT_GLUCOSE_TRANSPORTERS	9	4.10E-02
GO_DENDRITE_DEVELOPMENT	67	4.11E-02
GO_MONOVALENT_INORGANIC_CATION_TRANSMEMBRANE_TRANSPORTER_ACTIVITY2	27	4.13E-02
GO_REGULATION_OF_SYNAPSE_ASSEMBLY	50	4.23E-02
GO_HINDLIMB_MORPHOGENESIS	32	4.24E-02
KEGG_ASTHMA	13	4.27E-02
REACTOME_NEURONAL_SYSTEM	192	4.27E-02
GO_APOLIPOPROTEIN_BINDING	11	4.27E-02
GO_INORGANIC_ION_TRANSMEMBRANE_TRANSPORT	380	4.27E-02
GO_METENCEPHALON_DEVELOPMENT	79	4.39E-02
GO_SERTOLI_CELL_DIFFERENTIATION	13	4.39E-02
GO_HINDBRAIN_DEVELOPMENT	109	4.40E-02
GO_METAL_ION_TRANSPORT	376	4.41E-02
GO_HORMONE_ACTIVITY	36	4.41E-02
GO_RECEPTOR_SERINE_THREONINE_KINASE_BINDING	11	4.42E-02
GO_PHOSPHOLIPASE_C_ACTIVATING_G_PROTEIN_COUPLED_RECEPTOR_SIGNALING_PATHWAY	42	4.42E-02
KEGG_ALLOGRAFT_REJECTION	19	4.42E-02
GO_RESPONSE_TO_GROWTH_FACTOR	384	4.45E-02
GO_REGULATION_OF_ENDOTHELIAL_CELL_PROLIFERATION	77	4.46E-02
GO_UROGENITAL_SYSTEM_DEVELOPMENT	247	4.52E-02
GO_REGULATION_OF_METAL_ION_TRANSPORT	214	4.53E-02
GO_MOTOR_NEURON_AXON_GUIDANCE	27	4.53E-02
GO_REGULATION_OF_PROTEIN_BINDING	152	4.54E-02
GO_SERINE_TYPE_ENDOPEPTIDASE_INHIBITOR_ACTIVITY	36	4.55E-02
GO_ARTERY_MORPHOGENESIS	43	4.56E-02
GO_REGULATION_OF_SYNAPSE_STRUCTURE_OR_ACTIVITY	165	4.60E-02
GO_NEGATIVE_REGULATION_OF_SMOOTH_MUSCLE_CONTRACTION	14	4.61E-02
GO_MESENCHYMAL_TO_EPITHELIAL_TRANSITION	12	4.61E-02
GO_RESPIRATORY_BURST	7	4.61E-02
GO_SODIUM_ION_TRANSPORT	88	4.68E-02
GO_PROTEIN_FOLDING_IN_ENDOPLASMIC_RETICULUM	8	4.68E-02
GO_CHROMOCENTER	13	4.68E-02
GO_REGULATION_OF_ODONTOGENESIS_OF_DENTIN_CONTAINING_TOOTH	8	4.69E-02
REACTOME_SEMAPHORIN_INTERACTIONS	59	4.69E-02
GO_URETER_DEVELOPMENT	11	4.70E-02
GO_PROTEIN_LIPID_COMPLEX_BINDING	13	4.76E-02
GO_PLATELET_DERIVED_GROWTH_FACTOR_BINDING	9	4.77E-02
GO_SYNAPSE_ASSEMBLY	47	4.78E-02
GO_CYCLIC_NUCLEOTIDE_MEDIATED_SIGNALING	33	4.78E-02
GO_ION_CHANNEL_BINDING	91	4.78E-02
GO_PROSTATE_GLAND_MORPHOGENESIS	17	4.81E-02
GO_TRANSPORT_VESICLE_MEMBRANE	116	4.81E-02
REACTOME_AXON_GUIDANCE	215	4.81E-02

GO_REGULATION_OF_AXON_GUIDANCE	34	4.87E-02
PID_BETA_CATENIN_NUC_PATHWAY	68	4.87E-02
GO_POSITIVE_REGULATION_OF_ENDOTHELIAL_CELL_PROLIFERATION	55	4.91E-02
GO_COCHLEA_DEVELOPMENT	28	4.96E-02
GO_REGULATION_OF_OSSIFICATION	137	4.97E-02
GO_VENTRICULAR_SEPTUM_MORPHOGENESIS	25	4.99E-02

Table 2.5. List of "Ion Channeling Signaling" interaction network members upregulated in *CYP2J2*-silenced cardiomyocytes.

Gene Symbol	Gene Name	Location	Family
ASPH	aspartate beta-hydroxylase	Cytoplasm	enzyme
ATP1A3	ATPase Na+/K+ transporting subunit alpha 3	Plasma Membrane	transporter
ATP1B2	ATPase Na+/K+ transporting subunit beta 2	Plasma Membrane	transporter
ATP5PB	ATP synthase peripheral stalk-membrane subunit b	Cytoplasm	transporter
CA2	carbonic anhydrase 2	Cytoplasm	enzyme
CACNA1B	calcium voltage-gated channel subunit alpha1 B	Plasma Membrane	ion channel
CALU	calumenin	Cytoplasm	other
CAMKK2	calcium/calmodulin dependent protein kinase kinase 2	Cytoplasm	kinase
CANX	calnexin	Cytoplasm	other
CHRM4	cholinergic receptor muscarinic 4	Plasma Membrane	G-protein coupled receptor
CNTNAP1	contactin associated protein 1	Plasma Membrane	other
CNTNAP2	contactin associated protein like 2	Plasma Membrane	other
CPLX1	complexin 1	Plasma Membrane	transporter
CRTAC1	cartilage acidic protein 1	Extracellular Space	other
DACT1	dishevelled binding antagonist of beta catenin 1	Cytoplasm	other
DAG1	dystroglycan 1	Plasma Membrane	transmembrane receptor
DKK3	dickkopf WNT signaling pathway inhibitor 3	Extracellular Space	cytokine

EFEMP1	EGF containing fibulin extracellular matrix protein 1	Extracellular Space	enzyme
EZR	ezrin	Plasma Membrane	other
FBLN5	fibulin 5	Extracellular Space	other
FBN1	fibrillin 1	Extracellular Space	other
FGF12	fibroblast growth factor 12	Extracellular Space	other
GABBR2	gamma-aminobutyric acid type B receptor subunit 2	Plasma Membrane	G-protein coupled receptor
GFPT2	glutamine-fructose-6-phosphate transaminase 2	Cytoplasm	enzyme
GNAO1	G protein subunit alpha o1	Plasma Membrane	enzyme
HAP1	huntingtin associated protein 1	Cytoplasm	other
HSPA5	heat shock protein family A (Hsp70) member 5	Cytoplasm	enzyme
ITGA8	integrin subunit alpha 8	Plasma Membrane	other
KALRN	kalirin RhoGEF kinase	Cytoplasm	kinase
KCNA1	potassium voltage-gated channel subfamily A member 1	Plasma Membrane	ion channel
KCNA2	potassium voltage-gated channel subfamily A member 2	Plasma Membrane	ion channel
KCNC1	potassium voltage-gated channel subfamily C member 1	Plasma Membrane	ion channel
KCNC3	potassium voltage-gated channel subfamily C member 3	Plasma Membrane	ion channel
KCND3	potassium voltage-gated channel subfamily D member 3	Plasma Membrane	ion channel
KCNIP3	potassium voltage-gated channel interacting protein 3	Nucleus	transcription regulator
KCNMA1	potassium calcium-activated channel subfamily M alpha 1	Plasma Membrane	ion channel

LRP4	LDL receptor related protein 4	Extracellular Space	other
NFASC	neurofascin	Plasma Membrane	other
NOS2	nitric oxide synthase 2	Cytoplasm	enzyme
OPRD1	opioid receptor delta 1	Plasma Membrane	G-protein coupled receptor
P2RX2	purinergic receptor P2X 2	Plasma Membrane	ion channel
PLCB2	phospholipase C beta 2	Cytoplasm	enzyme
PTCH1	patched 1	Plasma Membrane	transmembrane receptor
RAB3B	RAB3B, member RAS oncogene family	Cytoplasm	enzyme
RASGRF1	Ras protein specific guanine nucleotide releasing factor 1	Cytoplasm	other
RHOA	ras homolog family member A	Cytoplasm	enzyme
SCN1B	sodium voltage-gated channel beta subunit 1	Plasma Membrane	ion channel
SCN2A	sodium voltage-gated channel alpha subunit 2	Plasma Membrane	ion channel
SCN5A	sodium voltage-gated channel alpha subunit 5	Plasma Membrane	ion channel
SGCB	sarcoglycan beta	Plasma Membrane	other
SGK1	serum/glucocorticoid regulated kinase 1	Cytoplasm	kinase
SHISA7	shisa family member 7	Plasma Membrane	other
SLIT2	slit guidance ligand 2	Extracellular Space	other
SNAP25	synaptosome associated protein 25	Plasma Membrane	transporter
SPARC	secreted protein acidic and cysteine rich	Extracellular Space	other
STX1B	syntaxin 1B	Plasma Membrane	other

SULF2	sulfatase 2	Plasma Membrane	enzyme
SV2A	synaptic vesicle glycoprotein 2A	Cytoplasm	transporter
SYT2	synaptotagmin 2	Cytoplasm	transporter
SYT6	synaptotagmin 6	Cytoplasm	transporter
THBD	thrombomodulin	Plasma Membrane	transmembrane receptor
VCAN	versican	Extracellular Space	other
YWHAB	tyrosine 3-monooxygenase/tryptophan 5-monooxygenase activation protein beta	Cytoplasm	transcription regulator

Table 2.6. List of the most significant upstream regulators predicted to be activated in CYP2J2-silenced cardiomyocytes.

Upstream Regulator	Molecule Type	Predicted Activation State	Activation z-score	P-value
HIF1A	transcription regulator	Activated	3.731	1.22E-06
SHH	peptidase	Activated	2.393	2.93E-06
TGFB1	growth factor	Activated	2.029	4.91E-06
EDN1	cytokine	Activated	2.129	7.23E-06
CTNNB1	transcription regulator	Activated	3.73	7.89E-06

Figures & Figure Legends

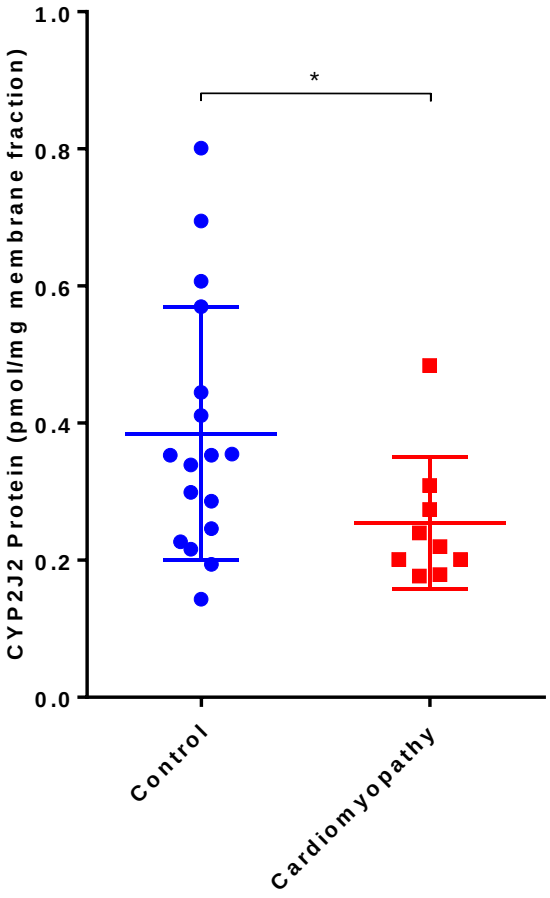

Figure 2.1. CYP2J2 protein content in ventricular tissue of Control (n = 17) and patients with cardiomyopathy (n = 9) as determined by protein mass spectrometry outlined in the methods section. CYP2J2 protein levels are significantly lower ($p < 0.05$) in cardiac tissues of individuals with non-ischemic cardiomyopathy compared to subjects with no known heart disease. *$p < 0.05$

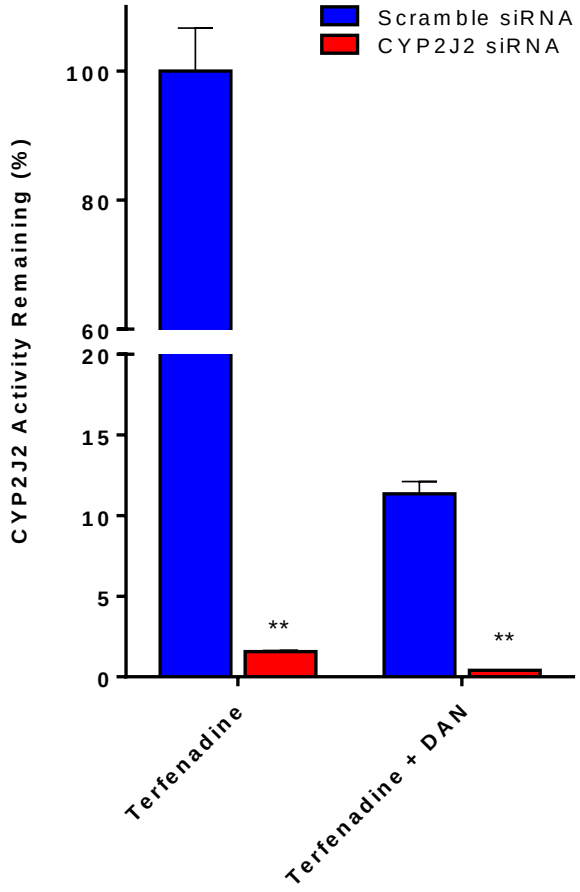

Figure 2.2. Relative mass spectrometric quantification of CYP2J2 activity in cells treated with either scrambled or CYP2J2 siRNA. Silencing with CYP2J2 siRNA for 72 hours significantly decreases ($p < 0.001$) CYP2J2 protein activity, as measured by terfenadine metabolism. In cells treated with CYP2J2 siRNA, activity is almost non-existent with very little hydroxy terfenadine detectable. Danazol, a known CYP2J2 inhibitor, was used to ascertain that the activity observed as due to CYP2J2, decreasing hydroxy terfenadine formation in scramble siRNA and CYP2J2 siRNA treated cells by over 90%. ** $p < 0.01$.

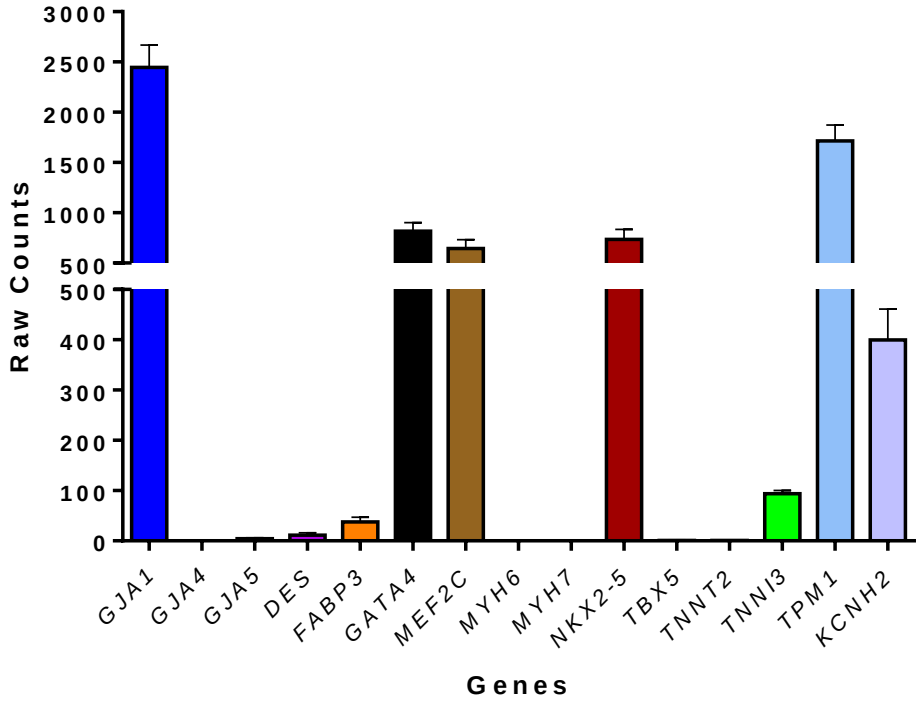

Figure 2.3. Cardiac marker genes identified in human cardiomyocyte cells using RNA-seq. Data presented are the average raw RNA-Seq counts of three biological triplicates. Cells were grown using Celprogen protocols and untreated in any way.

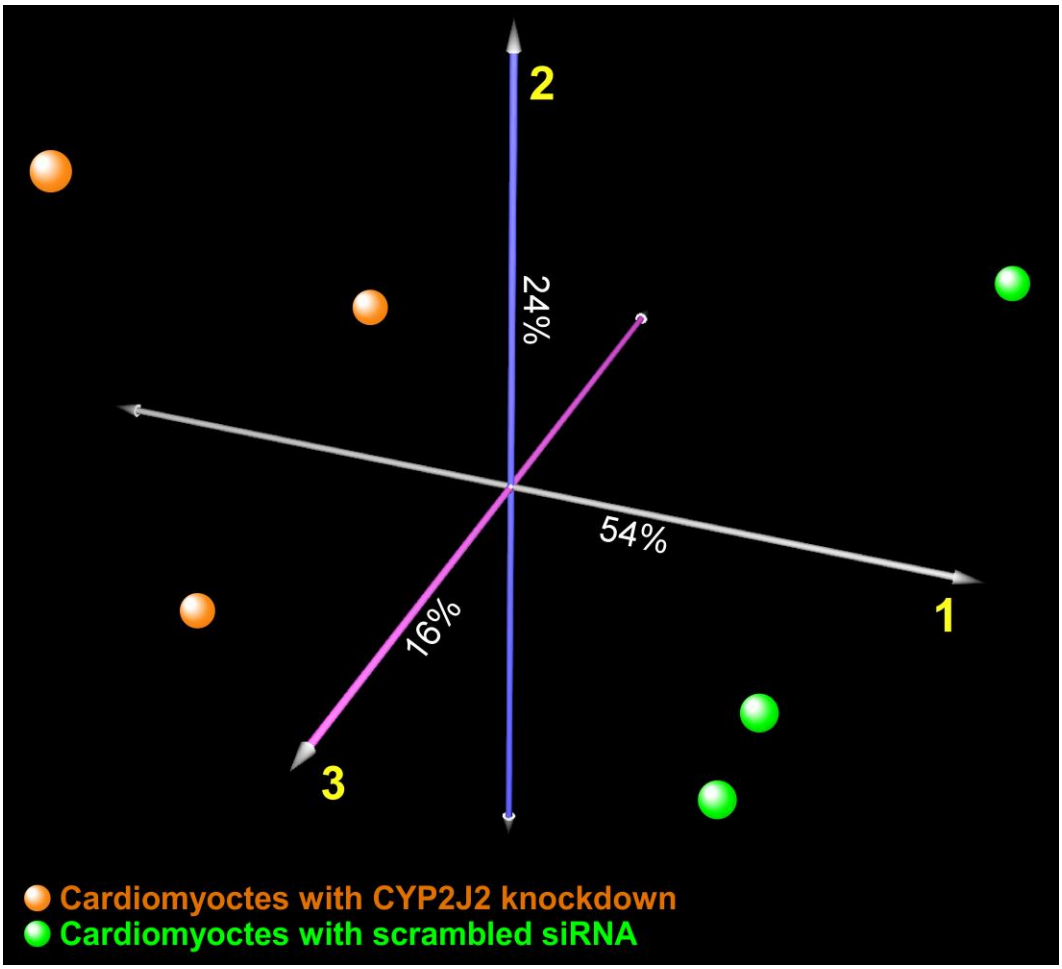

Figure 2.4. Multidimensional scaling using correspondence analysis of human cardiomyocyte transcriptome in CYP2J2-silenced samples (n = 3, orange spheres) and scrambled siRNA controls (n = 3, green spheres) demonstrates distinct segregation between the two conditions. The percentage of the overall gene expression variability captured by each orthogonal axis is shown, with the two experimental groups separating most prominently across the first component.

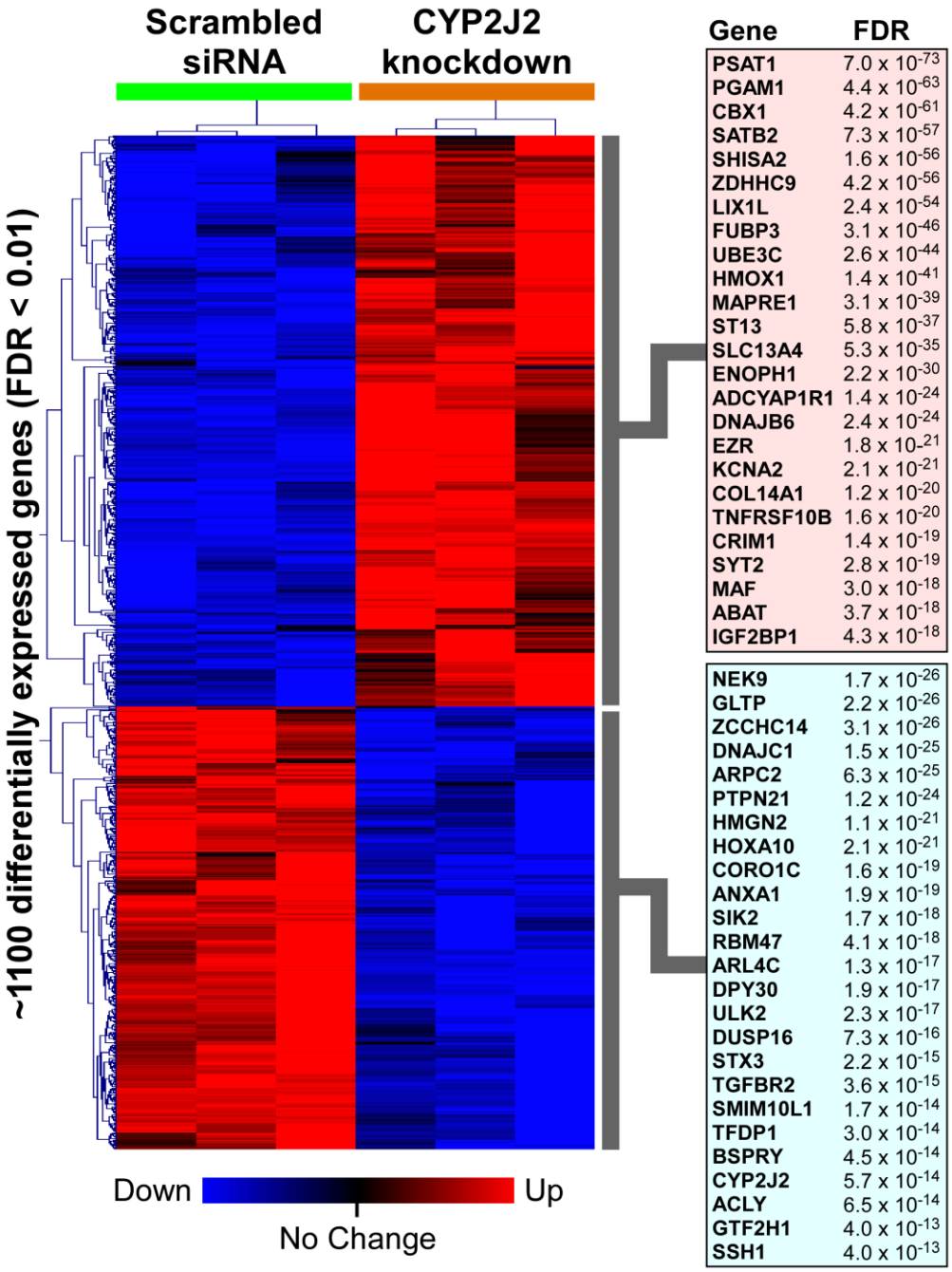

Figure 2.5. Hierarchical cluster analysis of approximately 1,100 differentially expressed genes following *CYP2J2* knockdown in human cardiomyocytes is shown as a heatmap. The top 25 up- and down-regulated genes have been labeled (Table 2.2). Note that, as expected, *CYP2J2* expression is significantly suppressed in the silenced group (FDR 5.7×10^{-14}).

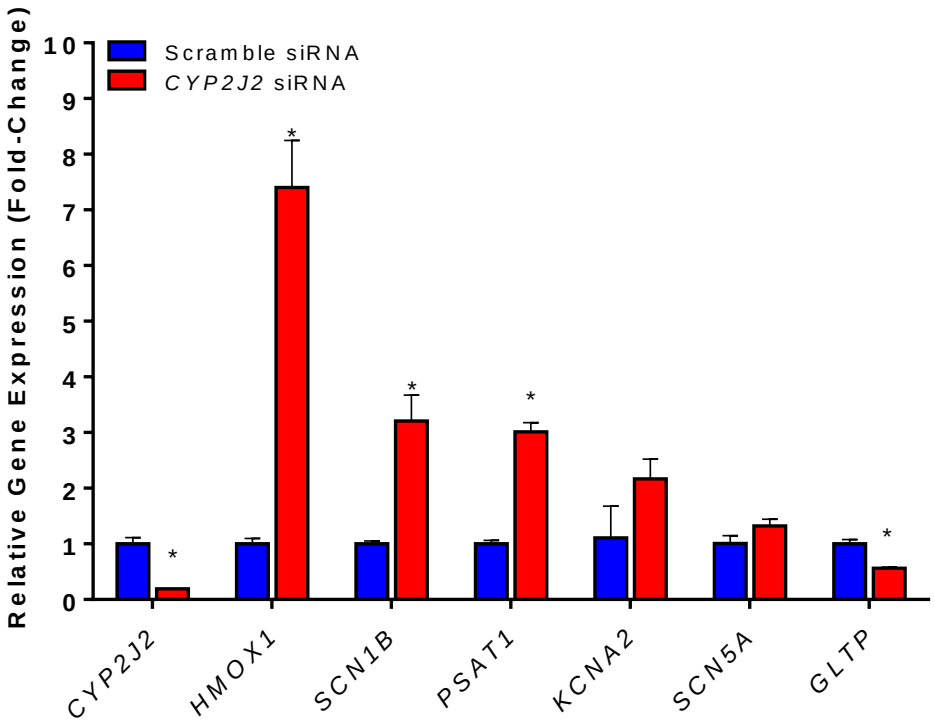

Figure 2.6. RT-PCR quantification of a subset of genes identified as altered by RNA-seq from an independent set of experiments. *HMOX1*, *SCN1B, PSAT1,* and *GLTP* were significantly altered by *CYP2J2* silencing, consistent with what was observed via RNA-seq. Additionally, *KCNA2* and *SCN5A* were up-regulated and consistent with the RNA sequencing findings but did not reach statistical significance. * $p < 0.05$.

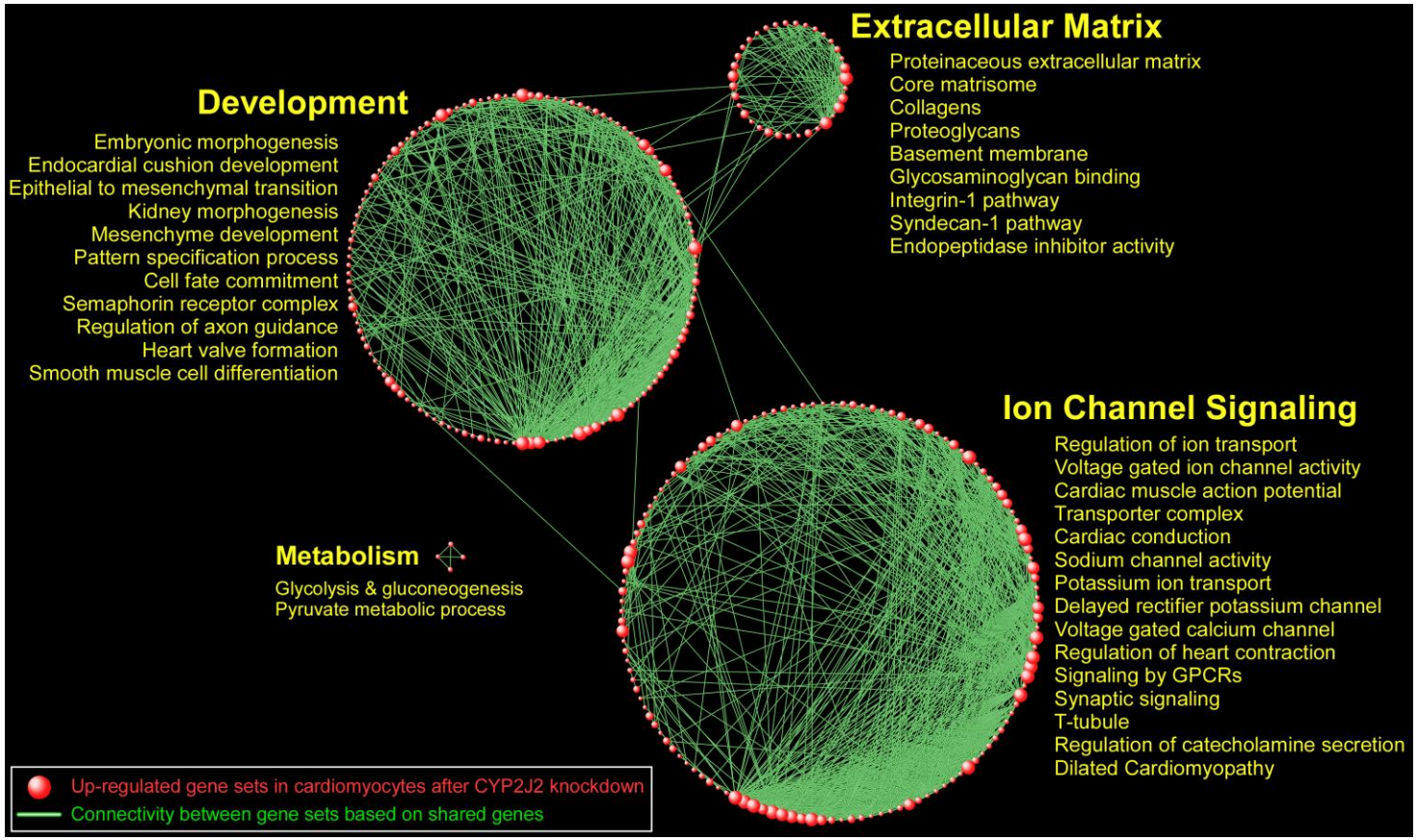

Figure 2.7. Network-based visual depiction of gene set enrichment analysis (GSEA) in adult ventricular myocytes after *CYP2J2* silencing. Each red sphere corresponds to an up-regulated gene set. Connectivity between the gene sets is based on 50% or greater overlap among their member genes. Note that the topology of the network is characterized by the emergence of biological modules comprises of highly interconnected gene sets with similar functional themes. Notable modules include “Ion Channel Signaling”, “Development”, “Extracellular Matrix”, and “Metabolism”. Representative pathways for each of these modules are shown and a complete list of enriched gene sets in Table 2.3.

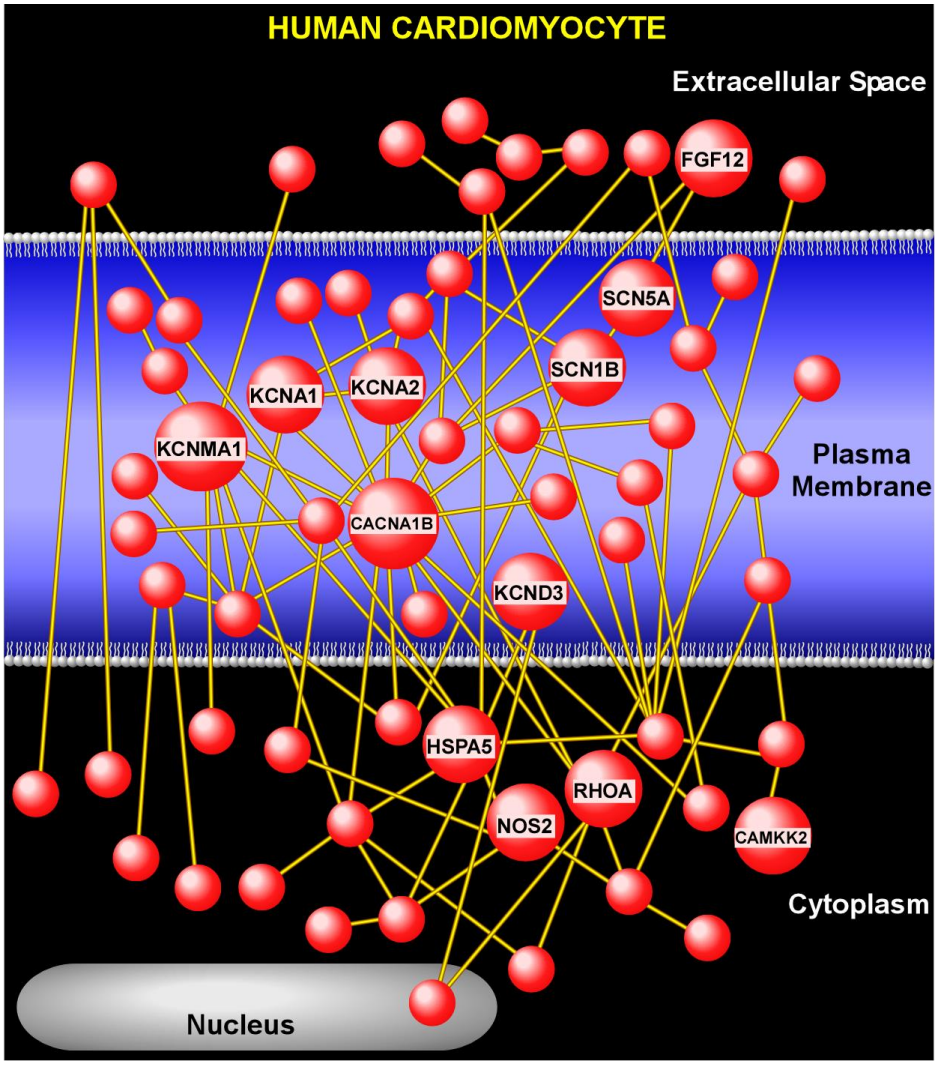

Figure 2.8. Gene product interaction network of "leading edge" members of gene sets mapping to the "Ion Channel Signaling" module. To enhance biological significance, we limited the "leading edge" genes to those with FDR < 0.01 and constructed the interaction network by incorporating only members with direct interactions. We have labeled several key nodes causing cardiac dysrhythmias including sodium (SCN1B, SCN5A), potassium (KCNA1, KCNA2, KCNMA1, KCND3), and calcium (CACNA1B) channels, as well as other genes linked to electrophysiologic abnormalities (FGF12, HSPA5, NOS2, RHOA, and CAMKK2). Full list of network nodes is Table 2.4.

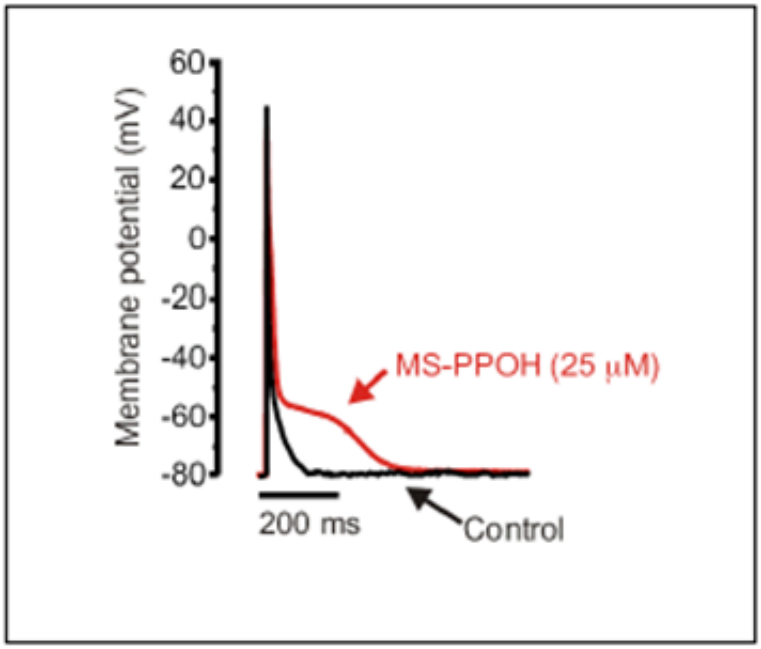

Figure 2.9. APD of ventricular myocyte isolated from an adult transgenic mouse overexpressing cardiac CYP2J2. Treatment of the cell with the CYP epoxygenase MS-PPOH (red trace) shows prolonged repolarization and overall AP compared to control (black trace).

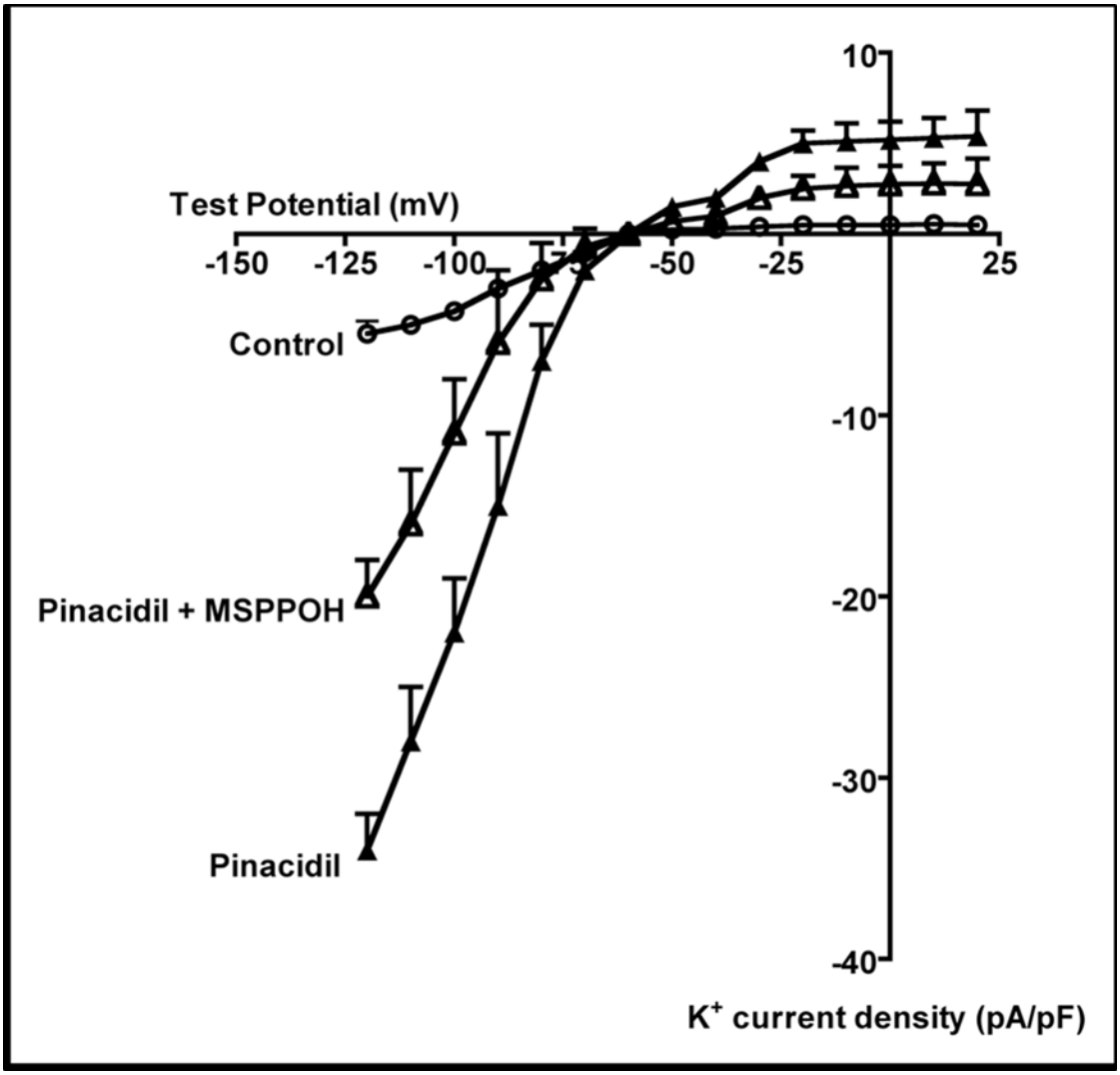

Figure 2.10. Representative ion density plot of isolated mouse cardiomyocytes subjected to whole-cell patch clamp. Untreated (control, open circles) show baseline current density at test potential ranges. Pinacidil-treated cells (pinacidil, filled triangles), exhibit increased current density as K^+ channels are pharmacologically activated. Finally, cells treated first with pinacidil, followed by the CYP epoxygenase inhibitor MSPPOH (pinacidil + MSPPOH, open triangles), exhibit decreased ion currents, showing that CYP epoxygenase inhibition has negative effects on K^+ channels activity.

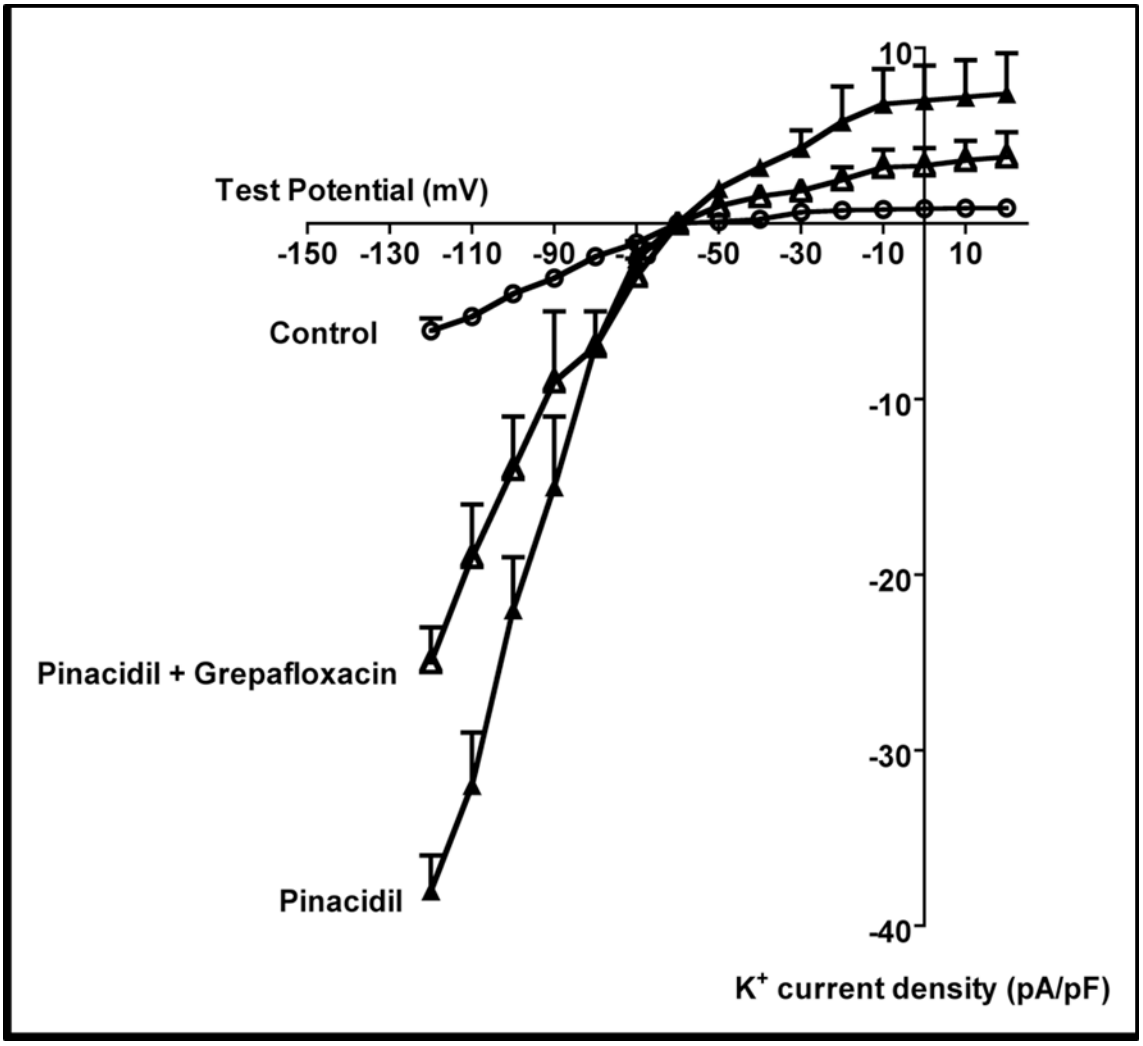

Figure 2.11. Representative ion density plot of isolated mouse cardiomyocytes subjected to whole-cell patch clamp. Untreated (control, open circles) show baseline current density at test potential ranges. Pinacidil-treated cells (pinacidil, filled triangles), have increase current density as K^+ channels are pharmacologically activated. Finally, cells treated first with pinacidil, followed by the CYP2J2 inhibitor grepafloxacin (pinacidil + Grepafloxacin, open triangles), exhibit decreased ion currents.

References

Aliwarga T, Evangelista EA, Sotoodehnia N, Lemaitre RN, and Totah RA (2018) Regulation of CYP2J2 and EET levels in cardiac disease and diabetes. *Int J Mol Sci* **19**.

Aliwarga T, Raccor BS, Lemaitre RN, Sotoodehnia N, Gharib SA, Xu L, and Totah RA (2017) Enzymatic and free radical formation of cis- and trans- epoxyeicosatrienoic acids in vitro and in vivo. *Free Radic Biol Med* **112**:131–140.

Bray NL, Pimentel H, Melsted P, and Pachter L (2016) Near-optimal probabilistic RNA-seq quantification. *Nat Biotechnol* **34**:525–527, Nature Publishing Group.

Chen L, Wang FY, Zeng ZY, Cui L, Shen J, Song XW, Li P, Zhao XX, and Qin YW (2017) MicroRNA-199a acts as a potential suppressor of cardiomyocyte autophagy through targeting Hspa5. *Oncotarget* **8**:63825–63834, Impact Journals LLC.

Cline MS, Smoot M, Cerami E, Kuchinsky A, Landys N, Workman C, Christmas R, Avila-Campilo I, Creech M, Gross B, Hanspers K, Isserlin R, Kelley R, Killcoyne S, Lotia S, Maere S, Morris J, Ono K, Pavlovic V, Pico AR, Vailaya A, Wang PL, Adler A, Conklin BR, Hood L, Kuiper M, Sander C, Schmulevich I, Schwikowski B, Warner GJ, Ideker T, and Bader GD (2007) Integration of biological networks and gene expression data using cytoscape. *Nat Protoc* **2**:2366–2382.

Eckle T, Kohler D, Lehmann R, Kasmi KCE, and Eltzschig HK (2008) Hypoxia-inducible factor-1 is central to cardioprotection a new paradigm for ischemic preconditioning. *Circulation* **118**:166–175.

El-Serafi I, Fares M, Abedi-Valugerdi M, Afsharian P, Moshfegh A, Terelius Y, Potácová Z, and

Hassan M (2015) Cytochrome P450 2J2, a new key enzyme in cyclophosphamide bioactivation and a potential biomarker for hematological malignancies. *Pharmacogenomics J* **15**:405–413, Nature Publishing Group.

Evangelista EA, Kaspera R, Mokadam NA, Jones III JP, and Totah RA (2013) Activity, inhibition, and induction of cytochrome P450 2J2 in adult human primary cardiomyocytes. *Drug Metab Dispos* **41**.

Evangelista EA, Lemaitre RN, Sotoodehnia N, Gharib SA, and Totah RA (2018) CYP2J2 expression in adult ventricular myocytes protects against reactive oxygen species toxicity. *Drug Metab Dispos* **46**.

Fellenberg K, Hauser NC, Brors B, Neutzner A, Hoheisel JD, and Vingron M (2001) Correspondence analysis applied to microarray data. *Proc Natl Acad Sci U S A* **98**:10781–10786.

Fer M, Dréano Y, Lucas D, Corcos L, Salaün JP, Berthou F, and Amet Y (2008) Metabolism of eicosapentaenoic and docosahexaenoic acids by recombinant human cytochromes P450. *Arch Biochem Biophys* **471**:116–125.

Giudicessi JR, Ye D, Tester DJ, Crotti L, Mugione A, Nesterenko V V., Albertson RM, Antzelevitch C, Schwartz PJ, and Ackerman MJ (2011) Transient outward current (I to) gain-of-function mutations in the KCND3-encoded Kv4.3 potassium channel and Brugada syndrome. *Hear Rhythm* **8**:1024–1032.

Goddeeris MM, Schwartz R, Klingensmith J, and Meyers EN (2007) Independent requirements for hedgehog signaling by both the anterior heart field and neural crest cells for outflow tract development. *Development* **134**:1593–1604.

Hennessey JA, Marcou CA, Wang Chuan, Wei EQ, Wang Chaojian, Tester DJ, Torchio M, Dagradi F, Crotti L, Schwartz PJ, Ackerman MJ, and Pitt GS (2013) FGF12 is a candidate Brugada syndrome locus. *Hear Rhythm* **10**:1886–1894.

Isserlin R, Merico D, Voisin V, and Bader GD (2014) Enrichment Map - a Cytoscape app to visualize and explore OMICs pathway enrichment results. *F1000Research* **3**, Faculty of 1000 Ltd.

Kaspera R, and Totah RA (2009) Epoxyeicosatrienoic acids: Formation, metabolism and potential role in tissue physiology and pathophysiology.

Ke Q, Xiao YF, Bradbury JAA, Graves JP, Degraff LM, Seubert JM, and Zeldin DC (2007) Electrophysiological Properties of Cardiomyocytes Isolated from CYP2J2 Transgenic Mice. *Mol Pharmacol* **72**:mol.

Kefaloyianni E, Bao L, Rindler MJ, Hong M, Patel T, Taskin E, and Coetzee WA (2012) Measuring and evaluating the role of ATP-sensitive K+ channels in cardiac muscle. *J Mol Cell Cardiol* **52**:596–607, Elsevier Ltd.

Koitabashi N, Danner T, Zaiman AL, Pinto YM, Rowell J, Mankowski J, Zhang D, Nakamura T, Takimoto E, and Kass DA (2011) Pivotal role of cardiomyocyte TGF-β signaling in the murine pathological response to sustained pressure overload. *J Clin Invest* **121**:2301–2312.

Krämer A, Green J, Pollard J, and Tugendreich S (2014) Causal analysis approaches in ingenuity pathway analysis. *Bioinformatics* **30**:523–530.

Larsen BT, Campbell WB, and Gutterman DD (2007) Beyond vasodilatation: non-vasomotor roles of epoxyeicosatrienoic acids in the cardiovascular system. *Trends Pharmacol Sci*

28:32–38.

Lauriol J, Keith K, Jaffré F, Couvillon A, Saci A, Goonasekera SA, McCarthy JR, Kessinger CW, Wang J, Ke Q, Kang PM, Molkentin JD, Carpenter C, and Kontaridis MI (2014) RhoA signaling in cardiomyocytes protects against stress-induced heart failure but facilitates cardiac fibrosis. *Sci Signal* **7**:ra100, American Association for the Advancement of Science.

Livak KJ, and Schmittgen TD (2001) Analysis of Relative Gene Expression Data Using Real-Time Quantitative PCR and the 2−ΔΔCT Method. *Methods* **25**:402–408, Academic Press.

Long QQ, Wang H, Gao W, Fan Y, Li YF, Ma Y, Yang Y, Shi HJ, Chen BR, Meng HY, Wang QM, Wang F, Wang ZM, and Wang LS (2017) Long noncoding RNA Kcna2 antisense RNA contributes to ventricular arrhythmias via silencing Kcna2 in rats with congestive heart failure. *J Am Heart Assoc* **6**, American Heart Association Inc.

Love MI, Huber W, and Anders S (2014) Moderated estimation of fold change and dispersion for RNA-seq data with DESeq2. *Genome Biol* **15**, BioMed Central Ltd.

Lu T, Hoshi T, Weintraub NL, Spector AA, and Lee H-C (2001) Activation of ATP-sensitive K+ channels by epoxyeicosatrienoic acids in rat cardiac ventricular myocytes. *J Physiol* **537**:811–827, Blackwell Publishing Ltd.

Manikandan P, and Nagini S (2018) Cytochrome P450 Structure, Function and Clinical Significance: A Review. *Curr Drug Targets* **19**:38–54.

McDonnell AM, and Dang CH (2013) Basic review of the cytochrome p450 system. *J Adv Pract Oncol* **4**:263–8, Harborside Press.

Michaud V, Frappier M, Dumas M, and Turgeon J (2010) Metabolic Activity and mRNA Levels

of Human Cardiac CYP450s Involved in Drug Metabolism. *PLoS One* **5**.

Ortiz de Montellano PR (2005) *Cytochrome P450 : structure, mechanism, and biochemistry*, Kluwer Academic/Plenum Publishers.

Parimon T, Yao C, Habiel DM, Ge L, Bora SA, Brauer R, Evans CM, Xie T, Alonso-Valenteen F, Medina-Kauwe LK, Jiang D, Noble PW, Hogaboam CM, Deng N, Burgy O, Antes TJ, Konigshoff M, Stripp BR, Gharib SA, and Chen P (2019) Syndecan-1 promotes lung fibrosis by regulating epithelial reprogramming through extracellular vesicles. *JCI Insight*, doi: 10.1172/jci.insight.129359.

Parks RJ, Ray G, Bienvenu LA, Rose RA, and Howlett SE (2014) Sex differences in SR Ca2+ release in murine ventricular myocytes are regulated by the cAMP/PKA pathway. *J Mol Cell Cardiol* **75**:162–173, Elsevier B.V.

Sakai S, Miyauchi T, Kobayashi M, Yamaguchi I, Goto K, and Sugishita Y (1996) Inhibition of myocardial endothelin pathway improves long-term survival in heart failure. *Nature* **384**:353–355.

Seubert J, Yang B, Bradbury JA, Graves J, Degraff LM, Gabel S, Gooch R, Foley J, Newman J, Mao L, Rockman HA, Hammock BD, Murphy E, and Zeldin DC (2004) Enhanced postischemic functional recovery in CYP2J2 transgenic hearts involves mitochondrial ATP-sensitive K+ channels and p42/p44 MAPK pathway. *Circ Res* **95**:506–14.

Si M, Trosclair K, Hamilton KA, and Glasscock E (2019) Genetic ablation or pharmacological inhibition of Kv1.1 potassium channel subunits impairs atrial repolarization in mice. *Am J Physiol - Cell Physiol* **316**:C154–C161, American Physiological Society.

Skepner JE, Shelly LD, Ji C, Reidich B, and Luo Y (2010) Chronic treatment with epoxyeicosatrienoic acids modulates insulin signaling and prevents insulin resistance in hepatocytes. *Prostaglandins Other Lipid Mediat* **94**:3–8.

Smith PK, Krohn RI, Hermanson GT, Mallia AK, Gartner FH, Provenzano MD, Fujimoto EK, Goeke NM, Olson BJ, and Klenk DC (1985) Measurement of protein using bicinchoninic acid. *Anal Biochem* **150**:76–85.

Spector AA, and Norris AW (2007) Action of epoxyeicosatrienoic acids on cellular function. *Am J Physiol Cell Physiol* **292**:C996–C1012.

Spiecker M, and Liao JK (2006) Cytochrome P450 Epoxygenase CYP2J2 and the Risk of Coronary Artery Disease. **16**:204–208.

Subramanian A, Kuehn H, Gould J, Tamayo P, and Mesirov JP (2007) GSEA-P: a desktop application for Gene Set Enrichment Analysis. *Bioinformatics* **23**:3251–3253, Narnia.

Subramanian A, Tamayo P, Mootha VK, Mukherjee S, Ebert BL, Gillette MA, Paulovich A, Pomeroy SL, Golub TR, Lander ES, and Mesirov JP (2005) Gene set enrichment analysis: A knowledge-based approach for interpreting genome-wide expression profiles. *Proc Natl Acad Sci U S A* **102**:15545–15550.

Wang Q, Shen J, Splawski I, Atkinson D, Li Z, Robinson JL, Moss AJ, Towbin JA, and Keating MT (1995) SCN5A mutations associated with an inherited cardiac arrhythmia, long QT syndrome. *Cell* **80**:805–811.

Watanabe H, Koopmann TT, Le Scouarnec S, Yang T, Ingram CR, Schott JJ, Demolombe S, Probst V, Anselme F, Escande D, Wiesfeld ACP, Pfeufer A, Kääb S, Wichmann HE,

Hasdemir C, Aizawa Y, Wilde AAM, Roden DM, and Bezzina CR (2008) Sodium channel β1 subunit mutations associated with Brugada syndrome and cardiac conduction disease in humans. *J Clin Invest* **118**:2260–2268.

Watanabe S, Horie T, Nagao K, Kuwabara Y, Baba O, Nishi H, Sowa N, Narazaki M, Matsuda T, Takemura G, Wada H, Hasegawa K, Kimura T, and Ono K (2014) Cardiac-specific inhibition of kinase activity in calcium/calmodulin-dependent protein kinase kinase-β leads to accelerated left ventricular remodeling and heart failure after transverse aortic constriction in mice. *PLoS One* **9**, Public Library of Science.

Westphal C, Spallek B, Konkel A, Marko L, Qadri F, DeGraff LM, Schubert C, Bradbury JA, Regitz-Zagrosek V, Falck JR, Zeldin DC, Müller DN, Schunck W-HH, and Fischer R (2013) CYP2J2 Overexpression Protects against Arrhythmia Susceptibility in Cardiac Hypertrophy. *PLoS One* **8**:e73490, Public Library of Science.

Xiao Y, Ke Q, Seubert JM, Bradbury JA, Graves J, Degraff LM, Falck JR, Krausz K, Gelboin H V, Morgan JP, and Zeldin DC (2004) Enhancement of Cardiac L-Type Ca 2 𝑎 Currents in Transgenic Mice with Cardiac-Specific Overexpression of CYP2J2. **66**:1607–1616.

Xu M, Bhatt DK, Yeung CK, Claw KG, Chaudhry AS, Gaedigk A, Pearce RE, Broeckel U, Gaedigk R, Nickerson DA, Schuetz E, Rettie AE, Leeder JS, Thummel KE, and Prasad B (2017) Genetic and nongenetic factors associated with protein abundance of flavin-containing monooxygenase 3 in human liver. *J Pharmacol Exp Ther* **363**:265–274, American Society for Pharmacology and Experimental Therapy.

Yamada Y, Kinoshita H, Kuwahara K, Nakagawa Y, Kuwabara Y, Minami T, Yamada C, Shibata J, Nakao Kazuhiro, Cho K, Arai Y, Yasuno S, Nishikimi T, Ueshima K, Kamakura

S, Nishida M, Kiyonaka S, Mori Y, Kimura T, Kangawa K, and Nakao Kazuwa (2014) Inhibition of N-type Ca2+ channels ameliorates an imbalance in cardiac autonomic nerve activity and prevents lethal arrhythmias in mice with heart failure. *Cardiovasc Res* **104**:183–193, Oxford University Press.

Yang S, Lin L, Chen J-X, Lee CR, Seubert JM, Wang Y, Wang H, Chao Z-R, Tao D-D, Gong J-P, Lu Z-Y, Wen Wang D, and Zeldin DC (2007) Cytochrome P-450 epoxygenases protect endothelial cells from apoptosis induced by tumor necrosis factor-␣ via MAPK and PI3K/Akt signaling pathways. *Am J Physiol - Hear Circ Physiol* **293**:H142–H151.

Yang S, Wei S, Pozzi A, and Capdevila JH (2009) The arachidonic acid epoxygenase is a component of the signaling mechanisms responsible for VEGF-stimulated angiogenesis. *Arch Biochem Biophys* **489**:82–91.

Zhang P, Xu X, Hu X, Van Deel ED, Zhu G, and Chen Y (2007) Inducible nitric oxide synthase deficiency protects the heart from systolic overload-induced ventricular hypertrophy and congestive heart failure. *Circ Res* **100**:1089–1098.

Zhang Y, El-sikhry H, Chaudhary KR, Batchu SN, Shayeganpour A, Jukar TO, Bradbury JA, Joan P, Degraff LM, Myers P, Rouse DC, Foley J, Zeldin DC, Seubert JM, Imig JD, Zhang Y, El-sikhry H, Chaudhary KR, Batchu SN, Shayeganpour A, Jukar TO, Bradbury JA, Graves JP, Degraff LM, Myers P, Rouse DC, Foley J, Nyska A, Zeldin DC, and Seubert JM (2012) Overexpression of CYP2J2 provides protection against doxorubicin-induced cardiotoxicity Overexpression of CYP2J2 provides protection against doxorubicin-induced cardiotoxicity. , doi: 10.1152/ajpheart.00983.2008.

Zhao Y, Wang Chunhong, Wang Cong, Hong X, Miao J, Liao Y, Zhou L, and Liu Y (2018) An

essential role for Wnt/β-catenin signaling in mediating hypertensive heart disease. *Sci Rep* **8**, Nature Publishing Group.

Chapter 3: CYP2J2 expression in adult ventricular myocytes is upregulated and protects against ROS toxicity

Significant portions of this chapter have been previously published in Drug Metabolism & Disposition (Evangelista *et al.*, 2018)

3.1 Introduction

Reactive oxygen species (ROS) are highly reactive entities that are naturally produced in the cells' mitochondria as metabolism byproducts. ROS are normally released as part of aerobic respiration and include hydrogen peroxide, superoxide and hydroxyl radicals, all of which are highly reactive and capable of oxidizing cellular lipids, proteins and nucleic acids (Schieber and Chandel, 2014). ROS are typically associated with oxidative stress within cells but in recent years, research has shown that ROS also play a role in cell signaling and cell survival (Finkel, 2011; Bouitbir *et al.*, 2012; Brieger *et al.*, 2012). In healthy cells, ROS levels are carefully maintained and managed with cellular antioxidants, such as glutathione and enzymes including superoxide dismutase and catalase, ensuring that ROS levels remain below toxic thresholds. In pathologic states, however, this careful balance is disrupted, and as ROS levels rise beyond healthy levels, cells enter a state of oxidative stress (Schieber and Chandel, 2014). Oxidative stress is associated with many disease states, including cardiovascular disease and diabetes (Giacco and Brownlee, 2010; Sugamura and Keaney, 2011).

Cardiovascular disease (CVD) is one of the leading causes of mortality in the US and worldwide (Benjamin *et al.*, 2019). CVD is a family of diseases involving the heart and blood vessels. These encompass hypertension, arrhythmias, coronary artery disease, myocardial infarctions, hypertrophy and heart failure. ROS and oxidative stress have been shown to be

important factors in the onset and progression of CVD, however, the exact role and mechanism of ROS is still a matter of debate (Sugamura and Keaney, 2011). In addition to a possible role in the etiology of cardiovascular diseases, ROS are also implicated in the cardiovascular toxicities of some drugs. Doxorubicin, for example, is an anthracycline anticancer agent that causes severe cardiotoxicity (Damiani *et al.*, 2016). One popular mechanism for doxorubicin's toxicity involves mitochondrial dysfunction and subsequent rise in cellular ROS levels (Ichikawa *et al.*, 2014; Damiani *et al.*, 2016).

Arachidonic acid (AA) is an omega-6 polyunsaturated fatty acid, which is a precursor to a myriad of signaling molecules including eicosanoids, leukotrienes, prostaglandins and thromboxanes (Sacerdoti *et al.*, 2016). In the 1980s, cytochrome P450 (CYP) enzymes were discovered to convert arachidonic acid to mono-hydroxyl metabolites and four cis regioisomers of epoxyeicosatrienoic acids (EETs) (Oliw *et al.*, 1982; Laniado-Schwartzman *et al.*, 1988; Oliw, 1994). Several animal models have demonstrated EETs to be protective in many disease states as well as against doxorubicin-induced cardiotoxicity (Zhang *et al.*, 2009; Cai *et al.*, 2013; Ma *et al.*, 2013; Westphal *et al.*, 2013; Chen *et al.*, 2015). EETs have gained increasing attention in CVD in the last two decades due to their involvement in angiogenesis, regulation of vasodilation, upregulation of eNOS and interactions with cardiac ion channels, highlighting their importance in overall cardiovascular health (Larsen *et al.*, 2007; Behm *et al.*, 2009; Campbell and Fleming, 2010; Pfister *et al.*, 2010). While initially thought to elicit a response through activation of an EET receptor, which remains elusive, EETs have been shown to affect cellular changes by activating key signaling pathways, for example the MAPK/ERK and Akt cascades (Yang *et al.*, 2007).

CYP2J2, the major CYP expressed in human heart tissue plays a prominent role in EET synthesis (Roman, 2002). Like other drug metabolizing CYPs, CYP2J2 is expressed in intestinal and hepatic tissue, but unlike other isoforms, it is expressed in extrahepatic tissues including the kidney, lungs, skeletal muscle and most prominently the heart (Wu *et al.*, 1996; Zeldin *et al.*, 1997; Delozier *et al.*, 2007; Michaud *et al.*, 2010; Evangelista *et al.*, 2013). The active site cavity for CYP2J2, determined from homology models, is comparable in volume to that of CYP3A4, the most prominent drug metabolizing CYP isoform, resulting in a similarly wide substrate array (Lee *et al.*, 2010, 2012).

Our group, and others, have previously shown CYP2J2 to be the dominant CYP isoform expressed in the heart, specifically in ventricular myocytes (Wu *et al.*, 1996; Delozier *et al.*, 2007; Michaud *et al.*, 2010; Evangelista *et al.*, 2013). In the heart, CYP2J2 is believed to be the predominant source of EETs. Given the importance of EETs in the heart and their reported abilities to protect against disease states and the role for CYP2J2 as a primary source of EETs in ventricular myocytes, we investigated the effects of ROS on CYP2J2 expression. Further, we experimentally determined the effects of reduced function or expression of CYP2J2 in cardiomyocytes on surviving ROS toxicity and tested if external EETs can mitigate these effects.

3.2 Materials & Methods

Chemicals & cell culture materials

Danazol and thiazolyl blue tetrazolium bromide (MTT) were obtained from Sigma-Aldrich (St. Louis, MO, USA) and used without further purification. Solvents and 30% hydrogen peroxide were purchased from Fisher Scientific (Waltham, MA, USA), also used without further purification. Adult derived primary human cardiomyocytes were obtained from Celprogen Inc. (San Pedro, CA, USA; cat #36044-15). Cell culture materials including media (complete growth media, cat #M36044-15S and phenol and serum-free media, cat #M36044-15PN) and cell culture flasks and plates pre-coated with extracellular matrix (cat #E36044-15) were obtained from Celprogen Inc. Cell growth media were further sterile filtered using a vacuum filter through a 0.22 μm polyethersulfone (PES) filter. Doxorubicin, (±) 5,6-*cis* epoxyeicosatrienoic acid (5,6-EET), (±) 8,9-*cis* epoxyeicosatrienoic acid (8,9-EET), (±) 11,12-*cis* epoxyeicosatrienoic acid (11,12-EET), and (±) 14,15-*cis* epoxyeicosatrienoic acid (14,15-EET) were obtained from Cayman Chemicals (Ann Arbor, MI) and used without further purification.

Cardiomyocyte cell culture

Cell culture was carried out following Celprogen's protocols. The cells obtained and used for these studies are adult derived ventricular cardiomyocytes. All experiments were carried out between passages 6 and 8 from receipt from Celprogen Inc. Passage numbers were determined by number of times cells were treated with trypsin since receipt from Celprogen which was designated passage 1 for the purposes of these experiments. Briefly, cells were maintained and expanded using Celprogen pre-coated flasks and plates and complete growth media with serum.

All experimental procedures involving treatments were carried out using serum and phenol free media unless otherwise stated. Cells used for RNA isolation and subsequent experiments were harvested by washing the cells still attached to the plate with 1X PBS. After washing, all liquid was aspirated from the wells and the entire plate was stored in -80 °C until further processing.

Gene expression following treatment with BHA, BHT, hydrogen peroxide, doxorubicin or EETs

Experiments to determine gene response to external factors were carried out using 12-well pre-coated plates from Celprogen Inc. Cells were plated at a density of approximately 250,000 cells per well and allowed to attach overnight at 37 °C and 5% CO_2. Cells were then washed with PBS and treated with butylated hydroxy anisole (BHA, 0, 1, 10, 100 μM), butylated hydroxytoluene (BHT, 0, 1, 10, 100 μM), hydrogen peroxide (0.01% v/v final concentration) or doxorubicin (20 μM or 5 μM final concentration) in serum-free media. Two concentrations of DOX were used in this study to determine the effects of DOX toxicity on the cells with impaired CYP2J2 expression and activity. A high concentration (20 μM) was chosen to induce maximal ROS formation in the cells over 24 hours. The effects of a lower concentration are also reported (5 μM) and was chosen to more closely mimic in vivo concentrations. Previously, the maximal in vivo concentration was determined to be between 2-5 μM (Greene *et al.*, 1983; Asperen *et al.*, 1999; Barpe *et al.*, 2010; Maillet *et al.*, 2016). The highest observed *in vivo* concentration was selected to achieve the greatest rise in intracellular ROS levels. Control vehicle treatments include serum-free media with PBS to serve as the BHA, BHT and hydrogen peroxide treatment controls and 0.1% DMSO for doxorubicin treatment controls. The cells were treated for either 6

hours (H_2O_2), 24 hours (doxorubicin), or 72 hours (BHA or BHT), after which they were washed and stored at -80 °C until RNA extraction.

Inhibition of CYP2J2 using danazol

Inhibition experiments were carried out using 12-well pre-coated plates from Celprogen Inc. Cells were plated at a density of 250,000 cells per well and allowed to attach overnight at 37 °C and 5% CO_2. Cells were then washed with PBS and the growth media was replaced with serum and phenol-free media containing 1 μM danazol (DAN) and either H_2O_2 (0.01%) or doxorubicin (5 μM or 20 μM final concentration). Controls include cells treated with vehicle only, with danazol only, and cells treated with hydrogen peroxide (0.01%) or doxorubicin (1 μM) alone. Experiments treating with hydrogen peroxide were carried out for six hours to avoid complete cell death while doxorubicin experiments were carried out for 24 hours. After each treatment period, cell viability was measured using an MTT assay as described below. A variation of the experiments outlined above were also carried out in the presence or absence of pyruvate (10 mM final concentration) to determine the effects of an antioxidant in the media (Franco *et al.*, 2007).

CYP2J2 gene silencing

Silencing of *CYP2J2* gene expression was achieved using the RNAiMAX lipofectamine (Thermo Fisher Scientific, Waltham MA) and the *CYP2J2* Trilencer siRNA or scrambled siRNA (Origene, Rockville, MD), using the manufacturer's suggested protocols, optimized for the cardiomyocyte system in terms of time and siRNA concentrations. Silencing of the *HPRT1* gene

using the Origene siRNA served as positive control for all gene knockdown experiments. Lipofectamine was delivered using a reverse transfection protocol. Briefly, the siRNA was reconstituted to a stock concentration of 20 μM per the manufacturer instructions and prepared with the lipofectamine using OptiMEM reduced serum media (Thermo Fisher Scientific, Waltham, MA) by diluting to a concentration of 50 nM. Cells were washed with warm (37 °C) PBS and harvested using trypsin. Following trypsinization, cells were pelleted, resuspended and diluted to a concentration of 200,000 cells/mL in complete media. The lipofectamine/siRNA stocks were added to each well to a final concentration of 10 nM siRNA (250 μL volume of 50 nM siRNA/lipofectamine in OptiMEM), followed by the cells (1 mL of cell suspension) for a final volume of 1250 μL in each well. The cells were incubated with the lipofectamine/siRNA for 72 hours, after which follow up experiments were performed.

In one set of experiments, media containing siRNA was removed and the cells were washed, with media replaced with complete growth media. Cells were then harvester at 0, 6, 12, and 24 hours following removal of siRNA containing media. Cells were then harvested, and gene expression assayed as described below.

In a different set of experiments, following siRNA silencing of the cells, wells were carefully washed with PBS before serum free media containing doxorubicin (20 or 5 μM) or DMSO (0.1%) were added for 24 hours. Rescue experiments were also carried out with the addition of pyruvate (10 mM) or 11,12-EET (5 or 50 nM) to determine if doxorubicin toxicity following gene silencing can be mitigated.

Measuring gene expression following EETs treatment

Experiments examining gene expression following EET addition were carried out using 12-well pre-coated plates. Cells were plated at a density of approximately 250,000 cells per well and allowed to attach overnight at 37 °C and 5% CO_2. The following day, the cells were washed with warm (37°C) PBS. After aspirating the PBS, the cells were treated with EETs (50 nM final concentration), either in combination (mix) or separately (individual isomers) in serum-free media for 1 hour. Negative controls were treated with serum-free media with < 0.1% ethanol. Cells were treated with external EETs for one hour, after which the treatment was aspirated, the cells were washed, and the plates were stored at -80 °C until RNA isolation.

Measuring mRNA levels

Total RNA was extracted using the MagMax 96 Total RNA Isolation kit (Thermo Fisher Scientific, Waltham MA). RNA quality (A_{260}/A_{280}) and quantity was determined using a Synergy HTX Multi-Mode Reader (BioTek, Winooski VT). Total RNA was then used to synthesize cDNA using the High Capacity RNA-to-cDNA kit (Thermo Fisher Scientific, Waltham MA). RT-PCR was then carried out using TaqMan (Thermo Fisher Scientific, Waltham MA) FAM reporter primers for the various genes screened (*CYP2J2, EPHX2, PLA2G4C, HMOX1, SOD1, SOD2, CAT,* and *GPX1*) as well as the housekeeping gene, *GusB.* Cycle threshold (C_T) values and the ΔC_T method followed by the $2^{\Delta CT}$calculation were used to determine the relative quantity of *CYP2J2* (and other genes) mRNA present relative to the *GusB* mRNA levels. The mRNA levels were first normalized to the housekeeping gene using the ΔC_T method and then the levels of expression in treated cells were compared to expression levels in untreated cells using the

$\Delta\Delta C_T$ calculation and relative gene expression levels were reported using the $2^{-\Delta\Delta CT}$ calculation (Livak and Schmittgen, 2001).

MTT assay for cell viability

Cell viability was determined using thiazolyl blue tetrazolium bromide (MTT) assays. Briefly, following treatment with siRNA and/or chemical, cells were treated with 5 μL of 12 mM MTT per mL of media (60 μM MTT final concentration). The cells were incubated with the MTT for 20 minutes at 37°C. Afterwards, the media was aspirated carefully and DMSO (600 μL) was added to each well, followed by 75 μL of Sorenson's glycine (100 mM glycine, 100 mM sodium chloride). The plate was placed on an orbital shaker for 5 min at 400 rpm. The absorbance from each well was measured using a Tecan Infinite M200 plate reader (Tecan, Männedorf, Switzerland) using the following protocol: 5 sec of orbital shaking with an amplitude of 1 mm, followed by 10 sec of wait time, and then absorbance measurement at 570 nm (9 nm bandwidth) using 670 nm (9 nm bandwidth) as the reference wavelength. A true zero signal was obtained by following the above protocol using plates that did not contain cells. Measurements were normalized to the absorbance in vehicle-treated control wells (set as 100% viability).

ROS formation assay

Reactive oxygen species formation was measured using 2',7'-dichlorodihydrofluorescein diacetate (H_2DCFDA, Thermo Fisher Scientific, Waltham MA). Cells were incubated in serum-free phenol-free media containing 20 μM H_2DCFDA for 30 minutes after siRNA and/or drug treatments to determine relative ROS levels in the cells. After incubation, 100 μL aliquots of the

media were transferred to a 96 well, black-walled, clear bottom plate (Thermo Fisher Scientific, Waltham MA). The fluorescence was captured and measured using a Synergy HTX Multi-Mode Reader (excitation wavelength of 485 nm/emission wavelength of 525 nm). Data were analyzed by normalizing signals to a control well subjected to similar conditions as described above, but with no cells present as the baseline ROS formation control.

Terfenadine Activity Assay

Cells were plated in 96 well plates at an approximate density of 10,000 cells per well and allowed to adhere to the plate for 24 hours in 100 μL of complete media. The cells were then washed with phosphate buffered saline (100 μL) and treated with either scrambled or CYP2J2 siRNA as described earlier. After 72 hours of incubation with siRNA, the wells were gently washed with warmed PBS and media replaced with complete media. A subset of cells was treated immediately with terfenadine, while others were cultured in complete media for 6 hours and 24 hours following removal of CYP2J2 siRNA. Activity was measured by dosing with terfenadine in serum-free media (1.5 μM final concentration containing 0.1 % DMSO). Control cells were dosed with serum free media with 0.1% DMSO. After 2 hours of incubation at 37 °C, the reaction was quenched by the addition of acetonitrile (100 μL) containing 0.1 μM midazolam as internal standard. Vigorous pipetting was then used to facilitate cellular detachment from the plate and lysis. The samples were centrifuged (3500 x g, 10 min), and 150 μL was transferred to a new 96 well plate for spectrometric analysis.

Terfenadine Metabolite Detection and Quantification

Metabolites and parent were quantified on a Sciex API 6500 LC/MS/MS (AB Sciex LLC, Framingham, MA) running Analyst software (v1.7) connected to a Waters Acquity I-class LC system equipped with a Waters autosampler (Waters Corp, Milford, MA). 10 μL of supernatant was injected on an Agilent Zorbax XDB C8-column (2.1 μm, 5 cm) column. For terfenadine, the mobile phase consisted of aqueous phase A: 10 mM ammonium acetate (pH 5.5) and organic phase B: 10 mM ammonium acetate in methanol and analyzed using the following gradient: mobile phase B: 0 -1 min, 30% ; 1-2 min, 30 to 70% , 2 - 4 min 70 to 100% , 4-6.5 min 100% , 6.5-6.6 min 100-30%. The column was re-equilibrated at initial conditions for 1.4 min. The flow rate was 0.3 ml/min. MS/MS-parameters: ion spray 5,500 V, temperature 450 °C, collision gas 6 L/min, ion gas 15 L/min, curtain gas 10 L/min. Compound detection: terfenadine (472.20 > 436.10; declustering potential (DP), 80; collision energy (CE) 37), hydroxy terfenadine (488.30 > 452.20; DP 90; CE 40), terfenadine acid (502.40 > 466.30; DP 100; CE 40) and midazolam (326.00 >291.20; DP 50; CE 30).

Data analysis

Experiments were performed as biological triplicates and the data reported as a mean ± standard deviation. All experiments were repeated at least two times on two separate days. Where appropriate, the reported values are the mean values of all experiments (representative of both inter-day and intra-day variability). Despite the variation in inter-day knockdown efficiency using siRNA to reduce *CYP2J2* experiment, only experiments with >80% knock-down efficiency is presented in this report. Statistical significance was determined using student t-tests with

unequal variances and using a threshold p-value of 0.05. Statistical analyses were performed using GraphPad Prism version 6.07 for Windows (GraphPad Software, La Jolla CA).

3.3 Results

Gene expression in the presence of antioxidants

Exposure to BHA or BHT for 72 hours results in dose-dependent decrease of *CYP2J2* expression (Figure 3.1). When cells are treated with BHA, expression drops 25% at 1 μM, 85% at 10 μM and 90% at 100 μM. *CYP2J2* expression levels decrease more drastically when exposed to BHT, with a 95% decrease observed at 10 μM and 100 μM, indicating that the maximal effect by BHT has likely occurred with exposure at 10 μM. Unlike exposure to BHA, however, exposure to BHT does not result in any significant change in expression levels at 1 μM (Figure 3.1).

Gene expression in the presence of ROS

In the presence of increased ROS in adult ventricular myocytes, *CYP2J2* expression is significantly increased in the cells (Figure 3.2). When exposed to 0.01% hydrogen peroxide for 6 hours, gene expression of *CYP2J2* increased by over 3-fold (Figure 3.2). Treating the cells with doxorubicin caused a dose-dependent increase in intracellular ROS levels (Figure 3.3). Treatment with doxorubicin at 5 μM and 20 μM over a 24-hour period caused over 2-fold increase in *CYP2J2* expression (Figure 3.2). In addition, when cells are treated with 5 μM DOX, the gene expression of several genes are affected, specifically those that encode antioxidant proteins (Figure 3.4). The most prominent increases were in the gene expression of *HMOX1* (7-fold) and *GPX1* (4-fold), which encode heme oxygenase 1 and glutathione peroxidase 1, respectively. Significant upregulation was also observed in the gene expression of *SOD1* and *CAT*, which encode superoxide dismutase 1 and catalase. Finally, modest but insignificant

increases in superoxide dismutase 2 (*SOD2)* were also observed. The upregulation in these genes were reversed, however, when cells were exposed to doxorubicin in the presence excess pyruvate, an antioxidant. (Figure 3.4).

CYP2J2 inhibition and ventricular myocytes survival under hydrogen peroxide stress

Cell survival in response to hydrogen peroxide in ventricular myocytes is dose dependent. There is significantly more cell death as the hydrogen peroxide concentration is increased. In the presence of danazol, a known CYP2J2 inhibitor (Lee *et al.*, 2012; Evangelista *et al.*, 2013), cells exposed to 0.01% hydrogen peroxide were less viable than cells with absence of inhibitor (Figure 3.5). In a series of three experiments carried out, all in triplicates, cells with CYP2J2 activity chemically inhibited were on average two-fold less viable compared to cells exposed only to hydrogen peroxide. Of note, danazol treatment alone had no significant effect on cell viability.

Effects of CYP2J2 silencing on ventricular myocytes

Using siRNA, *CYP2J2* expression was consistently reduced in adult ventricular myocytes by >80% (Figure 3.6). Experiments measuring *CYP2J2* mRNA levels at various time points following 72h of silencing showed that *CYP2J2* expression was restored to normal levels within 24h (Figure 3.7). Additionally, activity assays using terfenadine as a probe substrate show gradual increase of CYP2J2 activity following 72 hours of gene silencing. Despite complete recovery of gene expression over 24 hours, however, protein activity is not completely restored, only achieving 40% of the activity of scrambled siRNA treated cells (Figure 3.8).

Silencing *CYP2J2* had remarkable effects on several other genes, specifically *PLA2G4C*, and *EPHX2*, that encode human phospholipase A2 and soluble epoxide hydrolase proteins, respectively (Figure 3.6). Alterations in the expression of either protein would be expected to affect EET levels by affecting free arachidonic acid and EET degradation, respectively. Reduction in *CYP2J2* resulted in three-fold upregulation of *PLA2G4C* and a 30% reduction of *EPHX2* mRNA. Gene silencing effects on the expression of *HMOX1, SOD1, SOD2, CAT,* and *GPX1* were also probed. These genes encode heme oxygenase, superoxide dismutase (1 and 2), catalase, and glutathione peroxidase, respectively, all of which are ROS responsive enzymes. The most remarkable change observed was the seven-fold upregulation of *HMOX1* (Figure 3.6). The mRNA expression levels of the other four enzymes were also slightly elevated by *CYP2J2* gene silencing, although these changes were not significant when compared to scramble treated cells.

Silencing CYP2J2 increases cell death due to H_2O_2 exposure, an effect that is reversed by external EETs

Reduction of *CYP2J2* expression resulted in increased susceptibility to ROS toxicity (Figure 3.9). While siRNA treatment by itself did not affect cell viability, exposing the cells to 0.01% H_2O_2 following *CYP2J2* silencing resulted in significantly higher cell death. Cells treated with hydrogen peroxide following gene silencing had, on average, two-fold greater cell death than cells treated with scramble siRNA.

Further, the effects of reduced viability in the presence of ROS were mitigated if the cells were exposed to external EETs prior to ROS exposure. Externally supplementing the cells with

50 nM 11,12-EET for 30 min prior to hydrogen peroxide exposure significantly increased the cells' viability to levels similar to controls with normal CYP2J2 expression (Figure 3.9).

Ventricular myocytes with compromised CYP2J2 activity or expression are more susceptible to doxorubicin toxicity

Cells exposed to doxorubicin also experience dose-dependent toxicity. Further, treatment with doxorubicin also result in dose-dependent increases in intracellular ROS levels. In the absence of additional stresses, exposure to 5 μM for approximately 24 hours resulted in a modest increase in ROS levels and about a 25% loss of cell viability (Figure 3.3 and Figure 3.10). These numbers increase to an approximately 50% higher intracellular ROS concentration and up to a 50 % loss of cell viability when the dose is increased to 20 μM (Figure 3.3 and Figure 3.11). Further, when CYP2J2 protein activity is inhibited by danazol, cell viability in the presence of doxorubicin is much lower compared to cells not exposed to danazol at both concentrations tested. On average, cell viability was 1.5-fold and three-fold higher in cells exposed only to doxorubicin compared to cells exposed to doxorubicin and danazol simultaneously at 5 μM and 20 μM, respectively (Figure 3.10 and Figure 3.11).

Finally, mirroring the results of the cells exposed to hydrogen peroxide, adult ventricular myocytes are more susceptible to DOX toxicity when *CYP2J2* expression is reduced. On average, silencing *CYP2J2* expression reduced cell viability with doxorubicin treatment by up to 40% compared to doxorubicin-treated cells with normal *CYP2J2* expression. In addition, this decrease in viability is mitigated when cells are simultaneously treated with EETs, either in a mixture or individually. There were no marked differences between the different regioisomers of

EET in protecting against doxorubicin toxicity as all four regioisomers appear to have similar effects (Figure 3.12 and Figure 3.13).

EET effects on gene expression

Cells were treated with EETs for one hour to capture the early effects of gene expression, prior to the possible esterification of external EETs into the cell membrane for storage of hydrolysis by soluble epoxide hydrolase. Cells exposed to external EETs for only one hour exhibited very little variability in *CYP2J2* or *EPHX2* gene expression. Similarly, the gene expression of *HMOX1* and *PLA2G4C* changed very little over the one-hour incubation (Figure 3.12) except when the cells were treated with external 11,12-EET and 14,15-EET separately. *HMOX1* gene expression significantly increased two-fold over the one-hour treatment. Similarly, *PLA2G4C* was significantly upregulated by almost two-fold (1.8-fold change over untreated, Figure 3.14). Treatment with 11,12-EET and 14,15-EET exhibited similar effects on the genes that were surveyed. Neither 8,9-EET nor 5,6-EET had a significant effect on the surveyed gene expression.

3.4 Discussion

In this study, we determined the effects of ROS on *CYP2J2* expression in adult primary ventricular myocytes. A key finding was that *CYP2J2* expression decreases when ventricular myocytes are exposed to the antioxidants BHA and BHT, but increases in response to oxidative stress in cardiomyocytes, either from exogenous ROS or doxorubicin treatment. The downregulation of CYP2J2 is contradictory to previously published studies by Lee and Murray (Lee and Murray, 2010) where CYP2J2 expression was increased when HepG2 cells were exposed to BHA. This might be indicative of differential regulation of *CYP2J2* between the liver and the heart. In addition, HepG2 cells are derived from cancer tissue and CYP2J2 has been shown to be differentially regulated in cancers (Jiang *et al.*, 2005; Chen *et al.*, 2012). Our findings suggest a role for CYP2J2 in response to reactive oxygen species, with tight regulation that is turned off in the presence of high levels of antioxidants.

Upregulation of genes encoding antioxidant proteins were also observed during exposure to doxorubicin. These effects were lessened in the presence of an antioxidant, indicating that gene upregulation was linked to increased ROS levels and not an unrelated pathway. Further, inhibition of *CYP2J2* expression enhanced ROS-induced cell death, suggesting that CYP2J2 is part of the early defense mechanism in adult primary ventricular myocytes, one that may be attenuated when the cells are not under any oxidative stress. CYP2J2 has long been identified as a protective enzyme in the heart, through its metabolism of arachidonic acid (AA) to form epoxyeicosatrienoic acids (EETs) (Murray, 2016). In animal models, others have shown that overexpression of human CYP2J2 mitigates doxorubicin (Zhang *et al.*, 2009) cardiotoxicity and in 2010, Zordoky et al demonstrated that treating rats with doxorubicin for 24 hours shows a significant upregulation of *CYP2J3*, the rat orthologue of *CYP2J2* (Zordoky *et al.*, 2010) and in

2012, Alsaad et al. demonstrated that chronic DOX (14 days) treatment of rats showed no statistically significant change in *CYP2J3* expression, the rat orthologue of *CYP2J2* (Alsaad *et al.*, 2012). These data suggest a rapid transient response to the drug. This study is, however, to our knowledge is the first report where *CYP2J2* expression is upregulated in response to doxorubicin due to an increase in ROS in human adult ventricular myocytes. Further, while typical chemical CYP inducers such as phenobarbital and rifampicin are unable to affect CYP2J2 expression levels in cardiomyocytes, disease and stress markers have been shown to affect expression levels (Bystrom *et al.*, 2013; Evangelista *et al.*, 2013). Bystrom et al demonstrated that in response to bacterial LPS, *CYP2J2* is induced in human peripheral blood mononuclear cells and stimulates anti-inflammatory action in response to the presence of bacteria (Bystrom *et al.*, 2013). These results indicate regulation of *CYP2J2* expression as a general protective response against stresses that may increase ROS in various cell types.

The relative importance of CYP2J2 as a cardioprotective enzyme is attributed to its bioactivation of AA into EETs (Murray, 2016). The protective outcomes EETs exert, particularly where cardiac health is concerned, are numerous, though the exact mechanisms are not well defined. Among the CYPs, EET formation has been linked predominantly to the CYP2 family, with CYP2J2, CYP2C8 and CYP2C9 being putatively the most active isoforms involved in the cardiovascular system (Chaudhary *et al.*, 2009). We have previously shown CYP2J2 to be the major isozyme expressed in ventricular myocytes (Evangelista *et al.*, 2013). CYP2C8 and CYP2C9, in contrast, have greater expression levels in the endothelium of the vasculature where CYP2J2 is present at lower levels (Delozier *et al.*, 2007; Michaud *et al.*, 2010). Other groups demonstrated CYP2J2 to be chemically inducible in various cell lines including HepG2 cells however, induction in cardiomyocytes was not observed (Lee and Murray, 2010; Evangelista *et*

al., 2013). As the primary source of EETs in ventricular myocytes, it is likely that CYP2J2 expression is tightly regulated to preserve cardiac function, thus providing an explanation to its resistance to typical CYP inducers like phenobarbital and rifampicin.

Data from this study demonstrates that adult ventricular myocytes respond to elevated ROS levels by upregulating *CYP2J2* expression. In addition, this response is triggered either through the direct exposure of the cells to ROS or indirectly through exposure to doxorubicin and subsequent intracellular ROS elevation. Given the protective nature of EETs in cardiomyocytes, the upregulation of *CYP2J2* is likely a response designed to increase EET levels to counteract the toxicity of increased ROS levels. In our work, cells that were either pre-treated or co-treated with EETs when *CYP2J2* expression was knocked down experienced greater cell survival in response to ROS toxicity. In cases where we treated with doxorubicin, increases in ROS levels were mitigated by co-treatment with EETs as well. In addition, rescue by EETs against doxorubicin toxicity have identical effects to rescue with excess amounts of antioxidant, specifically pyruvate. The mechanism for this protection remains unknown although it is likely a result of EET signaling rather than direct reactions between ROS and EETs. The stoichiometry of EETs compared to hydrogen peroxide (i.e. 50 nM external EETs to rescue against the effects of mM hydrogen peroxide or μM doxorubicin concentrations) provides evidence against the latter mechanism. It is unlikely that EETs would be able to directly protect against levels that are in excess, and so signal amplification is the most likely cause of mitigation of any ROS toxicity observed.

This response to ROS by *CYP2J2* is unique to this isozyme because other drug metabolizing CYPs are typically down-regulated in times of disease and stress (Xu *et al.*, 2006; Morgan *et al.*, 2008; Morgan, 2009). This is of special interest considering evidence suggesting

an interplay between heme oxygenase 1 (HO-1) and EET analogs as mitigators of adipogenesis during metabolic syndrome, as demonstrated by Sodhi et al. and others (Sodhi *et al.*, 2009; Sacerdoti *et al.*, 2016). Data from this study suggests a link between CYP2J2 and HO-1, specifically at the transcriptional level. We showed that transient silencing of *CYP2J2* expression consistently led to *HMOX1* upregulation. Additionally, when 11,12-EETs or 14,15-EETs were added externally to the cells, *HMOX1* and *PLA2G4C* expression was elevated (Figure 3.14). *HMOX1*, the gene that encodes HO-1, is a gene sensitive to redox state of the cell. Phospholipase A2, encoded by the *PLA2G4C* gene, cleaves stored AA and EETs from the cell membrane, promoting increases in EET levels. The same effects, however, are not observed when a mixture of the four EETs is introduced (Figure 3.14). This discrepancy could be due to reduced overall concentrations of the 11,12- and 14,15-EET isomers, which may not have reached a threshold necessary to affect *HMOX1* expression. The observed data is intriguing for several reasons; first, all EET regioisomer, including 5,6-EET and 8,9-EET protected the cell from ROS toxicity but only 11,12- and 14,15-EET were capable of increasing *HMOX1* mRNA transcript suggesting one or more alternate pathways by which EET regioisomers protect against ROS damage. This is not the first report of different regioisomers exhibiting different effects. Others have reported varying effects among the four regioisomers. For example, Mitra et al. found that in some tumors, 14,15-EET affects human tumor growth but not the other three isomers (Mitra *et al.*, 2011). While 11,12-EET and 14,15-EET separately appear to protect cardiomyocytes through the heme oxygenase pathway, introducing a mixture of EETs to the cardiomyocytes diminished any effect on the gene expression of *HMOX1*. This could be indicative of opposing actions by different EET isomers, but this is unlikely since all four isomers exhibit an overall protective effect on the cells. In combination, a different pathway or pathways to rescue could be activated

by EETs, which is difficult to tease out, especially given that very little is known about the 5,6-EET and 8,9-EET isomers, including how they might exert their effects on the cells and the elusive nature of an EET receptor. Taken together, our data suggests a role, perhaps multiple roles, for EETs and CYP2J2 in the oxidative stress response of ventricular myocytes. A dose-response and a time-response effect of the separate EETs on ventricular myocytes is necessary to tease the effects of each regioisomer.

Interestingly, *CYP2J2* expression is non-responsive to any of the EET isoforms, indicating that the enzyme is not controlled directly by its metabolites. Expression may be directly dependent on the amount of ROS rather than through a feedback loop with its arachidonic acid products. This may explain why antioxidants are able to affect gene expression, through the reduction of ROS in the cells while EETs do not affect *CYP2J2* gene expression at all. It is also entirely possible that feedback control may occur not with the EETs, but with their soluble epoxide hydrolase products, the DHETs. This possibility is unlikely, however, since external EETs are also subject to this degradation pathway and there would have been an increase in DHETs as well.

There are several complicating factors with determining whether EETs might act in a feedback mechanism (either negative or positive) and the most difficult to overcome is that like arachidonic acid, EETs can be stored in the lipid bilayer. To date no study has been able to provide precise intracellular levels of free (non-esterified) EETs. It is therefore also difficult to determine how much externally added EETs remain as free EETs. These molecules may yet regulate *CYP2J2* expression, however, our study design did not allow for this determination.

Increased production of reactive oxygen species and the subsequent oxidative stress is a hallmark of many diseases including type II diabetes, neurodegenerative disease and heart

disease (Giacco and Brownlee, 2010; Sugamura and Keaney, 2011; Tsutsui *et al.*, 2011; Brieger *et al.*, 2012). While it is not the sole causative factor in any of these diseases, it is a prominent aspect. Our results suggest an interplay between *CYP2J2* expression and the oxidative state of the cell.

Based on the data obtained here and by others, one possible mechanism is that EETs, or at least two of the EET isomers, as indicated above, trigger signaling cascades resulting in the upregulation of *HMOX1* and other antioxidant enzymes. HO-1 has long been identified as a protective enzyme with regards to oxidative stress. It catalyzes the metabolism of heme into biliverdin and free iron and in the process releases carbon monoxide (CO), a gasotransmitter that can act as an antioxidant (Rochette *et al.*, 2013; Otterbein *et al.*, 2016). Small amounts of ROS are beneficial to the cell as they trigger cascades that promote cell survival and proliferation (Zhang *et al.*, 2016). In this context, where EETs have previously been shown to promote cell growth and survival, upregulation of *CYP2J2* might be expected. Further, upregulation of *HMOX1* by EET isomers may represent a means by which signals triggered by ROS are terminated. In this manner, CYP2J2 would be part of a response signal to trigger growth and survival, while simultaneously initiating the reduction of ROS levels, through the upregulation of HO-1, ensuring that cells are not overwhelmed by prolonged damage stemming from elevated ROS levels. Our work suggests that CYP2J2, through EET production, can protect the cell against increased ROS levels, but the pathway that leads to this protection has not been elucidated and will be further characterized in future work.

To conclude, the *CYP2J2* gene expression is responsive to increasing ROS levels. Cells treated with either hydrogen peroxide or doxorubicin, which causes a rise in ROS levels, exhibit an upregulation in *CYP2J2* expression. In addition to modulation of expression by ROS, other

markers of cardiac disease should be investigated to determine what may alter CYP2J2 levels. Given the wide range of effects exhibited by EETs, it is very likely that CYP2J2 may respond to multiple stress factors that threaten proper cardiac function.

Figures & Figure Legends

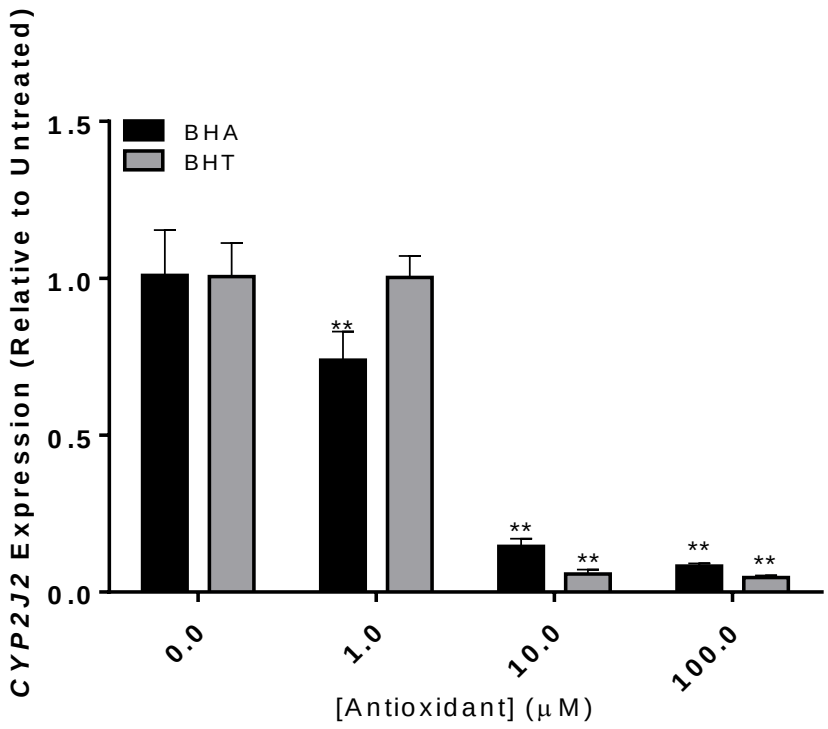

Figure 3.1. CYP2J2 expression in adult ventricular myocytes following 72h exposure to the antioxidants butylated hydroxyanisole and butylated hydroxytoluene. Decrease in expression shows a dose-dependent response to both antioxidants. Significance was determined using unpaired t-tests comparing expression at each concentration to the respective vehicle treated cells. ** $p < 0.01$.

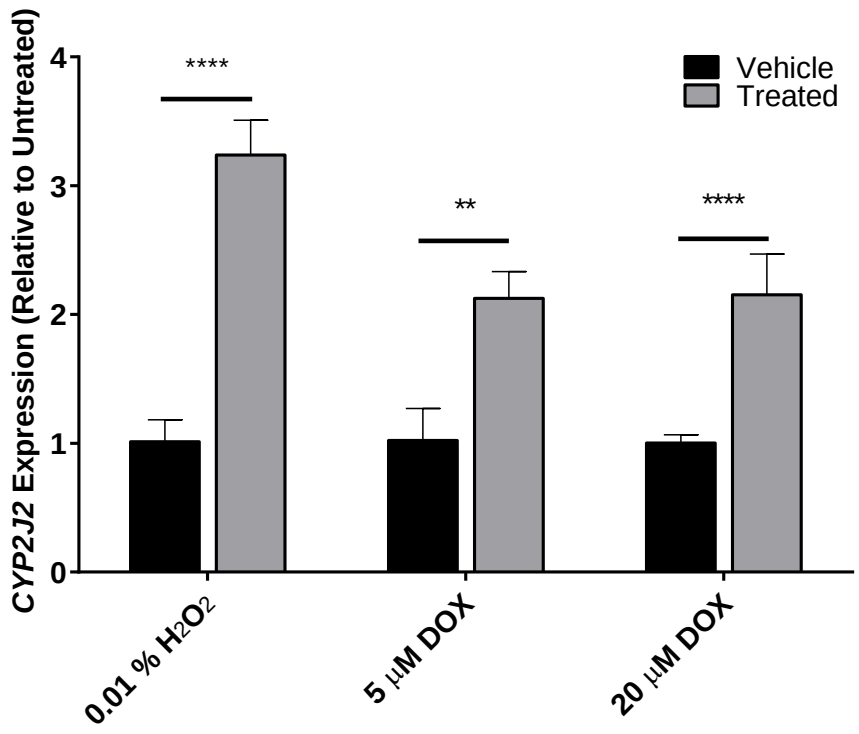

Figure 3.2. Ventricular myocytes treated with 0.01% H_2O_2 for six hours (left) and 20 μM doxorubicin for 24 hours (right). Each experiment was performed in triplicate (n=9 per condition). Data were normalized to vehicle treated cells (PBS for hydrogen peroxide and 0.1% DMSO for doxorubicin). Significance was determined using unpaired t-tests. **** $p < 0.0001$.

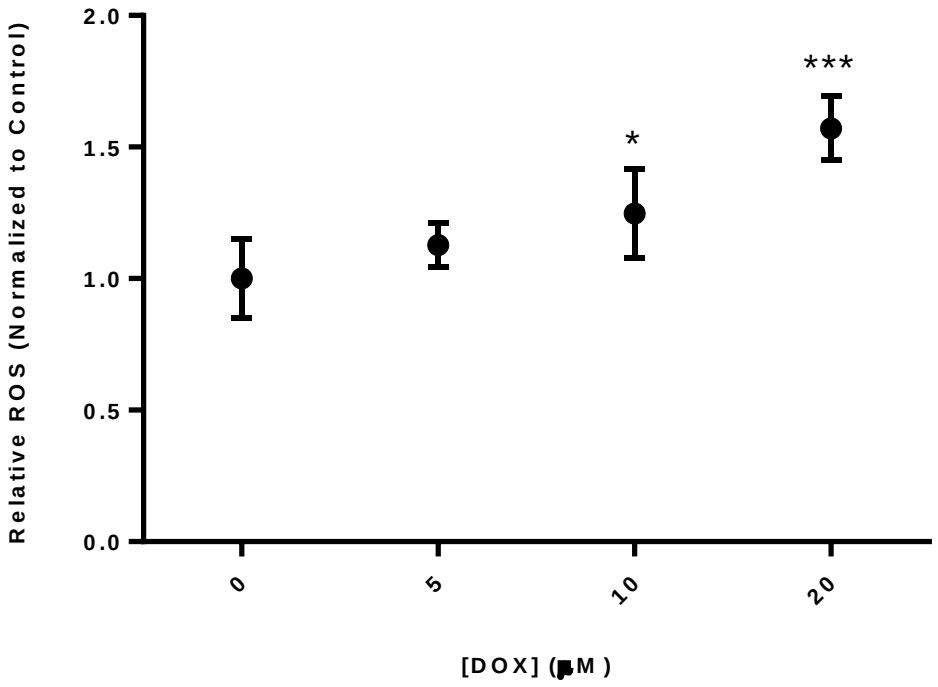

Figure 3.3. Relative ROS levels in adult human ventricular myocytes after 24 h of exposure to varying doxorubicin concentrations. Fluorescence values were normalized to vehicle control (0 μM DOX, 0.1% DMSO) to determine the relative intracellular ROS levels in cells with each concentration of DOX. Values reported are the mean ± SD of triplicates in a single experiment. Statistical significance was determined using unpaired t-tests. * $p < 0.05$, *** $p < 0.001$.

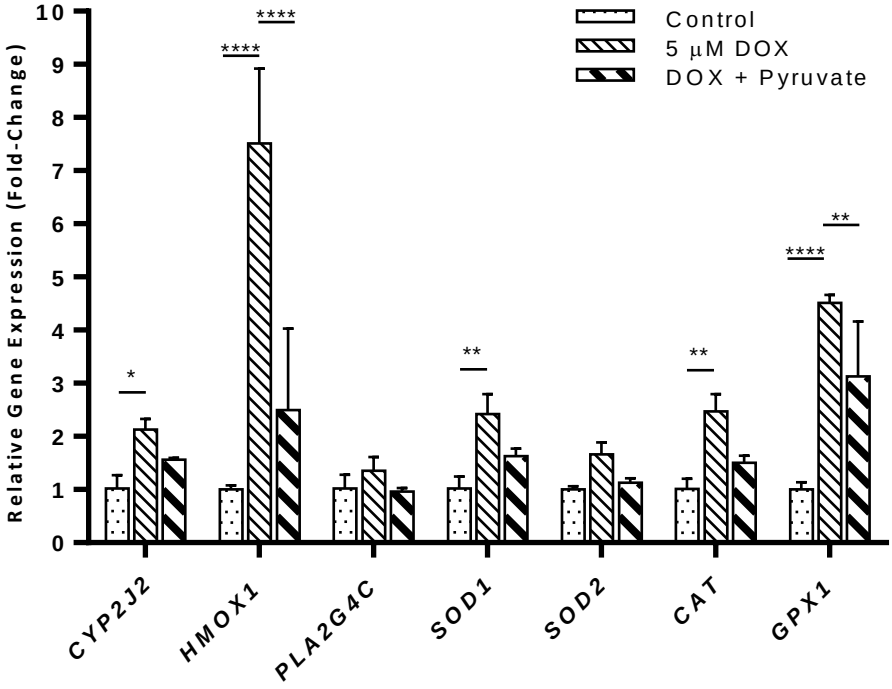

Figure 3.4. Fold changes in gene expression of a panel of genes following exposure of adult human ventricular myocytes to 5 μM doxorubicin, in the presence and absence of 10 mM pyruvate. Upregulation is mitigated when cells are exposed to doxorubicin (5 μM) and pyruvate (10 mM) simultaneously. Data shown are the mean ± SD of triplicates in a single experiment. Significance was determined using unpaired t-tests; * $p < 0.05$, ** $p < 0.01$, **** $p < 0.0001$.

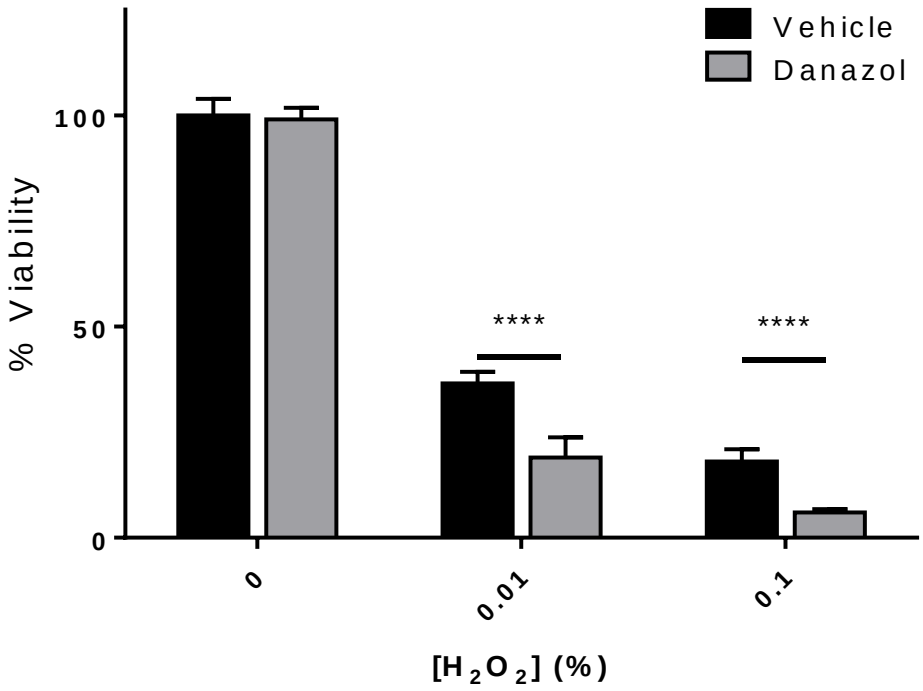

Figure 3.5. Adult ventricular myocytes treated with varying concentrations of hydrogen peroxide for six hours. Cells were co-treated with vehicle (0.1% DMSO) or 1 μM danazol, a known CYP2J2 inhibitor. The data presented are the mean and standard deviation of three separate experiments performed on three separate days, with each experiment in triplicate. Data are normalized to untreated cells. Significance determined using unpaired t-tests. **** $p < 0.0001$.

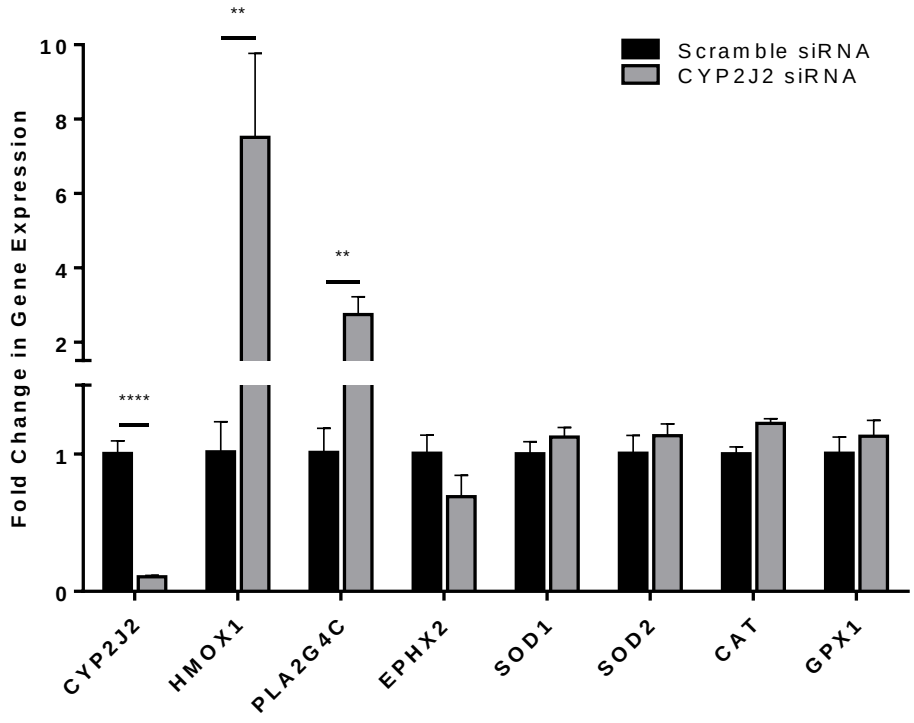

Figure 3.6. Representative figure of the effect of *CYP2J2* knocked down using siRNA for 72h on several genes. Data reported are a mean of a single experiment done in triplicates and the standard deviation. The experiment has been repeated multiple times on separate days. Data are normalized to control cells that were treated with scrambled siRNA, which were set to a value of one, to determine fold change in gene expression. Significance was determined using unpaired t-tests. ** $p < 0.01$ **** $p < 0.0001$.

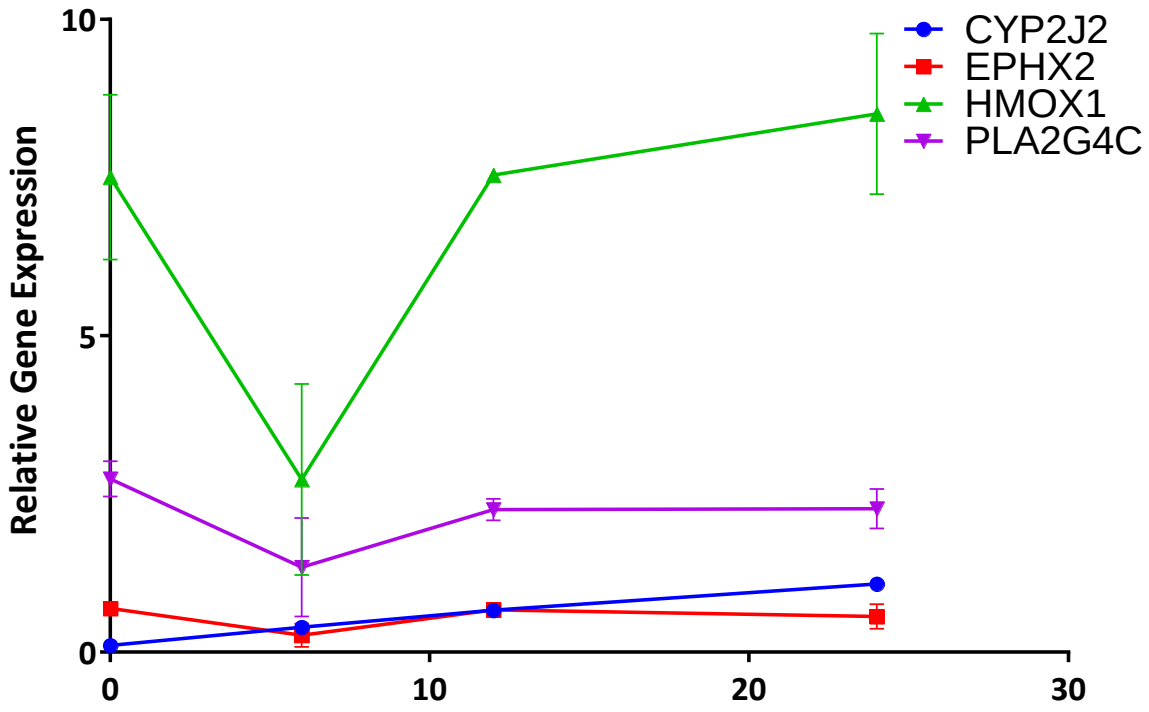

Figure 3.7. Representative plot of relative gene expression levels of *CYP2J2* (circles) and other genes related to EET production determined by RT-PCR following removal of siRNA. Data reported are a mean of a single experiment done in triplicates and the standard deviation. The experiment has been repeated multiple times on separate days, with similar results. Data are normalized to control cells that were treated with scrambled siRNA, which were set to a value of one, to determine fold change in gene expression.

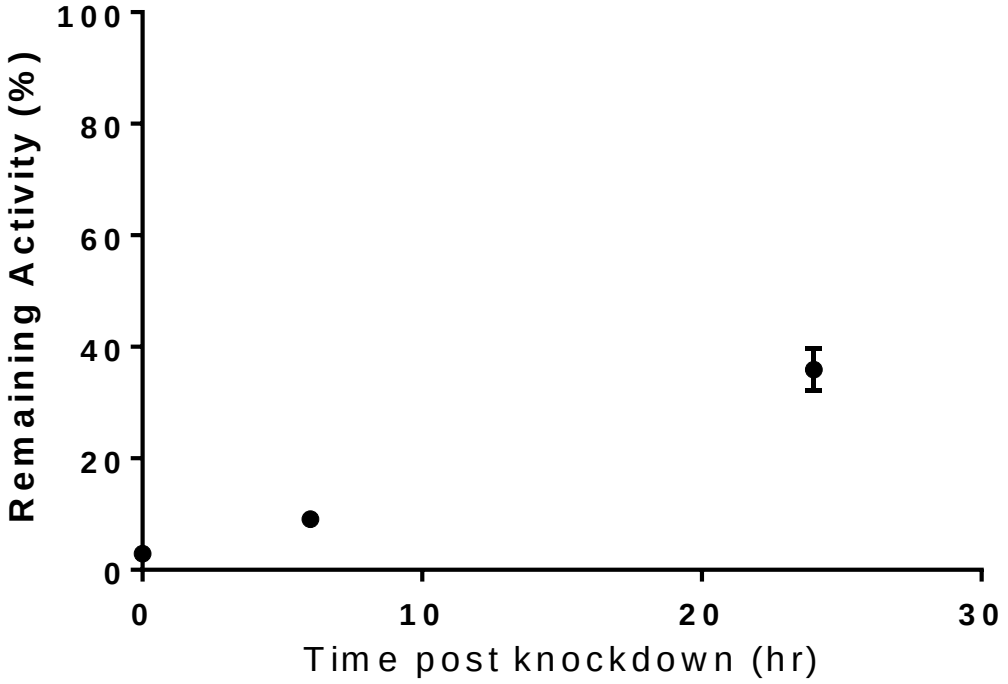

Figure 3.8. Representative plot of relative activity levels of CYP2J2 using terfenadine as a probe substrate following *CYP2J2* silencing. Data reported are a mean of a single experiment done in triplicates and the standard deviation. Data are normalized to the activity of scrambled siRNA treated cells for each time point, which were set to a value of 100 % activity, to determine fold change in gene expression.

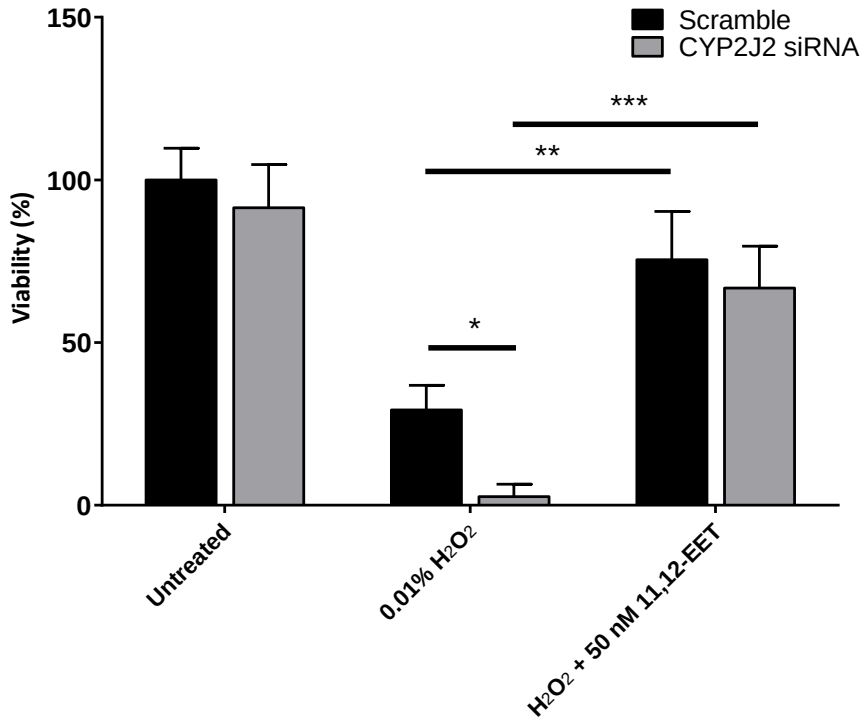

Figure 3.9. The effects of hydrogen peroxide treatment and 11,12-EET rescue on cells with diminished *CYP2J2* expression. Cells exposed to CYP2J2 siRNA were more susceptible to hydrogen peroxide toxicity compared to cells treated with scramble siRNA. The effect was reversed when cells were treated with 11,12-EET 30 min prior to hydrogen peroxide treatment following siRNA treatment. The data presented are the mean and standard deviation from a single experiment performed in triplicate and significance was determined using unpaired t-tests. * $p < 0.05$, ** $p < 0.01$, *** $p < 0.001$.

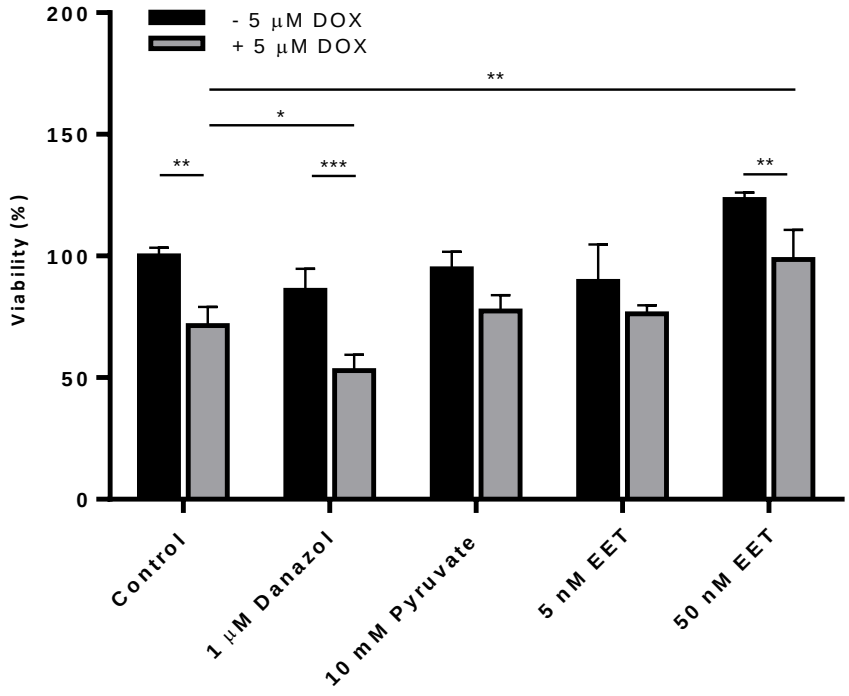

Figure 3.10. Cell viability of adult human ventricular myocytes treated with or without 5 μM DOX. Additional conditions (x-axis) were also tested in addition to exposure to doxorubicin. Data demonstrate that in the absence of additional stress, cell viability decreases 25% on average when exposed to doxorubicin (5 μM). When the CYP2J2 inhibitor danazol is added to this exposure, cell death is exacerbated. Finally, this decrease in cell viability is attenuated in the presence of either the antioxidant pyruvate or 11,12-EET (5 nM or 50 nM). The data presented on this figure are representative of the mean ± SD of triplicates in a single experiment. Significance was determined using unpaired t-tests; * $p < 0.05$, ** $p < 0.01$, *** $p < 0.001$.

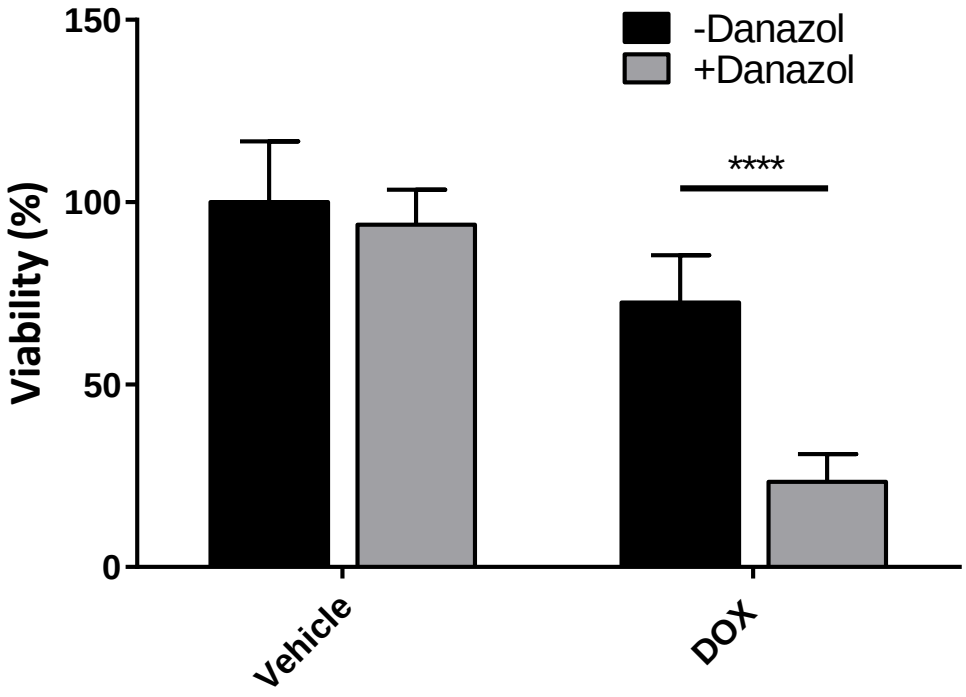

Figure 3.11. The effects of doxorubicin (20 μM for 24h) on adult cardiomyocyte viability in the presence and absence of the CYP2J2 inhibitor danazol. The effects of doxorubicin treatment are more pronounced when danazol is present. The data presented are the mean and standard deviation of three separate inter-day experiments, each done in triplicate. The data was normalized to cells that were treated with neither danazol nor doxorubicin. Significance was determined using unpaired t-tests. **** $p < 0.0001$.

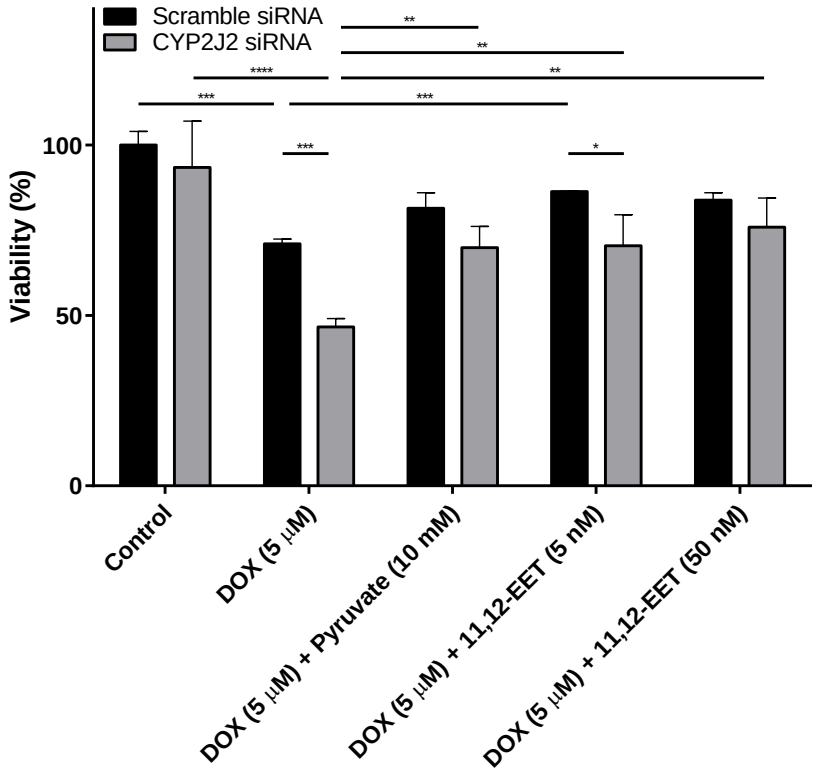

Figure 3.12. Cell viability of adult ventricular myocytes when *CYP2J2* is silenced and then exposed to doxorubicin (5 μM). Gene silencing by itself does not affect cell viability, however exposure to doxorubicin results in increased cell death with greater cell death occurring among cells with *CYP2J2* expression silenced. Additionally, this decrease in cell viability can be mitigated by the addition of the antioxidant pyruvate (10 mM) or 11,12-EET (5 nM or 50 nM). The data presented are the mean ± SD of triplicates in a single experiment. Significance was determined using unpaired t-tests; * $p < 0.05$, ** $p < 0.01$, *** $p < 0.001$, **** $p < 0.0001$.

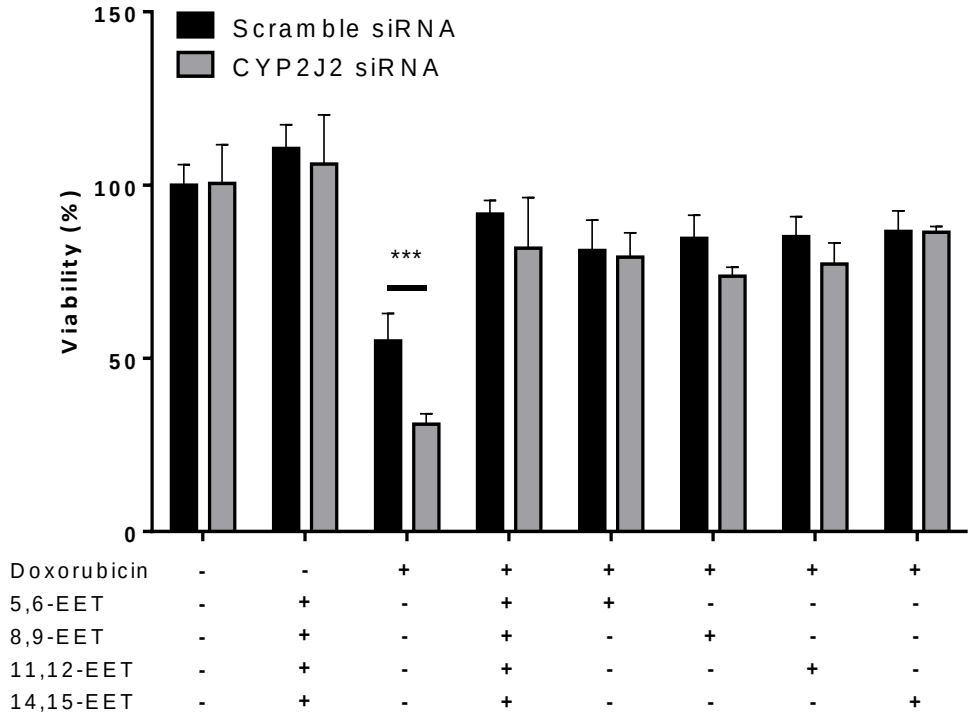

Figure 3.13. The effects of doxorubicin (20 μM, 24 h) on adult cardiomyocyte viability with reduced CYP2J2 expression due to 72 h silencing with siRNA. The effects of co-treatment with EETs (50 nM total) on cell viability, using either combination or individual EETs. The data presented are the mean and standard deviation of a single experiment in triplicate. Data were normalized to cells treated with scrambled siRNA for 72h, followed by vehicle treatment for 24 hours and p-values were determine using unpaired t-tests. *** $p < 0.001$.

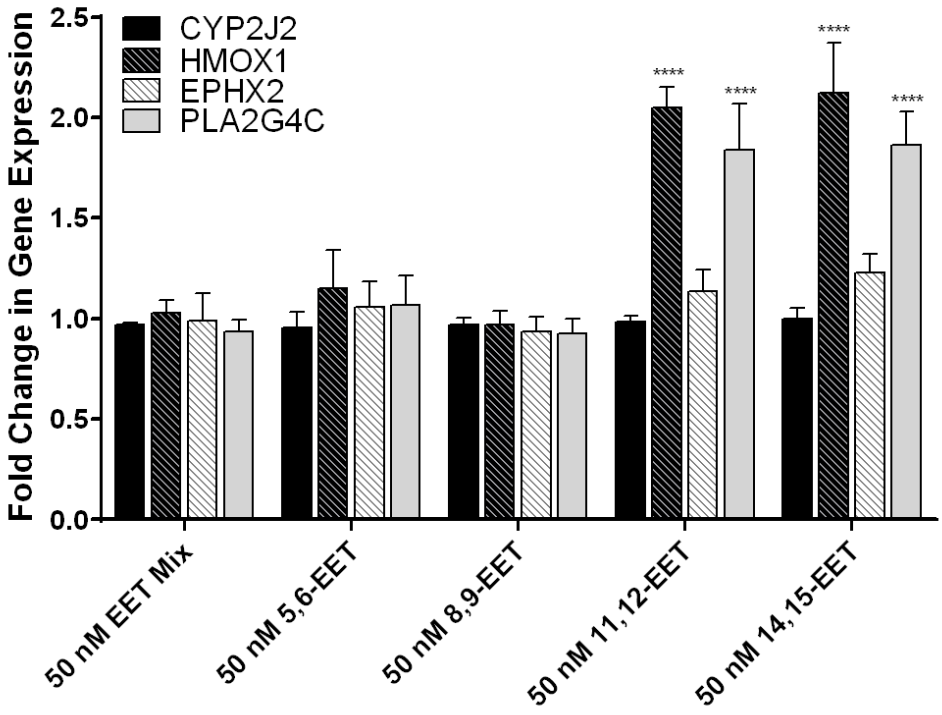

Figure 3.14. Gene expression in adult cardiomyocytes in response to EETs treatment, in combination or individually (50 nM total concentration). In combination, EETs do not appear to affect the gene expression of *CYP2J2, HMOX1, EPHX2,* or *PLA2G4C*. The same appears to be the case when cells are treated with 50 nM 5,6-EET or 8,9-EET. When the cells are treated with 11,12-EET or 14,15-EET however, *HMOX1* and *PLA2G4C* are upregulated up to 2-fold when compared to negative controls. Significance and p-values were determined using unpaired t-tests. **** $p < 0.0001$.

References

Alsaad AMS, Zordoky BNM, El-Sherbeni AA, and El-Kadi AOS (2012) Chronic doxorubicin cardiotoxicity modulates cardiac cytochrome P450-mediated arachidonic acid metabolism in rats. *Drug Metab Dispos* **40**:2126–2135.

Asperen J van, Tellingen O van, Tijssen F, Schinkel AH, and Beijnen JH (1999) Increased accumulation of doxorubicin and doxorubicinol in cardiac tissue of mice lacking mdr1a P-glycoprotein. *Br J Cancer* **79**:108–113, Nature Publishing Group.

Barpe DR, Rosa DD, and Froehlich PE (2010) Pharmacokinetic evaluation of doxorubicin plasma levels in normal and overweight patients with breast cancer and simulation of dose adjustment by different indexes of body mass. *Eur J Pharm Sci* **41**:458–463, Elsevier.

Behm DJ, Ogbonna A, Wu C, Burns-Kurtis CL, and Douglas SA (2009) Epoxyeicosatrienoic Acids Function as Selective, Endogenous Antagonists of Native Thromboxane Receptors: Identification of a Novel Mechanism of Vasodilation. *J Pharmacol Eperimental Ther* **328**:231–39.

Benjamin EJ, Muntner P, Alonso A, Bittencourt MS, Callaway CW, Carson AP, Chamberlain AM, Chang AR, Cheng S, Das SR, Delling FN, Djousse L, Elkind MS V, Ferguson JF, Fornage M, Jordan LC, Khan SS, Kissela BM, Knutson KL, Kwan TW, Lackland DT, Lewis TT, Lichtman JH, Longenecker CT, Loop MS, Lutsey PL, Martin SS, Matsushita K, Moran AE, Mussolino ME, O'Flaherty M, Pandey A, Perak AM, Rosamond WD, Roth GA, Sampson UKA, Satou GM, Schroeder EB, Shah SH, Spartano NL, Stokes A, Tirschwell DL, Tsao CW, Turakhia MP, VanWagner LB, Wilkins JT, Wong SS, Virani SS, and American Heart Association Council on Epidemiology and Prevention Statistics Committee

and Stroke Statistics Subcommittee (2019) Heart Disease and Stroke Statistics-2019 Update: A Report From the American Heart Association. *Circulation* **139**:e56–e528.

Bouitbir J, Charles A-L, Echaniz-Laguna A, Kindo M, Dé F, Daussin R, Auwerx J, Piquard F, Geny B, and Zoll J (2012) Opposite effects of statins on mitochondria of cardiac and skeletal muscles: a "mitohormesis" mechanism involving reactive oxygen species and PGC-1. *Eur Heart J* **33**:1397–1407.

Brieger K, Schiavone S, Miller Jr. FJ, and Krause K-H (2012) Reactive oxygen species: from health to disease. *Swiss Med Wkly*.

Bystrom J, Thomson SJ, Johansson J, Edin ML, Zeldin DC, Gilroy DW, Smith AM, and Bishop-Bailey D (2013) Inducible CYP2J2 and Its Product 11,12-EET Promotes Bacterial Phagocytosis: A Role for CYP2J2 Deficiency in the Pathogenesis of Crohn's Disease? *PLoS One* **8**.

Cai Z, Zhao G, Yan J, Liu W, Feng W, Ma B, Yang L, Wang J, Tu L, and Wang DW (2013) CYP2J2 overexpression increases EETs and protects against angiotensin II-induced abdominal aortic aneurysm in mice. *J Lipid Res* **54**:1448–1456, American Society for Biochemistry and Molecular Biology.

Campbell WB, and Fleming I (2010) Epoxyeicosatrienoic acids and endothelium-dependent responses. *Pflugers Arch* **459**:881–95.

Chaudhary KR, Batchu SN, and Seubert JM (2009) Critical Review Cytochrome P450 Enzymes and the Heart. *IUBMB Life* **61**:954–960.

Chen F, Chen C, Yang S, Gong W, Wang Y, Cianflone K, Tang J, and Wang DW (2012) Let-7b

inhibits human cancer phenotype by targeting cytochrome P450 epoxygenase 2J2. *PLoS One* **7**:e39197.

Chen G, Xu R, Zhang S, Wang Y, Wang P, Edin ML, Zeldin DC, and Wang DW (2015) CYP2J2 overexpression attenuates non-alcoholic fatty liver disease induced by high fat diet in mice. *Am J Physiol Endocrinol Metab* **308**:E97–E110.

Damiani RM, Moura DJ, Viau CM, Caceres RA, Henriques JAP, and Saffi J (2016) Pathways of cardiac toxicity: comparison between chemotherapeutic drugs doxorubicin and mitoxantrone. *Arch Toxicol* **90**:2063–2076.

Delozier TC, Kissling GE, Coulter SJ, Dai D, Foley JF, Bradbury JA, Murphy E, Steenbergen C, Zeldin DC, and Goldstein JA (2007) Detection of human CYP2C8, CYP2C9, and CYP2J2 in cardiovascular tissues. *Drug Metab Dispos* **35**:682–688.

Evangelista EA, Kaspera R, Mokadam NA, Jones III JP, and Totah RA (2013) Activity, inhibition, and induction of cytochrome P450 2J2 in adult human primary cardiomyocytes. *Drug Metab Dispos* **41**.

Evangelista EA, Lemaitre RN, Sotoodehnia N, Gharib SA, and Totah RA (2018) CYP2J2 expression in adult ventricular myocytes protects against reactive oxygen species toxicity. *Drug Metab Dispos* **46**.

Finkel T (2011) Signal transduction by reactive oxygen species. *J Cell Biol* **194**:7–15.

Franco R, Panayiotidis MI, and Cidlowski JA (2007) Glutathione depletion is necessary for apoptosis in lymphoid cells independent of reactive oxygen species formation. *J Biol Chem* **282**:30452–30465, American Society for Biochemistry and Molecular Biology.

Giacco F, and Brownlee M (2010) Oxidative Stress and Diabetic Complications. *Circ Res* **107**:1058–1070.

Greene RF, Collins JM, Jenkins JF, Speyer JL, and Myers CE (1983) Plasma pharmacokinetics of adriamycin and adriamycinol: implications for the design of in vitro experiments and treatment protocols. *Cancer Res* **43**:3417–21, American Association for Cancer Research.

Ichikawa Y, Ghanefar M, Bayeva M, Wu R, Khechaduri A, Prasad SVN, Mutharasan RK, Naik TJ, and Ardehali H (2014) Cardiotoxicity of doxorubicin is mediated through mitochondrial iron accumulation. *J Clin Invest* **124**:617–30.

Jiang J-G, Chen C-L, Card JW, Yang S, Chen J-X, Fu X-N, Ning Y-G, Xiao X, Zeldin DC, and Wang DW (2005) Cytochrome P450 2J2 promotes the neoplastic phenotype of carcinoma cells and is up-regulated in human tumors. *Cancer Res* **65**:4707–15.

Laniado-Schwartzman M, Davis KL, McGiff JC, Levere RD, and Abraham NG (1988) Purification and characterization of cytochrome P-450-dependent arachidonic acid epoxygenase from human liver. *J Biol Chem* **263**:2536–42.

Larsen BT, Campbell WB, and Gutterman DD (2007) Beyond vasodilatation: non-vasomotor roles of epoxyeicosatrienoic acids in the cardiovascular system. *Trends Pharmacol Sci* **28**:32–38.

Lee AC, and Murray M (2010) Up-Regulation of Human CYP2J2 in HepG2 Cells by Butylated Hydroxyanisole Is Mediated by c-Jun and Nrf2. *Mol Pharmacol* **77**:987–994.

Lee CA, Iii JPJ, Katayama J, Jiang Y, Freiwald S, Smith E, Walker GS, Totah RA, Al LEEET, Jones JP, Katayama J, Kaspera R, Jiang Y, Freiwald S, Smith E, Walker GS, Totah RA, Iii

JPJ, Katayama J, Jiang Y, Freiwald S, Smith E, Walker GS, Totah RA, and Al LEEET (2012) Identifying a selective substrate and inhibitor pair for the evaluation of CYP2J2 activity. *Drug Metab Dispos* **40**:943–951.

Lee CA, Neul D, Clouser-Roche A, Dalvie D, Wester MR, Jiang Y, Jones III JP, Freiwald S, Zientek M, Totah RA, Laboratories DJ, Diego S, California C a L, and Al LEEET (2010) Identification of Novel Substrates for Human Cytochrome. *Drug Metab Dispos* **38**:347–356.

Livak KJ, and Schmittgen TD (2001) Analysis of Relative Gene Expression Data Using Real-Time Quantitative PCR and the 2 ⁒⌬⌬C T Method. *METHODS* **25**:402–408.

Ma B, Xiong X, Chen C, Li H, Xu X, Li X, Li R, Chen G, Dackor RT, Zeldin DC, and Wang DW (2013) Cardiac-specific overexpression of CYP2J2 attenuates diabetic cardiomyopathy in male streptozotocin-induced diabetic mice. *Endocrinology* **154**:2843–56.

Maillet A, Tan K, Chai X, Sadananda SN, Mehta A, Ooi J, Hayden MR, Pouladi MA, Ghosh S, Shim W, and Brunham LR (2016) Modeling Doxorubicin-Induced Cardiotoxicity in Human Pluripotent Stem Cell Derived-Cardiomyocytes. *Sci Rep* **6**:25333, Nature Publishing Group.

Michaud V, Frappier M, Dumas M, and Turgeon J (2010) Metabolic Activity and mRNA Levels of Human Cardiac CYP450s Involved in Drug Metabolism. *PLoS One* **5**.

Mitra R, Guo Z, Milani M, Mesaros C, Rodriguez M, Nguyen J, Luo X, Clarke D, Lamba J, Schuetz E, Donner DB, Puli N, Falck JR, Capdevila J, Gupta K, Blair IA, and Potter DA (2011) CYP3A4 mediates growth of estrogen receptor-positive breast cancer cells in part by inducing nuclear translocation of phospho-Stat3 through biosynthesis of (±)-14,15-

epoxyeicosatrienoic acid (EET). *J Biol Chem* **286**:17543–59.

Morgan ET (2009) Impact of infectious and inflammatory disease on cytochrome P450-mediated drug metabolism and pharmacokinetics. *Clin Pharmacol Ther* **85**:434–438.

Morgan ET, Goralski KB, Piquette-Miller M, Renton KW, Robertson GR, Chaluvadi MR, Charles KA, Clarke SJ, Kacevska M, Liddle C, Richardson TA, Sharma R, Sinal CJ, and Dan L (2008) Regulation of Drug-Metabolizing Enzymes and Transporters in Infection, Inflammation, and Cancer. *Drug Metab Dispos* **36**:205–216.

Murray M (2016) CYP2J2 – regulation, function and polymorphism. *Drug Metab Rev* **48**:351–368.

Oliw EH (1994) Oxygenation of polyunsaturated fatty acids by cytochrome P450 monooxygenases. *Prog Lipid Res* **33**:329–54.

Oliw EH, Guengerich FP, and Oates JA (1982) Oxygenation of arachidonic acid by hepatic monooxygenases. Isolation and metabolism of four epoxide intermediates. *J Biol Chem* **257**:3771–81.

Otterbein LE, Foresti R, and Motterlini R (2016) Heme Oxygenase-1 and Carbon Monoxide in the Heart. *Circ Res* **118**:1940–1959.

Pfister SL, Gauthier KM, and Campbell WB (2010) Vascular Pharmacology of Epoxyeicosatrienoic Acids, in *Advances in Pharmacology* pp 27–59.

Rochette L, Cottin Y, Zeller M, and Vergely C (2013) Carbon monoxide: Mechanisms of action and potential clinical implications. *Pharmacol Ther* **137**:133–152.

Roman RJ (2002) P -450 Metabolites of Arachidonic Acid in the Control of Cardiovascular

Function. *Physiol Rev* **82**:131–185.

Sacerdoti D, Pesce P, Pascoli M Di, and Bolognesi M (2016) EETs and HO-1 cross-talk. *Prostaglandins Other Lipid Mediat* **125**:65–79.

Schieber M, and Chandel NS (2014) ROS Function in Redox Signaling and Oxidative Stress. *Curr Biol* **24**:453–462.

Sodhi K, Inoue K, Gotlinger KH, Canestraro M, Vanella L, Dong H, Kim VL, Manthati S, Reddy K, Falck JR, Schwartzman ML, and Abraham NG (2009) Epoxyeicosatrienoic Acid Agonist Rescues the Metabolic Syndrome Phenotype of HO-2-Null Mice. *J Pharmacol Exp Ther* **331**:906–916.

Sugamura K, and Keaney JF (2011) Reactive Oxygen Species in Cardiovascular Disease. *Free Radic Biol Med* **51**:978–92.

Tsutsui H, Kinugawa S, and Matsushima S (2011) Oxidative stress and heart failure. *Am J Physiol - Hear Circ Physiol* **301**:H2181–H2190.

Westphal C, Spallek B, Konkel A, Marko L, Qadri F, DeGraff LM, Schubert C, Bradbury JA, Regitz-Zagrosek V, Falck JR, Zeldin DC, Müller DN, Schunck W-HH, and Fischer R (2013) CYP2J2 Overexpression Protects against Arrhythmia Susceptibility in Cardiac Hypertrophy. *PLoS One* **8**:e73490, Public Library of Science.

Wu S, Moomaw CR, Tomer KB, Falck JR, and Zeldin DC (1996) Molecular cloning and expression of CYP2J2, a human cytochrome P450 arachidonic acid epoxygenase highly expressed in heart. *J Biol Chem* **271**:3460–8.

Xu D-X, Wang J-P, Sun M-F, Chen Y-H, and Wei W (2006) Lipopolysaccharide downregulates

the expressions of intestinal pregnane X receptor and cytochrome P450 3a11. *Eur J Pharmacol* **536**:162–170.

Yang S, Lin L, Chen J-X, Lee CR, Seubert JM, Wang Y, Wang H, Chao Z-R, Tao D-D, Gong J-P, Lu Z-Y, Wen Wang D, and Zeldin DC (2007) Cytochrome P-450 epoxygenases protect endothelial cells from apoptosis induced by tumor necrosis factor-␣ via MAPK and PI3K/Akt signaling pathways. *Am J Physiol - Hear Circ Physiol* **293**:H142–H151.

Zeldin DC, Foley J, Goldsworthy SM, Cook ME, Boyle JE, Ma J, Moomaw CR, Tomer KB, Steenbergen C, and Wu S (1997) CYP2J subfamily cytochrome P450s in the gastrointestinal tract: expression, localization, and potential functional significance. *Mol Pharmacol* **51**:931–943, American Society for Pharmacology and Experimental Therapy.

Zhang J, Wang X, Vikash V, Ye Q, Wu D, Liu Y, and Dong W (2016) ROS and ROS-Mediated Cellular Signaling. *Oxid Med Cell Longev* **2016**:4350918–4350965.

Zhang Y, El-Sikhry H, Chaudhary KR, Batchu SN, Shayeganpour A, Jukar TO, Bradbury JA, Graves JP, DeGraff LM, Myers P, Rouse DC, Foley J, Nyska A, Zeldin DC, and Seubert JM (2009) Overexpression of CYP2J2 provides protection against doxorubicin-induced cardiotoxicity. *Am J Physiol - Hear Circ Physiol* **297**:H37–H46, American Physiological Society.

Zordoky BNM, Anwar-Mohamed A, Aboutabl ME, and El-Kadi AOS (2010) Acute doxorubicin cardiotoxicity alters cardiac cytochrome P450 expression and arachidonic acid metabolism in rats. *Toxicol Appl Pharmacol* **242**:38–46.

Chapter 4: CYP2J2 regulation by hypoxia in adult ventricular myocytes

4.1 Introduction

Hypoxia is a physiological condition characterized by inadequate supply of oxygen to tissues, which leads to adverse consequences to the cells. Oxygen is a critical component of critical cellular processes, such as those involved in energy production through aerobic respiration and metabolism (Yeo, 2019). Hypoxia can be global, where the whole body is being deprived of oxygen, or it can be localized, where specific regions or tissues are not adequately oxygenated. Several conditions lead to hypoxia although not all of them are due to pathological origins. For example, high altitudes and strenuous exercise can reduce systemic oxygen and result in hypoxia. Alternatively, hypoxia can have pathological roots. Localized hypoxia, for example, can be caused by ischemia, where blood flow to specific tissues is blocked, leading to decreased oxygen supply, with significant effects on the physiological function of specific organ and organ systems. While hypoxia can affect any and all tissue types, its negative consequences on the cardiovascular system is of paramount importance.

In addition to having pathological roots, hypoxia is also linked to and can result in other pathologies, such as inflammation (Bartels *et al.*, 2013), cancer (Jiang *et al.*, 2005, 2009; Murray *et al.*, 2010), diabetes (Nyengaard *et al.*, 2004; Sada *et al.*, 2016; Norouzirad *et al.*, 2017), and cardiovascular disease (Semenza, 2014). Lack of oxygen can cause significant changes to various physiological processes at the cellular level (Abe *et al.*, 2017; Lee *et al.*, 2019). During strenuous exercise leading to global hypoxia, cells move from aerobic metabolism to anaerobic metabolism due to the lack of oxygen available to mitochondria (Yeo, 2019). Changes in gene expression, as consequences of hypoxia, are facilitated by the hypoxia inducible factor (HIF1)

pathway (Semenza, 1999; Taylor, 2008). HIF1 is a heterodimer, with α- and β-subunits, and is ubiquitously expressed. The α subunit, however, is immediately marked for degradation by HIFα-prolyl-4-hydroxylases in cells (Semenza, 1999; Marxsen *et al.*, 2004; Taylor, 2008). When oxygen levels are low or entirely absent, HIF1α degradation is halted, allowing the α and β units to dimerize and for the complex to translocate to the nucleus to accumulate and activate the expression of genes under its control, thus changing the mechanisms that allow for cell survival (Marxsen *et al.*, 2004; Kim *et al.*, 2006; Abe *et al.*, 2017).

There is significant evidence that CYP2J2 overexpression and EETs are protective against ischemia related injuries (Seubert *et al.*, 2004; Li *et al.*, 2012; Chaudhary *et al.*, 2013). Specifically, others have demonstrated a role for this enzyme in minimizing damage or enhancing recovery following ischemia-reperfusion injury, particularly in the heart (Seubert *et al.*, 2004; Imig, 2012; Chaudhary *et al.*, 2013; Chen *et al.*, 2014; Zhu *et al.*, 2020). Previously, Marden et al. demonstrated that expression of *CYP2J2* was downregulated in the HepG2 hepatocarcinoma-derived cell line cultured under hypoxic conditions (Marden *et al.*, 2003), indicating that hypoxia is able to modulate expression of this enzyme. Our lab previously investigated regulation of CYP2J2 in cardiomyocytes using butylated hydroxyanisole and butylated hydroxytoluene, compounds that other have shown to be able to increase *CYP2J2* expression in HepG2 cells (Lee and Murray, 2010; Evangelista *et al.*, 2013). Our findings were contrary to Lee et al., indicating that CYP2J2 may be differentially regulated between tissue types. The apparent importance that this enzyme plays in cardioprotection following injury due to periods of hypoxia and re-oxygenation highlights a need to understand how low oxygen levels affect *CYP2J2* expression and how loss of *CYP2J2* affects cell response to hypoxia.

Given the large body of evidence demonstrating a protective role for CYP2J2 and EETs in pathologies involving localized hypoxia, we measured the CYP2J2 protein level in human ventricular tissue from control patients compared with patients with ischemic cardiomyopathy. We also determined the effects of hypoxia on *CYP2J2* expression in a human adult-derived ventricular myocyte model using a hypoxic chamber to culture the cells under reduced oxygen tension, as well as cobalt chloride, a chemical used to mimic hypoxia, and compared changes observed when the cells' hypoxic response was activated by different stresses. Further, we silenced *CYP2J2* expression and then subjected ventricular myocytes to hypoxic stresses to determine any differences in the survival of cells under hypoxic conditions.

4.2 Materials & Methods

Adult ventricular cardiac tissue

Ventricular tissue from seventeen individuals (n = 17) with ischemic cardiomyopathy were compared to ventricular tissue from seventeen individuals (N = 17: 10 males, 7 females) with no known cardiac or cardiovascular health issues were used as the control group. As previously outlined in Chapter 2, the Institutional Review Board at University of Washington determined that since the tissue source was anonymous, it was not human research (NHR) and therefore waived the need for ethical review and informed consent. This policy was in accordance with Office for Human Research Protections guidelines (www.hhs.gov/ohrp/policy/cdebiol.html). Tissue acquisition and demographic information are further outlined in Chapter 2.

Ventricular tissue processing and mRNA and protein quantification

Tissues were processed and CYP2J2 protein content was measured via mass spectrometry as previously outlined in chapter 2, following previously published protocols (Smith *et al.*, 1985; Aliwarga *et al.*, 2017; Xu *et al.*, 2017). Likewise, *CYP2J2* mRNA content was measured by rtPCR as outlined previously in chapter 2.

Adult cardiomyocyte culture protocol

Adult ventricular myocytes used in experiments in this chapter were obtained from Celprogen Inc. (La Jolla, CA). Culturing and passage of cells followed previously published

studies and outlined in previous chapters (Evangelista et al., 2013, 2018). All experiments were performed between passages 5-8 upon receipt from the vendor.

General chemicals and reagents

Unless otherwise specified, all reagents and solvents used in this study were obtained from Millipore Sigma (Burlington, MA) and/or ThermoFisher Scientific (Waltham, MA) and used without further alterations.

Hypoxic Chamber

In order to subject the cardiomyocyte to a hypoxic environment, cells were cultured in the Eppendorf Galaxy 48 R with 0.1-19% oxygen control (Eppendorf, Hamburg, Germany). Hypoxic conditions were defined as near-anoxic with 1% or 2.5% O_2, 5% CO_2, and 37 °C. Oxygen content was controlled through displacement with Medipure N_2 gas (cat# NI 5.0 UH-T, Praxair, Danbury, CT). Control cells were cultured under normoxic conditions with unaltered atmospheric levels of O_2, 5% CO_2 and 37 °C.

Hypoxia Experiments

Adult ventricular myocytes were plated at a density of 200,000 cells/mL in either 12-well plates (1 mL/well, 200,000 cells per well) or 6-well plates (2 mL/well, 400,000 cells/well). The cells were incubated overnight in complete media, allowing them time to attach. After 24 hours, the media was refreshed, and the cells were either kept at normoxic conditions or transferred to

hypoxic conditions and kept in those conditions for the appropriate amount of time. Variations on this experiment include time under hypoxia (0, 0.5, 1, 4, 6, 24) and the level of hypoxia (1% and 2.5% O_2).

Cobalt chloride effects on cardiomyocyte CYP2J2 activity, expression and cell viability

Cobalt chloride ($CoCl_2$) was used as a chemical hypoxia mimetic, as previously established by others (Okail, 2010; Nag and Resnick, 2017). The effects of $CoCl_2$ on CYP2J2 activity, cell viability and gene expression were tested. In order to determine $CoCl_2$ effects on CYP2J2 activity, cells were plated at a density of 50,000 cells per well and allowed to attach overnight on a 96-well plate. The cells were then gently washed with PBS and treated with the probe substrate terfenadine (1.5 μM) as outlined in previous chapters. Cells were also co-treated with varying concentrations of $CoCl_2$ (5, 10, 50, 100, 500, 1000 μM). After 2 hours, the reaction was quenched by addition of 100 μL ice cold acetonitrile containing the midazolam internal standard (0.05 μM final concentration) to each well, followed by gentle pipetting to disrupt and lyse the cells. The plates were then centrifuged (3000 x g, 10 min, 4°C) to pellet the cell debris and 100 μL of the supernatant was transferred to a fresh 96-well plate. Mass spectrometric methods outlined in previous chapters were then used to quantify terfenadine alcohol to determine levels of CYP2J2 activity inhibition by $CoCl_2$. Activity levels were normalized to cells not exposed to $CoCl_2$.

Cell viability following $CoCl_2$ exposure was determined by treated cells (plated and allowed to attach overnight in complete media) with varying concentrations of $CoCl_2$ in serum free media (0, 0.5, 1, 2.5, 5, 10, 25, 50 μM) for 24 hours. After 24 hours, cell viability was

determined using an MTT assay, and normalized to the viability of untreated cells (0 μM $CoCl_2$). The concentration range for both cell viability and gene expression concentration course were chosen due to the results of the activity assay where appreciable CYP2J2 (>20%) inhibition was observed at 50 μM.

In order to determine the effects of $CoCl_2$ on gene expression, cells were plated on 12-well plates at a density of 200,000 cells/well and allowed to attach overnight in complete media. After 24 hours, the cells were washed and treated with varying concentrations of $CoCl_2$ (0, 0.5, 1, 2.5, 5, 10, 25, 50 μM). Following 24 hours in treatment media, cells were washed and harvested and stored in -80 °C until RNA isolation/purification.

CYP2J2 silencing, hypoxia/$CoCl_2$ toxicity, and EET rescue

CYP2J2 gene expression was decreased by at least 80% using CYP2J2 human siRNA Trilencer oligo duplexes (Origene, Rockville, MD; cat# SR301109) delivered by RNAi MAX lipofectamine (Thermo Fisher Scientific, Waltham, MA), using protocols previously described (Evangelista et al 2018). Scrambled siRNA was similarly prepared in lipofectamine and used to treat control cells. Briefly, the siRNA was prepared with the lipofectamine using OptiMEM reduced serum media (Thermo Fisher Scientific) to a concentration of 50 nM. Cells were washed with warm (37°C) PBS and harvested using trypsin. Following trypsinization, cells were pelleted, resuspended and diluted to a concentration of 100,000 cells/ml in complete medium. The lipofectamine/siRNA stocks were added to each well to a final concentration of 10 nM siRNA, followed by the cells. Cells were incubated with the lipofectamine/siRNA for 72 hours, after which cells were exposed to hypoxia or $CoCl_2$.

After treatment with siRNA, the siRNA containing media was removed and the cells were then exposed to hypoxic atmosphere or to $CoCl_2$. Cells exposed to hypoxic conditions were placed in a hypoxic (1% O_2) chamber for 24 hours. Cells were also treated with varying concentrations (20, 40 and 60 μM) of $CoCl_2$ for 24 hours. The concentrations selected were previously determined to have no effect on CYP2J2 activity and resulted in reasonable *CYP2J2* downregulation and loss in viability, thus the effects observed at these concentrations are due to $CoCl_2$ eliciting the hypoxic response in these cells rather than interference with CYP2J2 activity.

The effects of *CYP2J2* expression downregulation on hypoxia and $CoCl_2$ toxicity were further assessed with rescue experiments. *CYP2J2* gene expression was silenced with siRNA as described above, however, prior to exposure to hypoxic conditions or $CoCl_2$, the cells were pre-treated with an EET mixture of all four isomers, or individual isomers, (50 nM final concentration) for 60 minutes. After 60 minutes of exposure to EETs, the cells were cultured in hypoxic conditions or treated with $CoCl_2$ for 24 hours as described above and then an MTT assay was used to determine relative differences in viability between treated and control cells, normalizing to the viability of cells cultured in normoxic (18-20% O_2) or cells untreated with cobalt chloride in each group.

MTT Assays to determine adult ventricular myocyte viability

After 24 hours of exposure to hypoxia or cobalt chloride, thiazolyl blue tetrazolium bromide (MTT, Sigma Aldrich, St Louis, MO) assays were performed to determine the relative cell viability among the treatment groups as previously described (Evangelista et al 2018). Following exposure to $CoCl_2$, the cells were exposed to MTT (60 μM) and incubated for 20

minutes at 37 °C. The medium was then carefully removed, and the colorimetric dye was resuspended in DMSO (600 μL) and Sorenson's glycine (75 μL, 100 mM glycine and 100 mM sodium chloride). The absorbance from each well was measured using a Tecan Infinite M200 plate reader (Tecan, Männedorf, Switzerland) using the following protocol: 5 seconds of orbital shaking with an amplitude of 1 mm, followed by 10 seconds of wait time, and then absorbance measurement at 570 nm (9 nm bandwidth) using 670 nm (9 nm bandwidth) as the reference wavelength. A true zero signal was obtained by following the same protocol using plates that did not contain cells. Measurements were normalized to the absorbance in $CoCl_2$ untreated control wells (set as 100% viability).

Total RNA isolation and qPCR

Total RNA was extracted using the MagMax 96 Total RNA Isolation kit (Thermo Fisher Scientific, Waltham MA). Initial RNA quality (A260/A280) and quantity was determined using a Synergy HTX Multi-Mode Reader (BioTek, Winooski VT). Total RNA was used to synthesize cDNA using the High Capacity RNA-to-cDNA kit (Thermo Fisher Scientific, Waltham MA). RT-PCR was then carried out using TaqMan (Thermo Fisher Scientific, Waltham MA) FAM reporter primers for *CYP2J2* as well as a housekeeping gene, *GUSB*. We used TaqMan primers for *HMOX1, GPX1, SOD1, SOD2*, and *CAT* to assay for the expression levels of these genes by RT-PCR following *CYP2J2* knockdown. Lastly, *CA9* (gene encoding the protein carbonic anhydrase 9) expression was used as a reporter for determining whether the cells had initiated the hypoxic response, as the gene is responsive to HIF1 activation. Cycle threshold (C_T) values and the ΔC_T method followed by the $2^{\Delta CT}$calculation were used to determine the relative quantity of CYP2J2 (and other genes) mRNA present relative to the *GUSB*. The mRNA levels were first

normalized to the housekeeping gene using the ΔC_T method and then the levels of expression in treated cells were compared to expression levels in untreated cells using the $\Delta\Delta C_T$ calculation and relative gene expression levels were reported using the $2^{-\Delta\Delta CT}$ calculation (Livak and Schmittgen, 2001).

4.3 Results

CYP2J2 mRNA and protein is lower in the ventricular tissue of patients with ischemic heart conditions than patients with no known cardiac issues.

RT-PCR and proteomic analysis of adult ventricular tissues show that CYP2J2 mRNA and protein expression show that on average, cases with ischemic cardiomyopathy have lower CYP2J2 than the control population (individuals with no known cardiovascular and/or cardiac disease) at both the mRNA and protein levels (Figure 4.1). Control tissue had a mean relative expression level of 21.02 as normalized *GUSB* content with a standard deviation of 15.02. The mean protein content was 0.38 pmol/mg membrane fraction with a standard deviation of 0.18 pmol/mg membrane fraction. In contrast ischemic cases had a mean relative mRNA content of 16.30 as normalized to *GUSB* (standard deviation of 14.15) and a mean protein content of 0.28 pmol/mg membrane fraction (standard deviation of 0.14 pmol/mg membrane fraction). However, a T-test performed between control and cases show the differences in mRNA and protein are not statistically significant with p values of 0.42 and 0.15, respectively.

Hypoxic conditions cause a 2-fold decrease in *CYP2J2* expression.

RT-PCR analysis of RNA isolated from cells cultured in hypoxic conditions results have reduced *CYP2J2* expression (Figure 4.2). Preliminary experiments were conducted at 2.5% O_2 due to technical limitations. Experiments were then conducted at 1% O_2 to simulate more extreme hypoxic conditions. Data shows that regardless, at such near anoxic conditions, *CYP2J2* gene expression is reduced approximately 50% (2-fold) when compared to matched cells grown in normoxic conditions. Statistical analyses using t-tests comparing expression in hypoxia vs

normoxic controls show statistically significant decreases in *CYP2J2* expression ($p < 0.05$). In order to ascertain just how *CYP2J2* expression was affected by hypoxia over a 24-hour period, we cultured cells in 1% O_2 and harvested cells at 0.5, 1, 4, 6, and 25 hours. RTPCR analysis shows that over a 24-hour period, *CYP2J2* expression does not appear to decrease immediately, but changes in expression are evident after cells have been exposed to the hypoxic atmosphere for approximately 6 hours (Figure 4.3).

In addition to *CYP2J2*, we also looked at gene expression for *CA9*, a gene under the control of HIF-1 and expressed under hypoxic conditions, as well as several oxidative stress-related genes: *HMOX1*, *GPX1*, *SOD1*, and *SOD2* (Figure 4.4). Expression of *CA9* begins to increase by 4 hours, indicating that the hypoxic response was under way, and continue to increase until the 24-hour time point. Finally, the oxidative stress response genes were, like *CYP2J2*, downregulated and were about 50% the levels found in cells grown under normoxic conditions after 24 hours.

Hypoxic conditions adversely affect cell viability after 24 hours.

In addition to changes in gene expression, changes in cell viability were measured using MTT assays at 6 and 24 h subjected to hypoxia. At six hours, no significant changes in cell viability were detected. In contrast, culturing cells in hypoxia over 24 hours results in a 25% loss of viability compared to cells cultured in normoxic conditions (Figure 4.5).

$CoCl_2$ appreciably inhibits CYP2J2 activity at high concentrations.

In addition to environmental hypoxia, we also tested the effects of the chemical hypoxia mimetic agent $CoCl_2$. The capacity of $CoCl_2$ to inhibit CYP2J2 activity was first tested to ensure that any effects observed were not due to CYP2J2 inhibition over a wide range of concentrations (0, 5, 10, 50, 100, 500 and 1000 μM) in cells (Figure 4.6). Inhibition of activity was observed starting at 10 μM at about 5-10% inhibition, with more significant (~20%) loss in activity at 50 μM $CoCl_2$ using terfenadine to probe CYP2J2 enzymatic activity. CYP2J2 Activity was inhibited by 40%, 90% and 99% at 100, 500 and 1000 μM, respectively.

$CoCl_2$ downregulates *CYP2J2* expression, turns on the hypoxic response, and places the cells under oxidative stress.

Gene expression analysis of cells treated with varying concentrations of $CoCl_2$ demonstrated that *CYP2J2* expression levels decreased in a dose dependent manner, with significant decreases observed at 25 and 50 μM, with levels reaching 40% and 60% expression compared to control, respectively (Figure 4.7A). Lower concentrations did not affect *CYP2J2* expression levels significantly. Examining *CA9* expression indicated that HIF1 response was not initiated until treatment with 25 μM of $CoCl_2$. At 25 μM, *CA9* expression increased 2-fold while at 50 μM, expression spiked 6-fold, indicating that the hypoxic response is initiated when the cells are treated with 50 μM $CoCl_2$ for 24 hours (Figure 4.7B). Lastly, analysis showed that at the higher concentrations of $CoCl_2$ tested, the cells had begun upregulating oxidative response genes such as *HMOX1,* increasing 10-fold at 25 μM, and 70-fold at 50 μM $CoCl_2$ (Figure 4.7C). Other oxidative stress responsive genes were not significantly affected, although superoxide dismutase

1 and 2 (*SOD1* and *SOD2*) showed modest, though not significant, increases in expression at 50 μM of $CoCl_2$ (Figure 4.7D).

$CoCl_2$ leads to dose dependent loss of viability of adult ventricular myocytes over 24 hours.

Adult ventricular myocytes exposed to varying (0-50 μM $CoCl_2$) were less viable in a dose-dependent manner (Figure 4.8). The cells did not show appreciable loss of viability at low concentrations (0.5 and 1 μM), but exhibited a 25% loss at 2.5 μM, 40% at 5 μM, 45% at 10 μM, 60% at 25 μM, and 75% at 50 μM.

External EETs can protect against hypoxia induced cell death.

Adult ventricular myocyte increased cell death due to hypoxia or $CoCl_2$ can be counteracted by the addition of external EETs to serum-free media prior to exposure to these stresses. With no EETs applied, there are no differences between scramble and downregulated cell viability under normoxia or hypoxia (Figure 4.9, "No EETs"). Interestingly, when cells are pre-treated with a mix of EETs (50 nM total), cells cultured under hypoxic conditions exhibited no significant difference in viability with cells treated with scrambled siRNA and grown in normoxic conditions. Cell with silenced *CYP2J2* and pre-treated with EETs prior to hypoxia, however, showed decreased viability compared to the other groups (Figure 4.9, "Mix"). When assessing the effects of individual EET isomers, all four isomers individually were able to mitigate the effects of hypoxia on cell death, regardless of whether the cells were treated with scrambled or *CYP2J2* siRNA. Viability is also reduced when cells have *CYP2J2* downregulated, treated with individual EET isomers (50 nM) relative to cells with basal CYP2J2 levels in

normoxia, but are not exposed to hypoxia, though these values were not significant except when treated with 14,15-EET. Finally, exposure of scrambled siRNA treated cells to 8,9-, 11,12-, and 14,15-EET, individually, showed >40% increase in cell death. This effect was not observed in scrambled siRNA treated cells treated with 5,6-EET, but not placed under hypoxia.

External EETs protect against $CoCl_2$ toxicity in normal and *CYP2J2* downregulated cardiomyocytes.

Lastly, we examined the role of CYP2J2 in hypoxia-induced toxicity in human cardiomyocytes exposed to $CoCl_2$, a hypoxia mimetic (Figure 4.10). CYP2J2 knockdown using siRNA decreased cell viability following cobalt chloride treatment. At 20 and 40 μM $CoCl_2$, cells treated with CYP2J2 siRNA had a greater cell death compared with cells treated with scrambled siRNA. At 60 μM $CoCl_2$, no difference in cell viability was observed in the absence of EETs. On the other hand, pretreatment with EETs at a concentration of 50 nM increased cell viability upon exposure to $CoCl_2$ (Figure 4.10). At 20 μM cobalt chloride, EET pretreatment increased cell viability to about 65-70%. At higher $CoCl_2$ concentration, cell viability was increased to 55-65% at 40 μM and to 40-55% at 60 μM.

4.4 Discussion

This study aimed to examine the effect of hypoxia on *CYP2J2* gene expression and explored how downregulation of *CYP2J2* expression influences adult ventricular myocytes response to hypoxic stress. Data shows that when cardiomyocytes are subjected to hypoxic stress, *CYP2J2* expression is decreased by approximately 50% (Figures 4.2 and 4.7). This data agrees with ventricular tissue observations that CYP2J2 mRNA and protein are lower in patients with ischemic cardiomyopathy. This occurs regardless of whether hypoxic conditions are achieved by reduced O_2 tension or via hypoxia mimetic agents such as $CoCl_2$. This reduction in *CYP2J2* expression may likely be due to atmospheric oxygen being a substrate for the enzyme. Thus, with reduced oxygen levels, productive enzyme activity would also decrease and become an energetic burden for the cells to synthesize new protein. This would explain why expression is not immediately downregulated, but rather delayed.

Near anoxic conditions were selected in order to ensure the cells were stressed by a hypoxic environment. Oxygen concentrations were measured in the chamber, not in the flask containing the cells nor the cells themselves. Even at these levels, gene expression analysis of *CA9* demonstrated that cells did not exhibit signs of hypoxic stress until after 6 hours of hypoxic conditions. Even at severe hypoxia, nearing anoxia, for 24 hours, gene expression is not completely ablated, instead being reduced only to 50% compared to cells grown in normoxic conditions. A similar observation applies to oxidative stress responsive genes, such as catalase (*CAT*), superoxide dismutase (*SOD*), and glutathione peroxidase (*GPX1*). This apparent maximal reduction in *CYP2J2* gene expression may be due to the time limitation of the experiment and it is possible that given a longer duration in hypoxic environments could result in greater downregulation. Alternatively, this could be an indication of a tight regulation on this enzyme's

expression. Previously, our lab has examined the potential for canonical CYP inducers to alter expression of *CYP2J2*, but our results indicated that this CYP isoform was resistant to chemical induction in adult ventricular myocytes. A resistance to exogenous induction and complete downregulation indicates an important physiological role for this enzyme that cells need to tightly regulate, even when energy is limited.

CA9 expression was used as a marker to determine whether the cells were under hypoxic stress and interestingly, the cells responded differently in modulating gene expression of common oxidative stress related genes depending on how the hypoxic response was activated. When hypoxia is induced atmospherically, the cells also downregulated genes such as heme oxygenase, glutathione peroxidase, and superoxide dismutase. This is consistent with the expression and production of these enzyme becoming an energetic burden on the cells with decreasing levels of oxygen to stress the cells, but also to limit ATP production. The same trends are not seen when cells are subjected to chemically induced hypoxic state, however, as heme oxygenase and superoxide dismutase genes are upregulated. *HMOX1* is robustly overexpressed in the presence of $CoCl_2$ while *SOD1* and *SOD2* exhibit modest upregulation. This indicates that chemically inducing hypoxia may trigger other stress responses beyond hypoxia. *CA9* upregulation confirms that HIF1 is at least stabilized under experimental conditions and able to activate expression of genes under its influence. The effects are not isolated to HIF1 and the hypoxic response pathways. However, since $CoCl_2$ can inhibit CYP2J2 activity as well, we were limited in the concentration range we are able to use. It is unknown at this time how this compound affects ventricular myocytes at the concentration used, beyond what was experimentally observed utilizing our study design. If *HMOX1* expression levels are any indication, it is possible that beyond eliciting the hypoxic response, $CoCl_2$ also induces heme

degradation pathways, providing a potential mechanism for CYP2J2 inhibition. Further, induction of *HMOX1* appears to occur at roughly the same concentration that elicits the hypoxic response, though the oxidative stress response is markedly stronger than the hypoxic response – i.e. that the overexpression of *HMOX1* is stronger than the rise in expression of *CA9*. This is the opposite of what we observed in cells cultured in a hypoxic environment, where *HMOX1* expression is unchanged, while *CA9* is overexpressed. Taken together, these data suggest that while $CoCl_2$ does induce a true hypoxic response in adult ventricular myocytes, there are other responses triggered, confounding the conclusions that may be drawn from the data.

Previous work by our lab (Aliwarga et al., *in press*) and others have shown CYP2J2 and EETs to be protective against damage brought about by ischemia in a transgenic mouse model. Our cell model currently does not include a reperfusion aspect, as they were not subjected to a period of acclimation to atmospheric conditions. An extensive body of knowledge suggests that much of the damage from ischemic conditions is due to oxygen reperfusion rather than the hypoxic phase. Low available oxygen levels are dangerous to cell survival, however, the oxidative damage that occurs during reperfusion following short periods of hypoxia is equally threatening. Our data shows that in addition to *CYP2J2* being downregulated under atmospheric hypoxia, many other oxidative response genes are also downregulated, providing a potential explanation as to why reperfusion is destructive to the cells. This may also explain why ventricular myocytes reach an apparent maximal downregulation of about 50% and why overexpression of CYP2J2 is protective against ischemia-reperfusion.

Work outlined and presented in chapter 3 showed that *CYP2J2* was protective against oxidative stress and silencing expression subjected the cells to greater loss in viability when exposed to increased ROS levels. This response is similar to what is observed when cells have

CYP2J2 silenced and are exposed to $CoCl_2$. Gene expression of oxidative stress genes suggest that cobalt chloride simultaneously induces an oxidative response in ventricular myocytes, however, *CYP2J2* expression is elevated in response. This may be due to the short time scale of the experiment, although as previously mentioned, the oxidative stress response was much stronger than the hypoxic response due to $CoCl_2$. In this case, *CYP2J2* overexpression should take priority over the effects of hypoxia, but this is not what was observed. While genes responsive to oxidative stress, such as *HMOX1*, *SOD1*, and *SOD2*, showed an upward trend in expression, *CYP2J2* remained downregulated, implying that hypoxia and HIF1 may have priority control over this gene's expression in comparison with the presence of cellular oxidative stress in cardiomyocytes.

Finally, we sought to determine whether siRNA downregulation of *CYP2J2* affected the ability of ventricular myocytes to survive under hypoxic conditions. Data obtained shows no real difference in the viability of cells under hypoxia, regardless of *CYP2J2* expression levels, with scrambled siRNA or CYP2J2 siRNA treated cells the viability dropped 15-20% under hypoxic conditions. External EETs were added to reverse the effects of hypoxia. A mixture of EETs resulted in reversing the loss of viability in siRNA treated cells, both scrambled and CYP2J2, but CYP2J2 siRNA treated cells cultured in normoxic environment were 25% less viable. Further when individual EET isomers were added, the effects persisted, with the added effect that individual addition of 8,9-, 11,12-, and 14,15-EET also resulted in loss of viability for scrambled siRNA treated cells cultured in normoxic conditions. It is unclear why loss in viability of siRNA treated cells is only observed under normoxic conditions, while under hypoxic conditions, viability is rescued. Previous experiments have shown no change in viability to cells treated with EETs, as a mix or individually. The present experiments were repeated with similar results.

Thus, the effects seem to be linked to siRNA, possibly lipofectamine. In the absence of an additional external pressure on the cell, i.e. hypoxia, it is possible that cells treated with lipofectamine may have adverse responses to EETs. These observations, while interesting, require further studies to delineate.

In contrast, adult ventricular myocytes treated with external EETs are protected from $CoCl_2$-induced hypoxia when expressing basal levels of *CYP2J2*. In cases where levels of expression were downregulated by siRNA, cells became more sensitive to the toxic effects of $CoCl_2$. Thus, exposure to $CoCl_2$ at these concentrations indicate that cells with low levels of *CYP2J2* expression are more susceptible to toxicity. These data indicate that the cardioprotective effects of *CYP2J2* expression can be attributed to bioactivation of AA into EETs. Due to the presumed short half-life of EETs, it is unclear as to what the *in vivo* intracellular free concentrations of EETs are. Unfortunately, our study design did not include measurement of EETs in these treated cell sample. Their rapid metabolism by soluble epoxide hydrolase combined with the fact that they can be stored in the cell membrane in a manner similar to arachidonic acid makes quantification of free EETs at specific time points difficult to measure. Further studies investigating the relationship between EET concentrations and cellular effect will need to be carried out, with EET receptor targets identified and tested.

In summary, the effects of hypoxia on *CYP2J2* expression are modest, resulting in a 2-fold down regulation of expression, even at or near anoxic levels of O_2. Further, hypoxia regulation has priority over the oxidative stress response observed in previous chapters, likely as a means of energy conservation when oxygen levels are low. The apparently maximal downregulation by the cells, however, indicates that CYP2J2 may not be completely silenced due to its protective role. In the context of hypoxia, this may be during oxygen reperfusion when

the sudden increase in oxygen levels result in sudden increases in oxidative stress. Lastly, loss of CYP2J2 does not appear to adversely affect adult ventricular myocyte viability significantly, though the external addition of EETs mitigates any loss of viability resulting from hypoxia.

Figures & Figure Legends

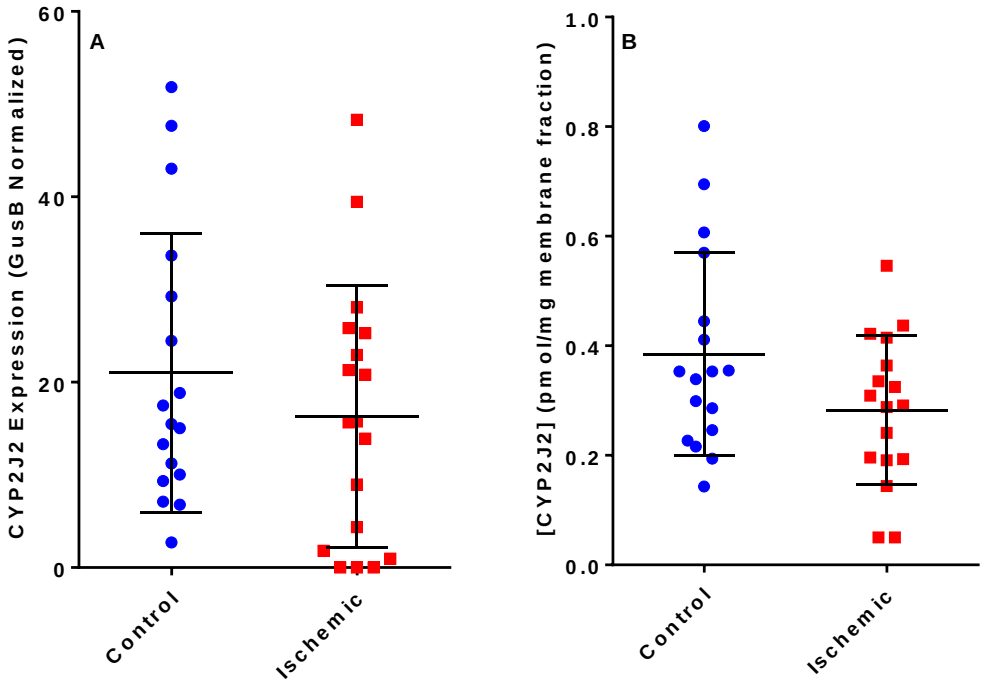

Figure 4.1. CYP2J2 mRNA and protein levels in ischemic cardiomyopathy human ventricular tissues (n=17) compared to control non-CVD ventricular tissue (n=17). On average, CYP2J2 levels are lower in ischemic tissues compared to healthy tissues at both the mRNA and protein levels. Statistical t-tests reveal that in our samples size, the means are not significantly different at either the mRNA (p=0.4) or protein (p=0.15) level.

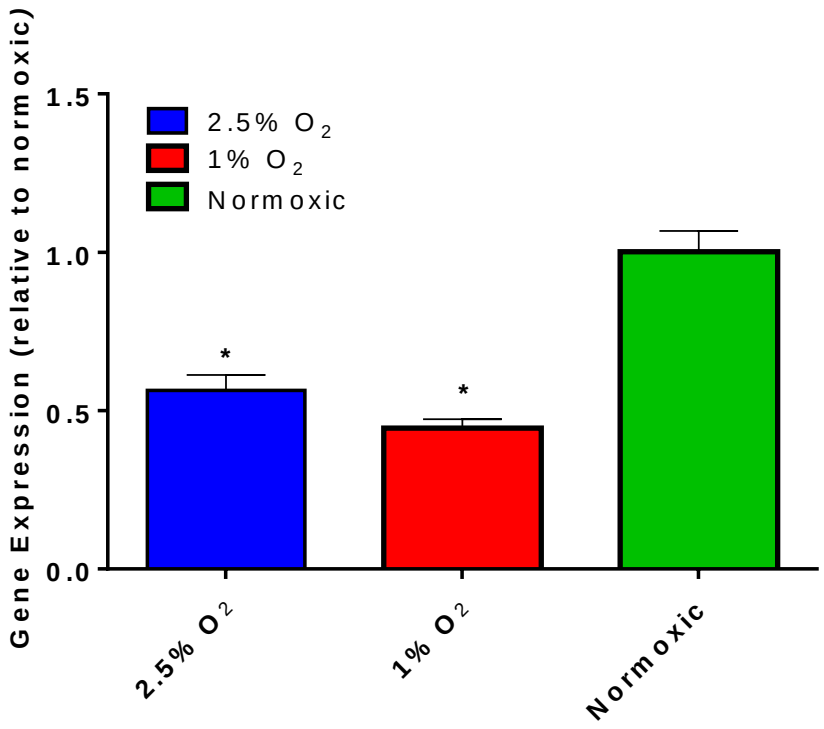

Figure 4.2. *CYP2J2* gene expression in adult ventricular myocytes when cultured under two concentrations of atmospheric oxygen, 1% and 2.5%. Expression was normalized to levels in cells cultured in normoxic (18% O_2). Statistical significance using t-tests comparing expression in hypoxic conditions to expression in normoxic conditions reveal a significant downregulation at the gene expression level. * $p < 0.05$.

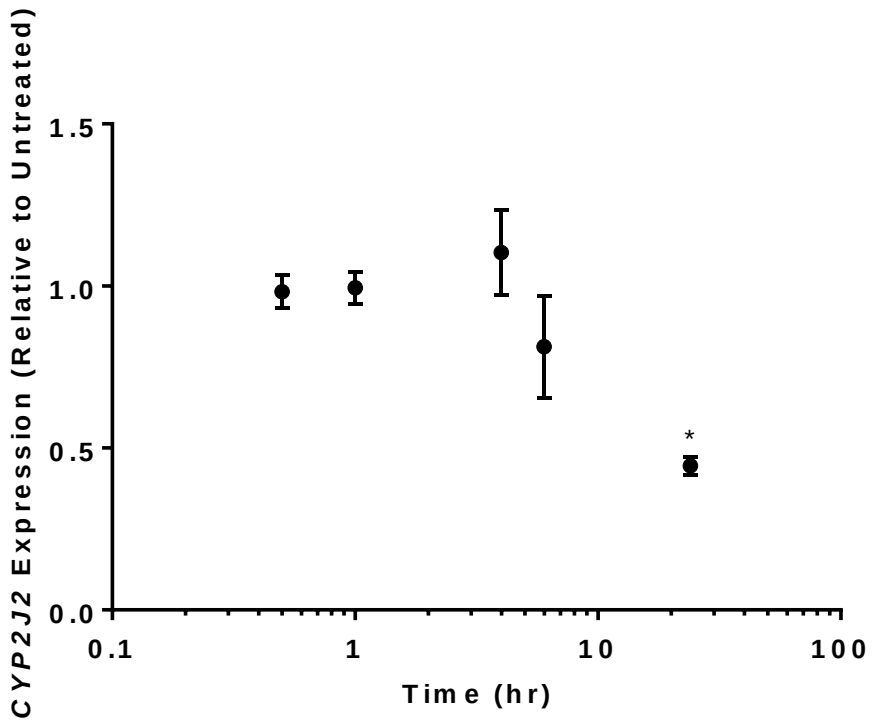

Figure 4.3. *CYP2J2* gene expression in adult cardiomyocytes cultured in hypoxic conditions (1% O_2) over 24 hours. Expression levels were assayed at 30 min, 1 hour, 4 hours, 6 hours, and 24 hours and show time dependent downregulation under hypoxic conditions, starting at 6 hours. After 24 hours in hypoxic conditions, *CYP2J2* expression is significantly decreased by 50% compared to cells grown under normoxic conditions. *$p < 0.05$.

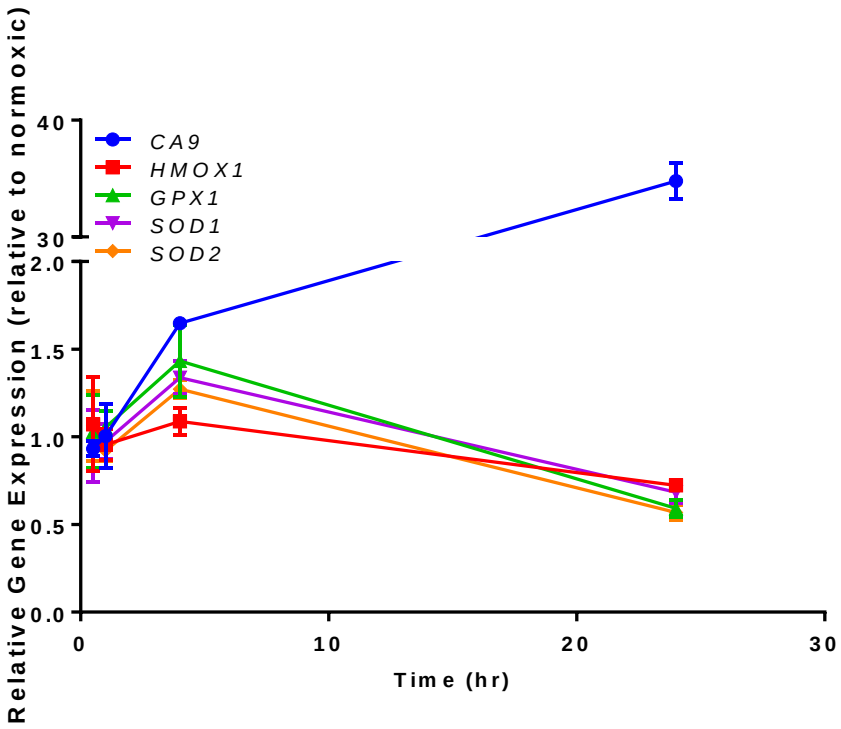

Figure 4.4. Gene expression of representative antioxidant genes in adult ventricular myocytes cultured in hypoxia (1% O_2) over 24 hours. *CA9* is a hypoxia responsive gene and is significantly overexpressed in ventricular myocytes under hypoxic stress over 24 hours. In contrast, *HMOX1*, *GPX1*, *SOD1*, and *SOD2* did not significantly change over the course of the experiment, but after 24 hours in a hypoxic environment, adult ventricular myocytes appear to downregulate these genes by as much as 50%.

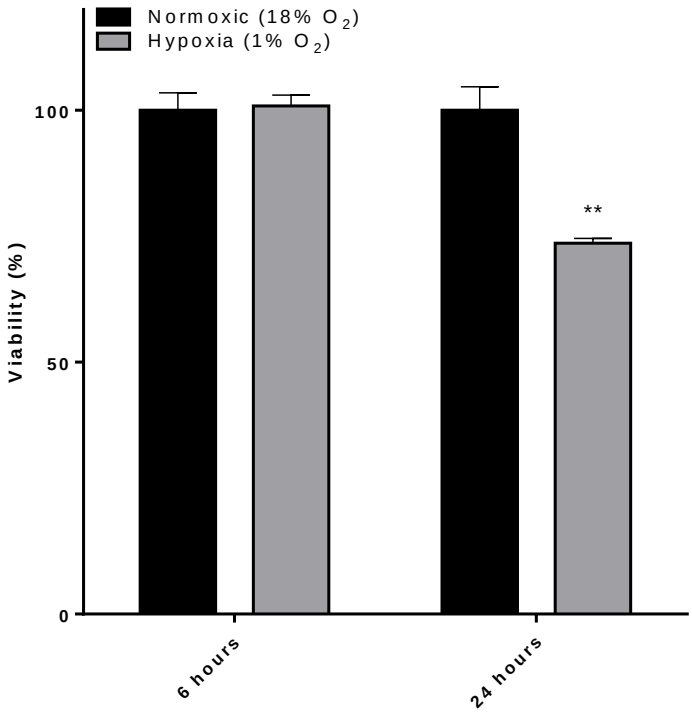

Figure 4.5. Cell viability of ventricular myocytes cultured in normoxia and hypoxia for 6 and 24 hours. No difference in viability was observed at 6 hours. At 24 hours, there was a 25% drop in cell viability of adult ventricular myocytes. A t-test of the means show the difference in viability between cells grown in normoxic and hypoxic environments are statistically significant. ** $p < 0.01$.

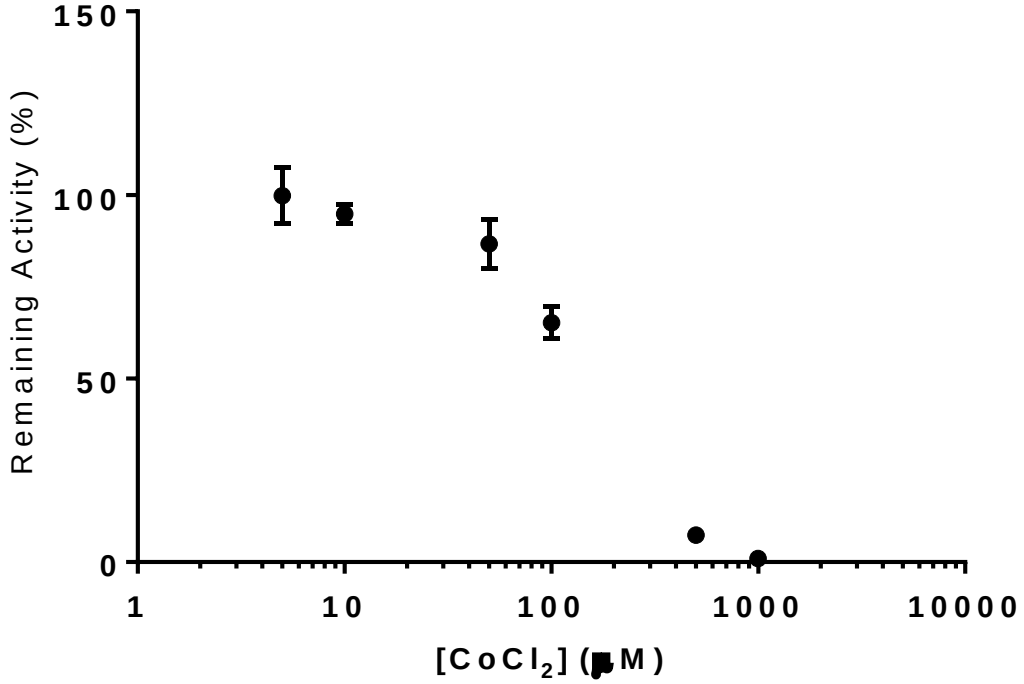

Figure 4.6. CYP2J2 activity in adult ventricular myocytes measured using terfenadine as a probe substrate in the presence of varying concentration of $CoCl_2$. Each point is the average of triplicates, and error bars represent the standard deviation of replicates. Activity begins to drop in the presence of 50 μM $CoCl_2$ (15% drop in activity), with greater loss in activity at higher concentrations.

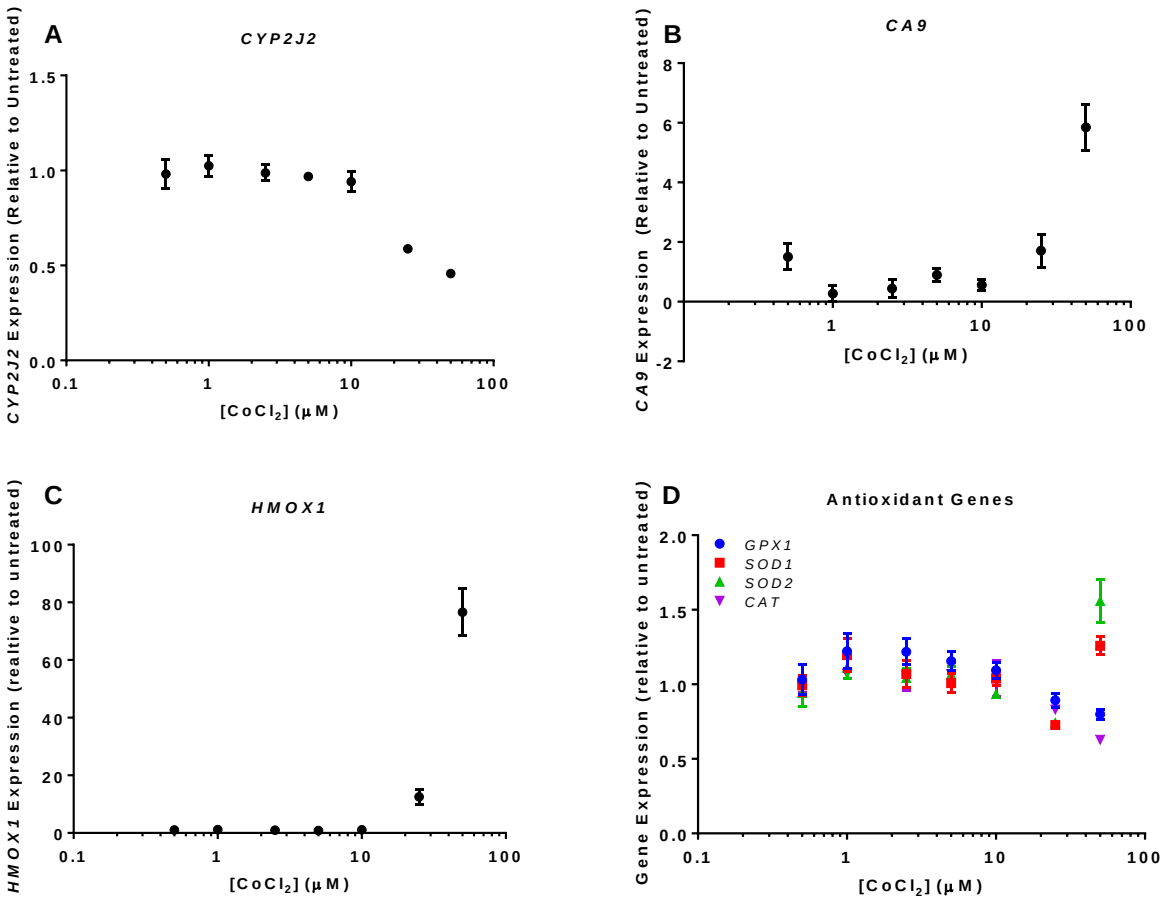

Figure 4.7. Gene expression changes of *CYP2J2* (A), *CA9* (B), *HMOX1* (C), and antioxidant genes (D) in ventricular myocytes at varying concentrations of $CoCl_2$. *CYP2J2* is downregulated by 50% at the highest concentration tested (50 μM). *CA9* and *HMOX1* expression begins to rise at 20 μM $CoCl_2$ with increased expression at 50 μM $CoCl_2$, the highest concentration tested. Finally, no significant changes in expression levels were observed with *GPX1* and *CAT*. In contrast, superoxide dismutase isoforms rise modestly at 50 μM $CoCl_2$.

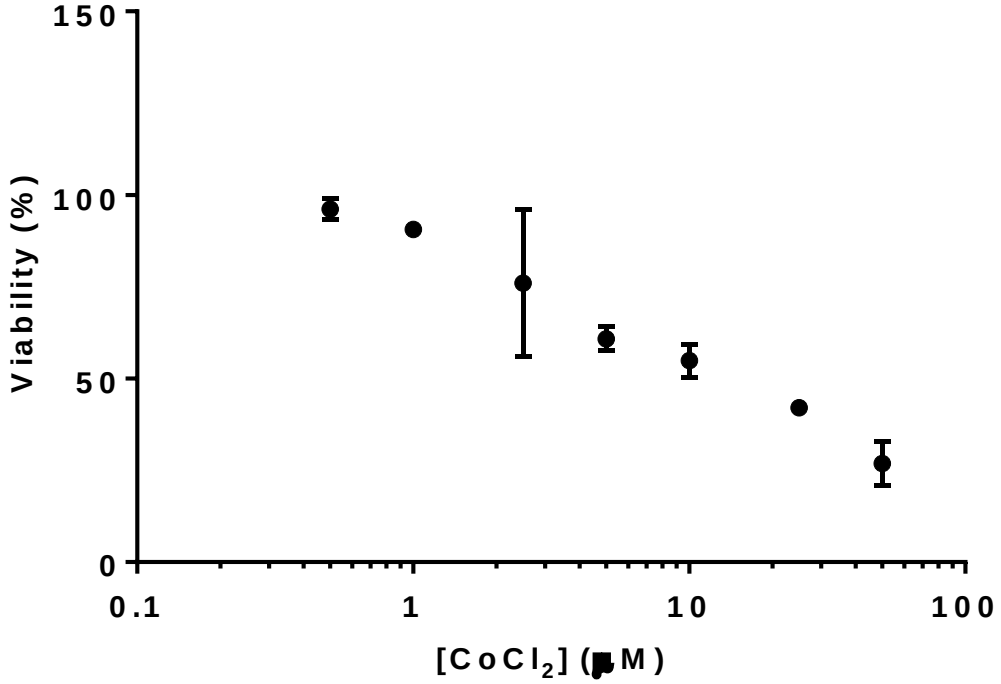

Figure 4.8. Viability of cells treated with varying concentrations of $CoCl_2$. Adult ventricular myocyte viability decreases in a dose-dependent manner, with loss observed starting at low μM concentrations. At the highest concentration tested (50 μM), cell viability decreased 70%.

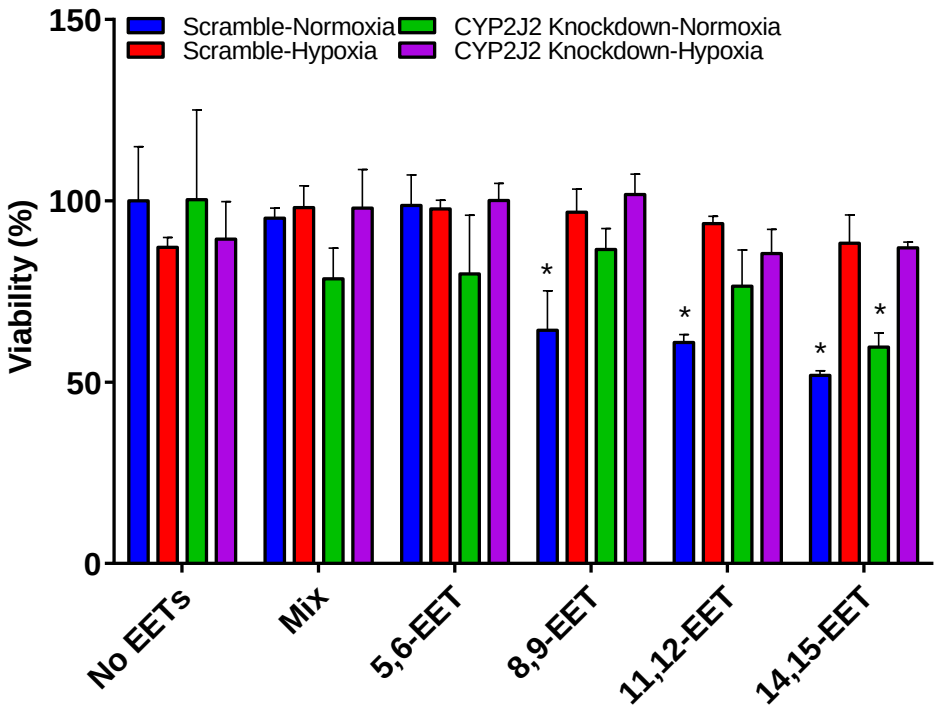

Figure 4.9. Adult ventricular myocyte viability due to hypoxia in the absence and presence of EETs, added as a mixture or individual isomers. In the absence of EETs, there are no differences between scramble and downregulated cell viability under normoxia or hypoxia. Cells pre-treated with a mix of EETs (50 nM total) showed no significant difference in viability when cells are treated with scrambled siRNA and grown under normoxic conditions. Cell with CYP2J2 knocked down and pre-treated with EETs prior to hypoxia, exhibited decreased viability compared to the other groups. All four isomers, added individually, mitigated the effects of hypoxia on cell death. Lastly, viability is reduced when cells have *CYP2J2* downregulated and treated with individual EET isomers (50 nM) but are not exposed to hypoxia and exposure of scrambled siRNA treated cells to 8,9-, 11,12-, and 14,15-EET, individually, showed >40% loss of viability. * $p < 0.05$.

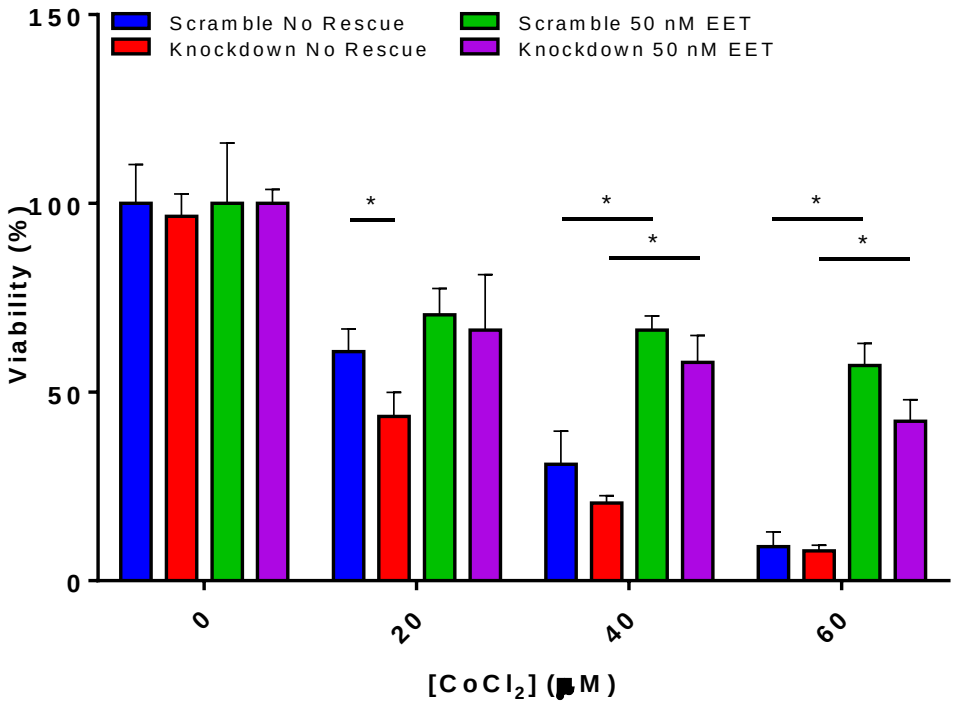

Figure 4.10. Cell viability in human adult derived ventricular myocytes exposed to varying doses of $CoCl_2$ for 24 hours following 72 hours of lipofectamine treatment and either scrambled siRNA or CYP2J2 siRNA. *CYP2J2* expression appears to be protective against $CoCl_2$ as cells with expression reduced by at least 80% are more susceptible to $CoCl_2$ toxicity. Cells that were exposed to an EET mixture (12.5 nM each isomer, 50 nM total EETs) for 1 hour after *CYP2J2* knockdown and before $CoCl_2$ appear to be protected from $CoCl_2$ toxicity. * indicates $p < 0.05$.

References

Abe H, Semba H, and Takeda N (2017) The Roles of Hypoxia Signaling in the Pathogenesis of Cardiovascular Diseases. *J Atheroscler Thromb* **24**:884–894, Japan Atherosclerosis Society.

Aliwarga T, Raccor BS, Lemaitre RN, Sotoodehnia N, Gharib SA, Xu L, and Totah RA (2017) Enzymatic and free radical formation of cis- and trans- epoxyeicosatrienoic acids in vitro and in vivo. *Free Radic Biol Med* **112**:131–140.

Bartels K, Grenz A, and Eltzschig HK (2013) Hypoxia and inflammation are two sides of the same coin. *Proc Natl Acad Sci U S A* **110**:18351–2.

Chaudhary KR, Zordoky BNM, Edin ML, Alsaleh N, El-Kadi AOS, Zeldin DC, and Seubert JM (2013) Differential effects of soluble epoxide hydrolase inhibition and CYP2J2 overexpression on postischemic cardiac function in aged mice. *Prostaglandins Other Lipid Mediat* **104**–**105**:8–17, Elsevier Inc.

Chen W, Zheng G, Yang S, Ping W, Fu X, Zhang N, Wang DW, and Wang J (2014) CYP2J2 and EETs Protect against Oxidative Stress and Apoptosis in Vivo and in Vitro Following Lung Ischemia/Reperfusion. *Cell Physiol Biochem* **33**:1663–80.

Evangelista EA, Kaspera R, Mokadam NA, Jones III JP, and Totah RA (2013) Activity, inhibition, and induction of cytochrome P450 2J2 in adult human primary cardiomyocytes. *Drug Metab Dispos* **41**.

Evangelista EA, Lemaitre RN, Sotoodehnia N, Gharib SA, and Totah RA (2018) CYP2J2 expression in adult ventricular myocytes protects against reactive oxygen species toxicity. *Drug Metab Dispos* **46**.

Imig JD (2012) Epoxides and soluble epoxide hydrolase in cardiovascular physiology. *Physiol Rev* **92**:101–30.

Jiang J-G, Chen C-L, Card JW, Yang S, Chen J-X, Fu X-N, Ning Y-G, Xiao X, Zeldin DC, and Wang DW (2005) Cytochrome P450 2J2 promotes the neoplastic phenotype of carcinoma cells and is up-regulated in human tumors. *Cancer Res* **65**:4707–15.

Jiang J-G, Fu X-N, Chen C-L, and Wang D-W (2009) Expression of cytochrome P450 arachidonic acid epoxygenase 2J2 in human tumor tissues and cell lines. *Ai Zheng* **28**:93–6.

Kim J, Tchernyshyov I, Semenza GL, and Dang C V (2006) HIF-1-mediated expression of pyruvate dehydrogenase kinase: a metabolic switch required for cellular adaptation to hypoxia. *Cell Metab* **3**:177–85.

Lee AC, and Murray M (2010) Up-Regulation of Human CYP2J2 in HepG2 Cells by Butylated Hydroxyanisole Is Mediated by c-Jun and Nrf2. *Mol Pharmacol* **77**:987–994.

Lee JW, Ko J, Ju C, and Eltzschig HK (2019) Hypoxia signaling in human diseases and therapeutic targets. *Exp Mol Med* **51**:68.

Li R, Xu X, Chen C, Yu X, Edin ML, Degraff LM, Lee CR, Zeldin DC, and Wang DW (2012) Cytochrome P450 2J2 is protective against global cerebral ischemia in transgenic mice. *Prostaglandins Other Lipid Mediat* **99**:68–78, Elsevier Inc.

Livak KJ, and Schmittgen TD (2001) Analysis of Relative Gene Expression Data Using Real-Time Quantitative PCR and the 2−ΔΔCT Method. *Methods* **25**:402–408, Academic Press.

Marden NY, Fiala-Beer E, Xiang S, and Murray M (2003) Role of activator protein-1 in the down-regulation of the human CYP2J2 gene in hypoxia. *Biochem J* **373**:669–80.

Marxsen JH, Stengel P, Doege K, Heikkinen P, Jokilehto T, Wagner T, Jelkmann W, Jaakkola P, and Metzen E (2004) Hypoxia-inducible factor-1 (HIF-1) promotes its degradation by induction of HIF-alpha-prolyl-4-hydroxylases. *Biochem J* **381**:761–7.

Murray GI, Patimalla S, Stewart KN, Miller ID, and Heys SD (2010) Profiling the expression of cytochrome P450 in breast cancer. 202–211.

Nag S, and Resnick A (2017) Stabilization of hypoxia inducible factor by cobalt chloride can alter renal epithelial transport. *Physiol Rep* **5**:e13531.

Norouzirad R, González-Muniesa P, and Ghasemi A (2017) Hypoxia in Obesity and Diabetes: Potential Therapeutic Effects of Hyperoxia and Nitrate. *Oxid Med Cell Longev* **2017**:5350267.

Nyengaard JR, Ido Y, Kilo C, and Williamson JR (2004) Interactions between hyperglycemia and hypoxia: implications for diabetic retinopathy. *Diabetes* **53**:2931–8.

Okail MS Al (2010) Cobalt chloride , a chemical inducer of hypoxia-inducible factor-1 a in U251 human glioblastoma cell line. *JSCS* **14**:197–201, Japanese Association for Dental Science.

Sada K, Nishikawa T, Kukidome D, Yoshinaga T, Kajihara N, Sonoda K, Senokuchi T, Motoshima H, Matsumura T, and Araki E (2016) Hyperglycemia Induces Cellular Hypoxia through Production of Mitochondrial ROS Followed by Suppression of Aquaporin-1. *PLoS One* **11**:e0158619.

Semenza GL (2014) Hypoxia-inducible factor 1 and cardiovascular disease. *Annu Rev Physiol* **76**:39–56.

Semenza GL (1999) Regulation of mammalian O2 homeostasis by hypoxia-inducible factor 1. *Annu Rev Cell Dev Biol* **15**:551–78.

Seubert J, Yang B, Bradbury JA, Graves J, Degraff LM, Gabel S, Gooch R, Foley J, Newman J, Mao L, Rockman HA, Hammock BD, Murphy E, and Zeldin DC (2004) Enhanced postischemic functional recovery in CYP2J2 transgenic hearts involves mitochondrial ATP-sensitive K+ channels and p42/p44 MAPK pathway. *Circ Res* **95**:506–14.

Smith PK, Krohn RI, Hermanson GT, Mallia AK, Gartner FH, Provenzano MD, Fujimoto EK, Goeke NM, Olson BJ, and Klenk DC (1985) Measurement of protein using bicinchoninic acid. *Anal Biochem* **150**:76–85.

Taylor CT (2008) Mitochondria and cellular oxygen sensing in the HIF pathway. *Biochem J* **409**:19–26.

Xu M, Bhatt DK, Yeung CK, Claw KG, Chaudhry AS, Gaedigk A, Pearce RE, Broeckel U, Gaedigk R, Nickerson DA, Schuetz E, Rettie AE, Leeder JS, Thummel KE, and Prasad B (2017) Genetic and nongenetic factors associated with protein abundance of flavin-containing monooxygenase 3 in human liver. *J Pharmacol Exp Ther* **363**:265–274, American Society for Pharmacology and Experimental Therapy.

Yeo E-J (2019) Special issue on hypoxia. *Exp Mol Med* **51**:69.

Zhu Y, Ding A, Yang D, Cui T, Yang H, Zhang H, and Wang C (2020) CYP2J2-produced epoxyeicosatrienoic acids attenuate ischemia/reperfusion-induced acute kidney injury by activating the SIRT1-FoxO3a pathway. *Life Sci* **246**:117327.

Chapter 5: CYP2J2 regulation and protection of ventricular myocytes cultured under type 2 diabetes stressors

5.1 Introduction

Diabetes is a disease characterized by dysfunctions in the body's ability to produce (type 1) or respond to (type 2) the hormone insulin (Luo and Wang, 2011). The resulting consequence is that the body ultimately becomes hyperglycemic due to chronically high blood glucose levels. Diabetes also results in dysregulation of carbohydrate, lipid, and protein metabolism (DeFronzo *et al.*, 2015) and is often associated with other pathological states such as obesity, hypertension, and inflammation. The combination of these pathological states lead to chronic stresses at the cellular level, the most prevalent being hypoxia from increased O_2 consumption due to hyperglycemia and obesity (Nordquist *et al.*, 2015) and chronic elevated oxidative stress due to increased ROS production, possibly as a result of metabolic dysregulation, particularly lipid metabolism (Asmat *et al.*, 2016). If untreated, diabetes could lead to various diseases including cardiovascular, kidney, and neurological diseases, among others (Brownlee *et al.*, 2016).

Animal studies have overwhelmingly shown a protective role for EETs, and thus CYP2J2, in the etiology and progression of diabetes (Wang *et al.*, 2010; Chen *et al.*, 2011; Ma *et al.*, 2013; Abraham *et al.*, 2014; Li *et al.*, 2015; Dai *et al.*, 2017). Animal studies using transgenic mice with cardiac-specific human CYP2J2 expression demonstrated improved glucose and insulin plasma levels, as well as improved glucose tolerance and uptake compared to their wild type counterparts when challenged with a high fat diet and streptozotocin exposure (Ma *et al.*, 2013). The transgenic mice were protected from the cardiovascular consequences of diabetes, specifically myocardial hypertrophy, which the investigators attributed to the activation

of the PPAR-γ and MAPK pathways, along with higher atrial natriuretic peptide (ANP) production. Beyond cardiovascular effects, CYP2J2 overexpression in endothelial cells also mitigated damage to the kidneys in streptozocin-induced diabetic mice (Chen *et al.*, 2011). Others have demonstrated that CYP2J2 overexpression resulted in attenuated inflammatory responses in isolated hepatocytes in diabetic mice (Li *et al.*, 2015). Inflammatory pathways leading to elevated cytokine levels are thought to be an important factor in the development of type II diabetes (Li *et al.*, 2015). In addition, Li et al also showed that CYP2J2 expression activated the PPAR-γ pathway, which they reasoned could lead to decreased dyslipidemia in their animal models by increasing adipogenesis diabetes. Together, these studies demonstrate CYP2J2 and CYP2J2-mediated production of EETs are involved in the development, progression and sequelae of diabetes.

Given the large body of evidence supporting a protective function for CYP2J2 in the initiation and progression of diabetes, as well as the cardioprotection conferred by CYP2J2 when cells are exposed to ROS and hypoxia as demonstrated in previous chapters, we sought to determine the effect of type 2 diabetes serum on *CYP2J2* regulation in adult ventricular myocytes. We then altered CYP2J2 expression using siRNA and determined cell viability cultured in type 2 diabetic serum compared to normal serum. Finally, we explored how protection pathways in adult ventricular myocytes are altered when cells are cultured in type 2 diabetes serum compared to control.

5.2 Materials & Methods

General materials, reagents and compounds.

Unless otherwise specified, all reagents and solvents used in this study were obtained from Millipore Sigma (Burlington, MA) and/or ThermoFisher Scientific (Waltham, MA) and used without further purification. Human serum was obtained from BioIVT (Westbury, NY). Control normal serum was obtained from a pool of relatively healthy individuals with no history of type 2 diabetes, aliquoted into 1 mL portions and stored frozen in -20 °C until added to serum-free media for experiments. Serum pooled from 36 type 2 patients taking only metformin. As with the control serum, pooled diabetic serum was aliquoted into 1 mL aliquots, and frozen at -20 °C until use. Metformin (MET) for experiments was obtained through Dr. Ed Kelly's lab at the University of Washington, Department of Pharmaceutics. Recombinant human interleukin-6 (IL6) (cat # PHC0065) and tumor necrosis factor alpha (TNFα) (cat # PHC3015) were obtained commercially from ThermoFisher Scientific (Waltham, MA).

Adult ventricular cardiac tissue

Cardiac tissue from seventeen individuals (n = 27) undergoing Left Ventricular Assist Device (LVAD). As outlined in Chapter 2, the Institutional Review Board at University of Washington determined that since the tissue source was anonymous, it was exempt from the human research (NHR) requirements and therefore waived the need for ethical review and informed consent. This policy is in accordance with Office for Human Research Protections guidelines (www.hhs.gov/ohrp/policy/cdebiol.html). These case tissues were divided into non-diabetic (n=17) and diabetic (n=10) groups based on the presence of antidiabetic agents (insulin,

metformin, etc.) on medication list obtained at the time of tissue procurement. More information on tissue acquisition and demographics of the tissue donors are provided in Chapter 2.

Cardiac tissue processing and proteomic quantification of CYP2J2

Cardiac tissue was processed using protocols outlined in Chapter 2, as reported by Aliwarga et al. for sample preparation (Aliwarga *et al.*, 2017), Smith et al. for BCA protein quantification (Smith *et al.*, 1985) and Xu et al. for sample preparation and proteomic mass spectrometry analysis (Xu *et al.*, 2017). CYP2J2 was quantified in cardiac tissue samples using mass spectrometry. Liquid chromatography and mass spectrometric properties are outlined in detail in chapter 2.

Adult ventricular myocytes

Adult derived ventricular myocytes used in these experiments were obtained commercially from Celprogen Inc. (San Pedro, CA) and as outlined in previous chapters, all cell culture materials and media were obtained directly from the vendors. Cells were cultured and passaged using vendor's protocols, outlined in previous chapters and published studies (Evangelista *et al.*, 2013, 2018), with no modifications except that cell media were further sterile filtered through a 0.22 μm polyether sulfone membrane prior to use.

Adult ventricular myocyte treatment with metformin

Adult ventricular myocytes were plated at a density of 200,000 cells/mL in 12 well plates (1 mL/well). The cells were allowed to attach for 24 hours at 37 °C and 5% CO_2. After 24 hours, the wells were washed and serum-free cardiomyocyte media with metformin (2 mM) added, a concentration based on previous published studies and within measured physiologically relevant concentrations (Williams *et al.*, 2013; Kajbaf *et al.*, 2016; Samuel *et al.*, 2017). The experiment proceeded for 72h, with fresh media changes at 24h and 48h. Cells were harvested at 24, 48, and 72 hours for total RNA isolation and RT-PCR analysis of *CYP2J2* gene expression. Cell viability was assessed at 24, 48, and 72 hours by thiazolyl blue tetrazolium bromide (MTT) assay.

CYP2J2 inhibition and gene silencing experiments in adult cardiomyocyte cultured with human serum

To determine the effect type 2 diabetes on *CYP2J2* expression, cells were cultured in media containing human serum. Control cells were cultured in serum-free media containing pooled healthy human serum (10% v/v) to replace the BSA. Treated cells were cultured in serum-free media containing pooled human serum from type 2 diabetic patients (10% v/v). Two time points were studied: 12 hours and 48 hours. Cells were plated at a density of 200,000 cells/mL in 12-well plates (1 mL/well), in Celprogen complete cardiomyocyte media and incubated for 24 hours (37 °C and 5% CO_2) to allow cells to adhere. After 24 hours, cells were washed, and the media replaced with serum-free media supplemented with human serum. At each time point, cells were harvested for total RNA isolation for RTPCR analysis of gene expression. Additionally, ROS levels were measured at each time point using 2',7'-

dichlorodihydrofluorescein diacetate (H_2DCFDA) and cell viability was assessed with MTT assays.

To determine the impact of loss of CYP2J2 activity, cells were cultured in human serum as described previously, in the presence and absence of danazol (DAN), the CYP2J2 specific inhibitor used in experiments in previous chapters. Briefly, cells were plated as described. After allowing 24 hours for the cells to attach, media was changed from Celprogen's growth media to serum-free media containing human serum. Cells were also simultaneously treated with either DMSO (0.1% vehicle control) or danazol (1 μM).

Similar experiments were performed with *CYP2J2* expression silenced as outlined in Chapter 2, and in published protocols (Evangelista *et al.*, 2018). Briefly, cells were treated with RNAiMAX lipofectamine (Thermo Fisher Scientific, Waltham MA) and *CYP2J2* Trilencer siRNA or scrambled siRNA (Origene, Rockville, MD). *HPRT1* silencing using Origene siRNA was the positive control. Lipofectamine was delivered using a reverse transfection protocol, where siRNA was reconstituted to a stock concentration (20 μM) and prepared with lipofectamine using OptiMEM reduced serum media (Thermo Fisher Scientific, Waltham, MA) by diluting the mixture to a concentration of 50 nM. The lipofectamine/siRNA mixture was incubated at room temperature for at least 10 minutes, during which time cells were washed, trypsinized, pelleted, resuspended and diluted to a concentration of 200,000 cells/mL in complete media. The lipofectamine/siRNA stocks were added to individual wells a 12-well plate to a final concentration of 10 nM siRNA (250 μL volume of 50 nM siRNA/lipofectamine in OptiMEM), followed by the cells (1 mL of cell suspension) for a final volume of 1250 μL in each well. The cells were incubated with lipofectamine/siRNA for 72 hours. Following gene silencing, cells were washed and then cultured in human serum as described above.

Ventricular myocyte cultured with varying glucose concentrations

Cell were plated as previously described in 12-well plates. After culturing for 24 hours to allow cells to attach, complete media was aspirated, and the cells were washed with PBS. Serum-free media supplemented with 0, 4, 6, and 8 mM (final concentration) of glucose was then added to the wells. These concentrations were selected based on the clinically relevant fasting blood sugar levels of normal (below 5.6 mM), pre-diabetic (5.6-7.0 mM) and diabetic (above 7 mM). The glucose treatments were carried out over 48 hours, with media refresh at 24 hours. Cardiomyocytes were harvested at 24 and 48h and viability as assessed using MTT assays.

Cardiomyocyte treated with IL6 and TNFα

Cells were plated in 12 well plates as previously described. After culturing for 24 hours to allow cells to attach to the plate, the cells were washed and media replaced with serum-free media with varying concentrations (0, 2, 20, and 200 pg/mL) of either IL6 or TNFα. These concentrations were selected as physiologically relevant concentrations for these cytokines, where healthy individuals typically have 1-2 pg/mL circulating concentrations, with a 10-fold increase under chronic inflammation, and finally 100- to 1000- fold increases under fatal sepsis (Hack *et al.*, 1989; Waage *et al.*, 1989; Ruotsalainen *et al.*, 2010; Mirza *et al.*, 2012; Chen *et al.*, 2017). The cells were treated with cytokines for 30 mins, 2 hours, and 24 hours. Cardiomyocytes were isolated at each time point and MTT assays performed to asses cell viability. Additionally, total RNA was isolated and gene expression assessed by RTPCR for *CYP2J2*, *HMOX1, CAT, GPX1, SOD1* and *SOD2*.

MTT assay for cell viability

Cell viability was determined using thiazolyl blue tetrazolium bromide (MTT) assays. Briefly, following treatment with siRNA and/or chemical, cells were treated with 5 μL of 12 mM MTT per mL of media (60 μM MTT final concentration). The cells were incubated with the MTT for 20 minutes at 37°C. Afterwards, the media was aspirated carefully and DMSO (600 μL) was added to each well, followed by 75 μL of Sorenson's glycine (100 mM glycine, 100 mM sodium chloride). The plate was shaken on an orbital shaker for 5 min at 400 rpm. The absorbance from each well was measured using a Tecan Infinite M200 plate reader (Tecan, Männedorf, Switzerland) using the following protocol: 5 sec of orbital shaking with an amplitude of 1 mm, followed by 10 sec of wait time, and then absorbance measurement at 570 nm (9 nm bandwidth) using 670 nm (9 nm bandwidth) as the reference wavelength. A true zero signal was obtained by following the above protocol using plates that did not contain cells. Measurements were normalized to the absorbance in vehicle-treated control wells (set as 100% viability).

ROS formation assay

Reactive oxygen species formation was measured using 2',7'-dichlorodihydrofluorescein diacetate (H_2DCFDA, Thermo Fisher Scientific, Waltham MA). Cells were incubated in serum-free phenol-free media containing 20 μM H_2DCFDA for 30 minutes after siRNA and/or drug treatments to determine relative ROS levels in the cells. After incubation, 100 μL aliquots of the media were transferred to a 96 well, black-walled, clear bottom plate (Thermo Fisher Scientific, Waltham MA). The fluorescence was captured and measured using a Synergy HTX Multi-Mode Reader (excitation wavelength of 485 nm/emission wavelength of 525 nm). Data were analyzed

by normalizing signals to a control well subjected to similar conditions as described above, but with no cells present as the 0 ROS formation control.

Total RNA Isolation and qPCR

Total RNA was extracted using the MagMax 96 Total RNA Isolation kit (Thermo Fisher Scientific, Waltham MA) from adult derived human ventricular myocytes. RNA was isolated from human ventricular tissues by homogenizing tissues in 1 mL Trizol Reagent (Thermo Fisher Scientific, Waltham, MA) using an Omni Bead Ruptor homogenizer (Omni Intl., Kennesaw, GA) with 4 ceramic beads in each tube. After homogenization, purification continued using PureLink RNA Mini Kit (Thermo Fisher Scientific, Waltham, MA) and following the manufacturer protocol. Briefly, the lysate was incubated at room temperature for 5 mins, after which chloroform (200 μL) was added to the tube and the mixture shaken vigorously for 15 seconds by hand. Phase separation was achieved by centrifugation at 4 °C and 13,000 x g for 15 mins. The upper phase was transferred to an RNAse free tube and diluted 1:1 with 100 % ethanol. Any precipitate was dispersed by inversion of the tube. RNA was then captured on spin columns provided by the kit mentioned above, washed and eluted in RNAse-free water (30 μL).

Initial RNA quality (A260/A280) and quantity was determined using a Synergy HTX Multi-Mode Reader (BioTek, Winooski VT). In order to determine CYP2J2 siRNA knockdown efficiency, total RNA was used to synthesize cDNA using the High Capacity RNA-to-cDNA kit (Thermo Fisher Scientific, Waltham MA). RT-PCR was then carried out using TaqMan (Thermo Fisher Scientific, Waltham MA) FAM reporter primers for *CYP2J2* as well as a housekeeping gene, *GUSB*. Other TaqMan FAM reporter primers utilized, specific to other genes

being assessed as described in previous sections. Cycle threshold (C_T) values and the ΔC_T method followed by the $2^{\Delta CT}$calculation were used to determine the relative quantity of CYP2J2 (and other genes) mRNA present relative to the *GUSB*. The mRNA levels were first normalized to the housekeeping gene using the ΔC_T method and then expression levels in treated cells were compared to levels in untreated cells using the $\Delta\Delta C_T$ calculation. Relative gene expression levels were reported using either the $2^{\Delta CT}$ for comparison of gene expression levels between hearts using *GUSB* as the housekeeping standard or the $2^{-\Delta\Delta CT}$ calculation for comparison of differences in gene expression between treated and untreated cells (Livak and Schmittgen, 2001).

5.3 Results

CYP2J2 is lower in diabetic cardiac tissue compared to controls at both mRNA and protein levels

Real time-PCR analysis of total RNA isolated from human ventricular tissues demonstrates that control ventricular tissue had mean *CYP2J2* mRNA levels of 21-fold higher than *GUSB* housekeeping levels (range from 2.7-51.8), non-diabetic case tissue had mean levels 25.1-fold higher than *GUSB* (range: 4.4-48.3) and type 2 diabetic case tissue had mean levels 13.7-fold higher than *GUSB* levels (range: 1.0-35.1). T-tests comparing means between groups indicate the difference between non-diabetic and diabetic cases are statistically significant with a p-value of 0.012 (Figure 5.1).

Proteomic analysis of CYP2J2 protein expression in the same ventricular tissue indicates that in control tissues, there was an average of 0.38 pmol CYP2J2/mg membrane fraction (range: 0.14-0.80). Non-diabetic cases had a mean of 0.28 pmol CYP2J2/mg membrane fraction (range: 0.05-0.55) and diabetic cases had a mean of 0.22 pmol CYP2J2/mg membrane fraction (range: 0.05-0.34). T-tests comparing means between groups showed the difference between control tissue and diabetic case tissue are statistically significant with a p-value of 0.015 (Figure 5.1).

Oxidative stress related genes expression in cardiac tissue is variable

Gene expression of various oxidative stress genes for heme oxygenase 1, catalase, glutathione peroxidase, and superoxide dismutase 1 and 2 (*HMOX1*, *CAT*, *GPX1*, *SOD1*, and *SOD2*, respectively) in human ventricular tissue were also measured by RT-PCR. *HMOX1* levels were not statistically significant between control, non-diabetic cases, and diabetic cases (Figure

5.2A), with mean *HMOX1* levels (fold relative to *GUSB* levels) of 2.8, 2.8 and 1.3, respectively. Similarly, mean *CAT* mRNA levels were not significantly different, with mean levels (fold relative to *GUSB*) of 6.9, 8.9 and 6.9 in control, non-diabetic cases and diabetic cases, respectively (Figure 5.2B).

GPX1 levels were interestingly higher in case tissue compared to control tissues, with diabetic tissue expressing higher levels of *GPX1* mRNA. The mean levels of *GPX1* (fold relative to *GUSB*) transcripts in ventricular tissues were 38.1 in controls, 52.7 in non-diabetic cases, and 60.1 in diabetic cases. T-tests indicate a statistical difference between the mean *GPX1* transcripts in tissue and in diabetic case tissues ($p = 0.011$). *SOD1* levels were similar between groups with average mRNA levels (fold relative to *GUSB*) of 46.3, 42.0, and 33.5 in control, non-diabetic cases and diabetic cases, respectively. While there is a trend for lower expression of this gene in cases, particularly in diabetic cases, t-tests indicate these differences to statistically insignificant. Finally, *SOD2* mRNA levels were also similar among the three groups, with average levels (relative to *GUSB*) of 44.0, 58.4, and 32.6 in control, non-diabetic and diabetic ventricular tissues, respectively. As with *SOD1* levels, diabetic tissue *SOD2* levels were lower than in the other groups, but t-tests indicate these differences are not significant.

Metformin does not affect *CYP2J2* expression

Real time-PCR analysis of total RNA isolated from ventricular myocytes exposed to metformin reveal that compared to control treated cells, MET-treated cells had an average of 8% lower *CYP2J2* mRNA (Figure 5.3) at the different concentrations tested. The experiment was

repeated three times, each time with biological triplicates. The data presented is the average of nine measurements. This difference is not statistically significant.

Type 2 diabetic serum stimulates downregulation of *CYP2J2* gene in ventricular myocytes

Culturing adult ventricular myocytes in human serum derived from type 2 diabetic individuals results in a 75% downregulation in *CYP2J2* expression in12 hours. Surprisingly, culturing the cells in type 2 diabetic serum for 48 hours yields only a 50% downregulation of *CYP2J2* expression (Figure 5.4). The differences in gene expression between cells grown in healthy serum and cells grown in type 2 diabetic serum are significant as determined by t-tests ($p < 0.01$).

Type 2 diabetes serum does not increase ROS regardless of CYP2J2 inhibition status

No significant differences in ROS levels were observed in cells cultured in media supplemented with human serum derived from type 2 diabetic individuals, compared to cells grown in media supplemented with healthy human serum (Figure 5.5). Further, when CYP2J2 activity is inhibited in the presence of danazol (1 μM), there continued to be no difference in the ROS levels measure in the cells by H_2DCFDA.

Inhibiting CYP2J2 activity chemically or by silencing *CYP2J2* expression results in greater cell death

Cardiomyocytes were first cultured in human serum and co-treated with the CYP2J2 inhibitor DAN. After 12 hours, there were little differences in cell viability, except in cells cultured with type 2 diabetic serum co-treated with DAN where viability significantly dropped to 58%. After 48 hours, cardiomyocytes in healthy serum media co-treated with DAN dropped to 80% viability. In contrast, the viability of cells grown in type 2 diabetic serum significantly dropped to 63% and 34% in the presence and absence of DAN, respectively, compared to cells grown in healthy serum with no DAN for 48 hours. (Figure 5.6).

Similarly, the viability of cardiomyocytes treated with scrambled or *CYP2J2* siRNA and then transferred to media supplemented with human serum were measured (Figure 5.7). After 12 hours in human serum, cells cultured in diabetic serum, but treated with scrambled siRNA, dropped to 75% viability. At 48 hours, cell viability in the same conditions (healthy serum, scrambled siRNA) dropped to 60%. Cells that had CYP2J2 silenced were 90% and 46% viable at 12h and 48h, respectively in healthy human serum-containing media. When cultured in type 2 diabetic serum media, cardiomyocyte viability is 66% and 30% at 12h and 48h, respectively, when CYP2J2 is silenced (Figure 5.7).

Glucose treatment does not change cardiomyocyte viability

MTT assays indicate that glucose does not significantly affect viability in ventricular myocytes at the concentrations tested (4, 6, and 8 mM), compared to no glucose controls. Instead, there were increases in the average cell viability at both time points, particularly at 4 and

6 mM, which were more pronounced at 24 hours, with a maximum increase of 40% in cardiomyocyte cell viability at 4 mM glucose (Figure 5.8).

IL6 and TNFα do not significantly affect cardiomyocyte viability and result in short-lived minor decreases in gene expression.

When cardiomyocytes were treated with cytokines IL6 and TNFα at varying concentrations, only slight decreases in cell viability were observed (Figure 5.9). Small changes of ~ 10% decrease in viability occurred at all three time points. At 30 min, viability dropped to 89% with 20 pg/mL IL6 and 87% with 20 pg/mL TNFα. At 2 h, viability dropped to 87% with 200 pg/mL of IL6. Finally, after 24 hours of cytokine treatment, viability dropped to 89% when cells were treated with 20 pg/mL IL6 or 2 pg/mL TNFα. T-tests indicate that these observed decreases in viability due to cytokine treatment of cardiomyocytes are not significant.

Gene expression for *CYP2J2*, *HMOX1, CAT, GPX1, SOD1* and *SOD2* in cardiomyocytes were not significantly altered over the 24-hour treatment with cytokines (Figure 5.10). The greatest change in gene expression occurs at 2 hours at the highest concentration tested (200 pg/mL). *CYP2J2* expression is downregulated approximately 20% in cells exposed to the cytokines IL6 and TNFα (200 pg/mL) for 2 hours. At 24 hours, these changes have either remained the same as what was observed at 2 hours or rebounded to normal expression.

5.4 Discussion

This chapter focused on examining the effects of type 2 diabetes on *CYP2J2* expression in adult ventricular myocytes. Key findings were that 1- Diabetes downregulates *CYP2J2* expression. Analysis of cardiac tissue indicates that CYP2J2 mRNA and protein levels were significantly lower in patients with cardiac conditions and diabetes than either control individuals or patients with cardiac conditions but were not diabetic. This was confirmed in human adult-derived primary ventricular myocytes. It should be noted that the type 2 diabetic serum was derived from patients with type 2 diabetes that were on MET only as their diabetic medication. Thus, the effects of Metformin on *CYP2J2* expression were tested and confirmed to be negligible. 2- Culturing cells in human serum derived from type 2 diabetic patients resulted in downregulation of cardiomyocyte *CYP2J2* gene expression. This is in agreement with previous studies examining CYP expression in diabetes models and finding that CYP expression and activity is reduced in diabetes (Dostalek *et al.*, 2011; Jarrar *et al.*, 2018; Gravel *et al.*, 2019).

Interestingly, downregulation was greater when measured at 12 hours following exposure to type 2 diabetic serum (75% decrease in expression) than at 48 hours (50% decrease in expression). Previously, in Chapter 3, data were presented showing that *CYP2J2* expression rebounded rapidly when knocked down with siRNA. The observations in this chapter, therefore, may be an extension of that as the cells adjust to insulting factors contained in the human sera used. It is possible that there is a maximum threshold for downregulation of this gene and that ventricular myocytes will counteract downregulation due to external forces in order to return expression levels back to normal. This is supported by the findings that CYP2J2 is protective against the pressures forced on ventricular myocytes by type 2 diabetes in agreement with the

literature. Along these lines, inhibition of protein activity by DAN and *CYP2J2* gene silencing by siRNA caused greater cell death compared to controls, supporting a cardioprotective role.

One limitation of this investigation is that the sera used, both healthy and type 2 diabetic, were not fully characterized making it difficult to determine what exactly in diabetic serum is responsible for these changes. Therefore, we sought to determine whether individual factors typically associated with diabetes could affect *CYP2J2* expression. To this end, we tested whether ROS, hyperglycemia, and inflammatory cytokines usually associated with diabetes may be responsible for the changes in *CYP2J2* expression.

Changes in oxidative stress were immediately ruled out, since data measuring ROS levels indicated that cellular ROS levels were largely unchanged when ventricular myocytes were cultured with human serum. In addition, as presented in previous chapters, oxidative stress causes an upregulation in *CYP2J2* gene expression, thus the downregulation observed in the presence of diabetic serum is unlikely due to higher ROS.

Hyperglycemia, one of the hallmarks of type 2 diabetes, could not be conclusively tested with the current study design. Initial experiments indicated that a hyperglycemic environment did not significantly affect cell viability. Follow-up studies measuring glucose levels in Celprogen media and human serum using a glucometer, however, indicated that this is because this cell line is naturally cultured in hyperglycemic media. Glucose measurements using a glucometer (data not shown) identified glucose levels in the complete growth media obtained from Celprogen to be naturally hyperglycemic (glucose > 10 mM), making delineation of glucose effects on gene expression difficult. Further studies are needed to isolate the effects of high glucose on *CYP2J2* expression and activity in ventricular myocytes. However, our cell model is likely not the best model for such studies.

Lastly, we investigated the effects of two cytokines typically associated with type 2 diabetes. Interleukin-6 (IL6) is a known pro-inflammatory cytokine with various physiological functions and is associated with development of type 2 diabetes (Kristiansen and Mandrup-Poulsen, 2005; Rehman *et al.*, 2017; Rodrigues *et al.*, 2017). IL6 has been found to be elevated in individuals with chronic type 2 diabetes. Similarly, tumor necrosis factor alpha (TNFα) is another cytokine with a wide range of physiological effects associated with type 2 diabetes pathogenesis and progression (Mirza *et al.*, 2012; Swaroop *et al.*, 2012; Akash *et al.*, 2018). Primarily, these cytokines have been linked to the development of insulin resistance in type 2 diabetes. RNASeq data had previously identified the IL6 receptor (*IL6R*) and TNFα receptor (*TNFRSF1A*) as being expressed in our ventricular myocyte model. We therefore sought to determine how these associated cytokines affected gene expression of *CYP2J2* and other genes associated with cellular oxidative stress.

The results are inconclusive in that expression of the genes investigated appeared to be downregulated, but only slightly, towards the early time points of experiments that captured an early cellular response. These results are partially reversed by 24 hours, however, and there are many reasons for this. The most likely reason is that cytokines are short-lived with half-lives being around 1-2 hours (Waage *et al.*, 1989). These measurements are *in vivo*, however, and to date, there are no reports of degradation kinetics *in vitro*. There is precedent for determining cytokine effects on CYP expression showing that CYP expression is downregulated in HepG2 hepatocarcinoma cells (Aitken and Morgan, 2007). The concentrations used by these investigators, were quite high – 10 ng/ml – which is 10,000-fold higher than physiologically relevant concentrations in healthy individuals. Future studies may need to focus on treating

ventricular myocytes at higher concentrations to yield more definitive results, particularly as initial time points indicate a downregulation of *CYP2J2* expression.

It is possible that the unique combination of oxidative stress, cytokines and hyperglycemia present in the type 2 diabetes result in the downregulation of *CYP2J2* but the same effect cannot be detected when these factors are tested individually. Another potential limitation of this study is that we were only able to acutely expose cells to the type 2 diabetic serum. Diabetes is a chronic condition and the most serious complications often manifest long after the initial onset. Future work validating the changes observed in ventricular myocytes under chronic exposure are necessary. In addition, deeper scrutiny of the global effects of type 2 diabetes on ventricular myocytes would provide better insight on the findings herein. Similar to Chapter 2, RNASeq would provide greater insight on the global changes in the transcriptome when exposed to type 2 diabetic serum.

In summary, the present investigation agrees with literature that CYP enzymes are downregulated in type 2 diabetes by showing the downregulation of CYP2J2 in ventricular myocytes. In addition, *CYP2J2* downregulation and CYP2J2 chemical inhibition both result in increased cell death when cardiomyocytes were cultured in type 2 diabetic serum, reinforcing CPY2J2's role as a cardioprotective enzyme. Given the apparent importance of *CYP2J2* in the human heart, greater understanding of how type 2 diabetes modulates this enzyme and determining altered pathways that are CYP2J2-dependent in the heart may provide insight on how cardiovascular health can be preserved in patients with type 2 diabetes.

Figures & Figure Legends

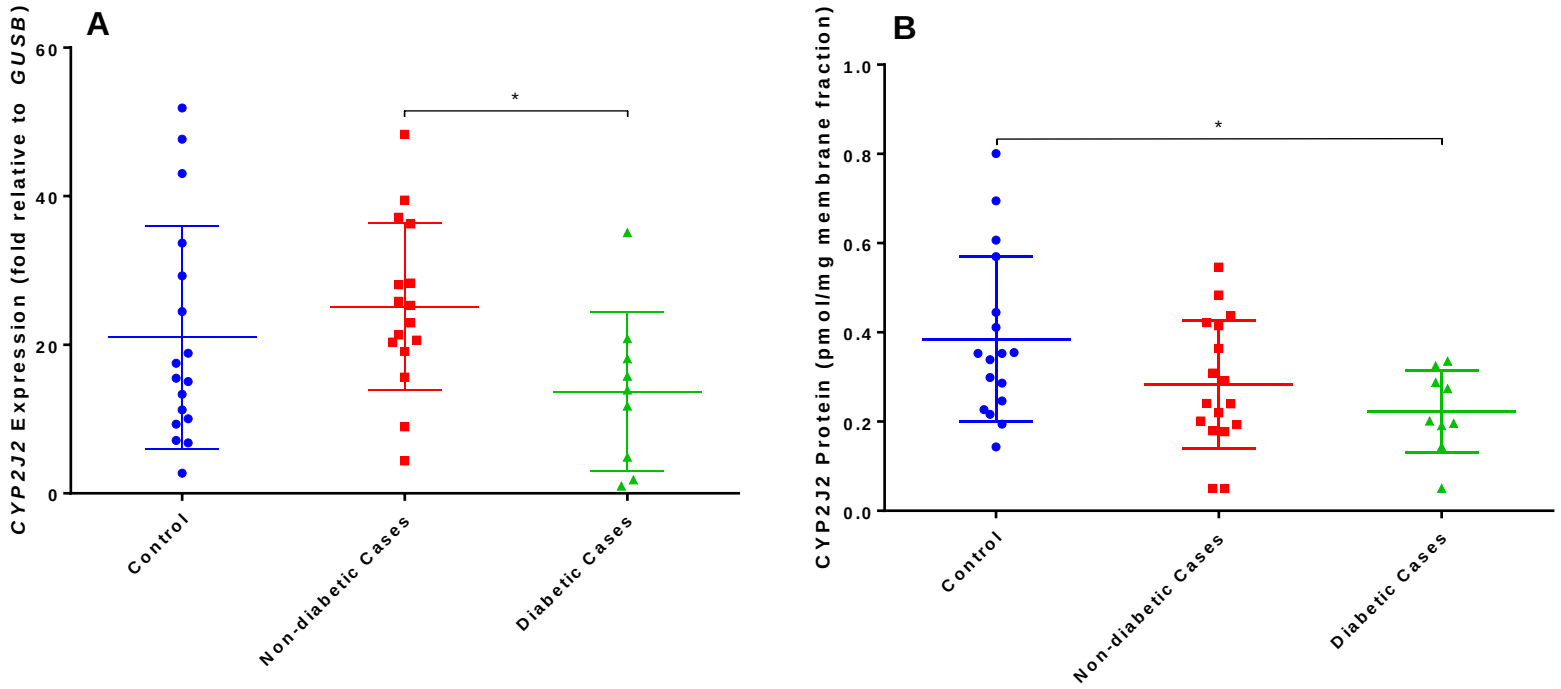

Figure 5.1. Measured CYP2J2 mRNA (A) and protein (B) levels in human cardiac tissue. At both transcript and protein levels, average CYP2J2 levels were lower in diabetic patients than either control or non-diabetic case patients. T-tests indicate mean mRNA levels were significantly lower in diabetic cases than non-diabetic cases. Similarly, mean protein levels were significantly lower in diabetic cases than in control tissues. * $p < 0.05$.

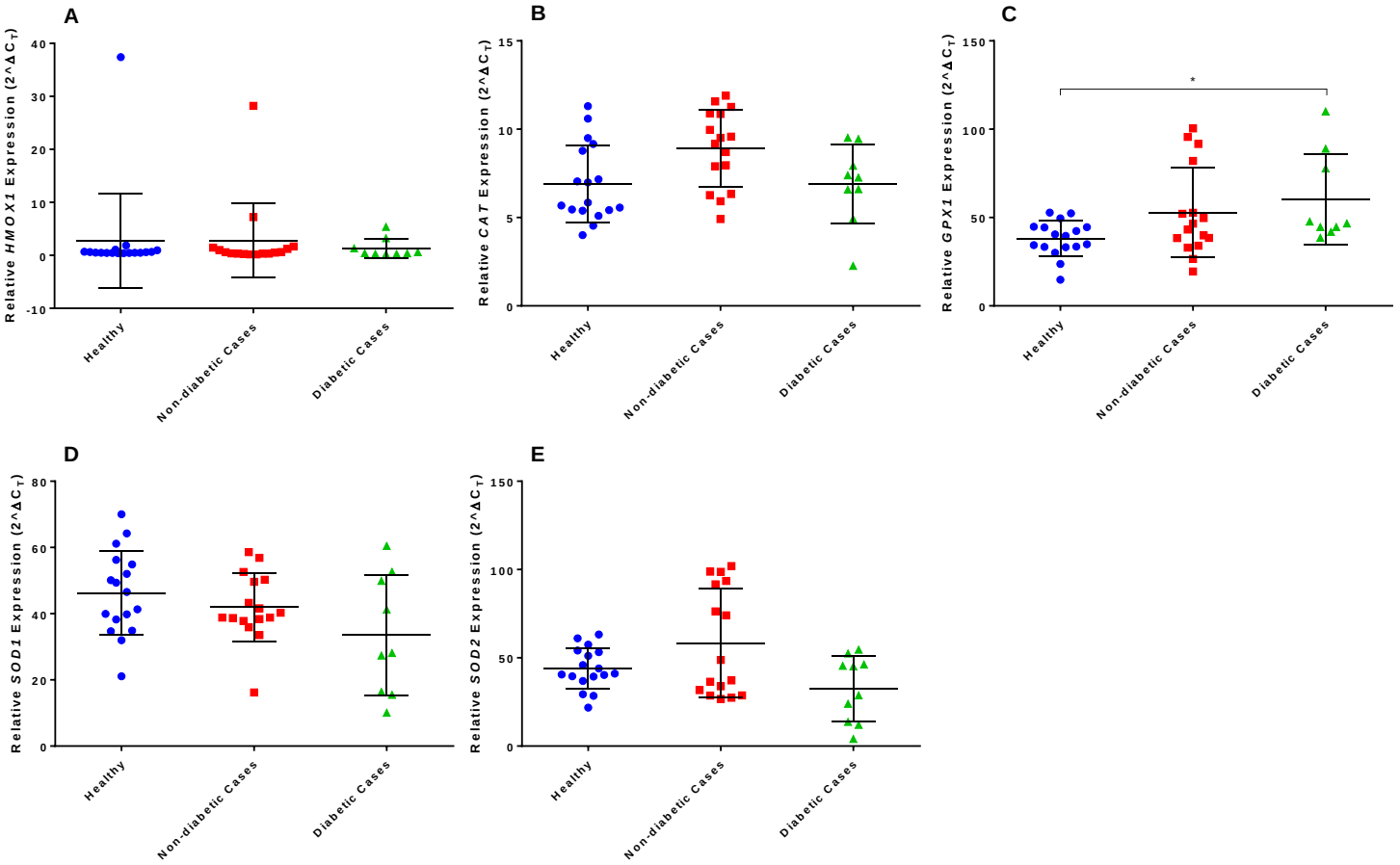

Figure 5.2. mRNA levels of (A) *HMOX1*, (B) *CAT*, (C) *GPX1*, (D) *SOD1*, and (E) *SOD2*. T-tests comparing the means between groups indicate no statistically significant differences in the mean transcript levels between groups in any of the genes investigated, except for lower *GPX1* levels in control ventricular tissue compared to diabetic case tissue, which was significant. * $p < 0.05$.

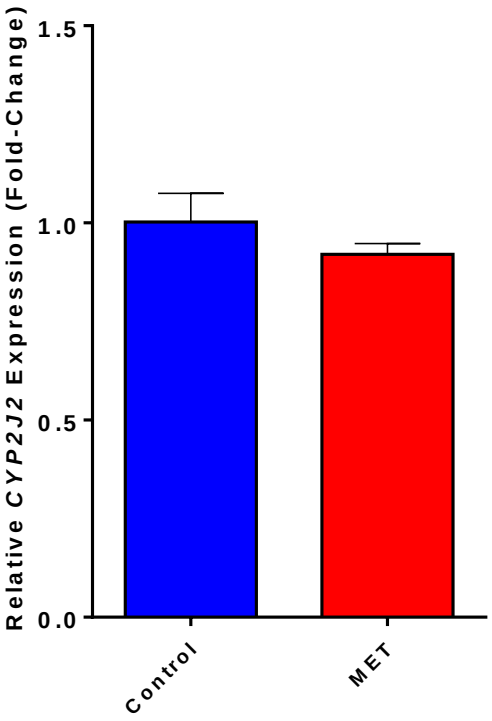

Figure 5.3. CYP2J2 expression in adult cardiomyocytes treated with 2 mM metformin (MET) and vehicle control. Cells treated with MET are 92% viable. A t-test indicates this difference to be insignificant.

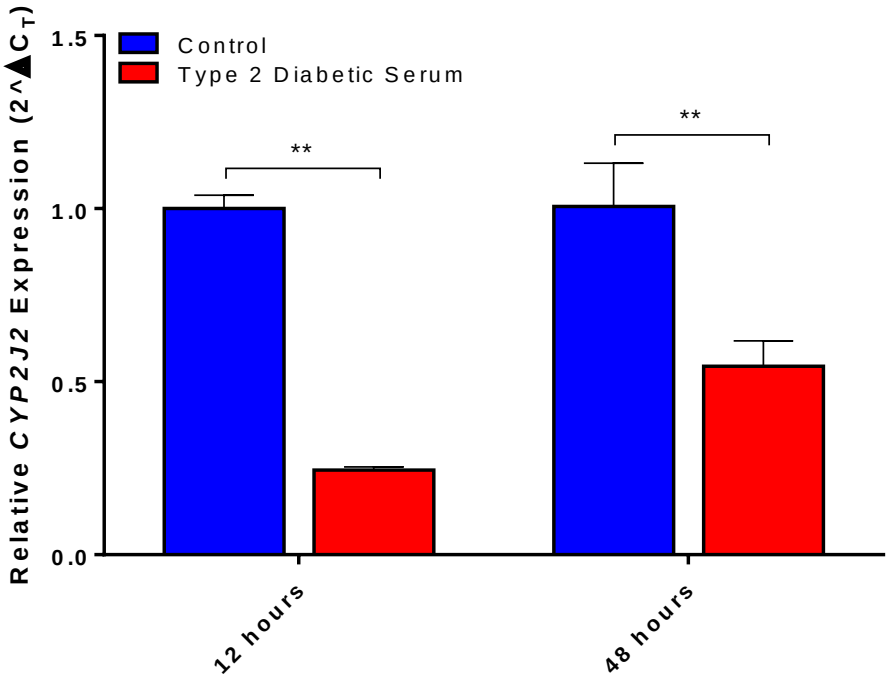

Figure 5.4. *CYP2J2* expression changes when cells are cultured in media supplemented with human type 2 diabetic serum. After 12 hours in human serum, cells in type-2 diabetic human serum downregulate *CYP2J2* by 75%. At 48 hours, this downregulation is at 50%. ** $p < 0.01$.

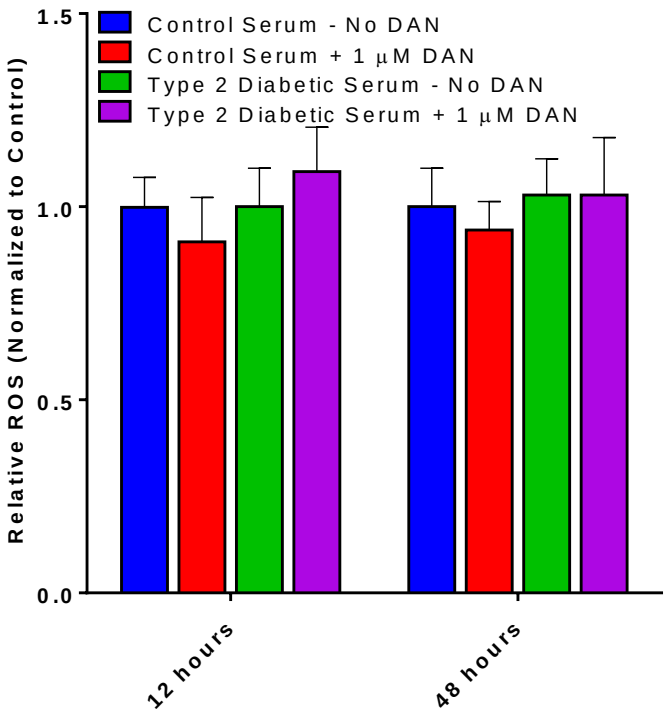

Figure 5.5. Relative ROS levels in cells cultured with human serum, with and without DAN. There is no difference in ROS levels between different treatment groups.

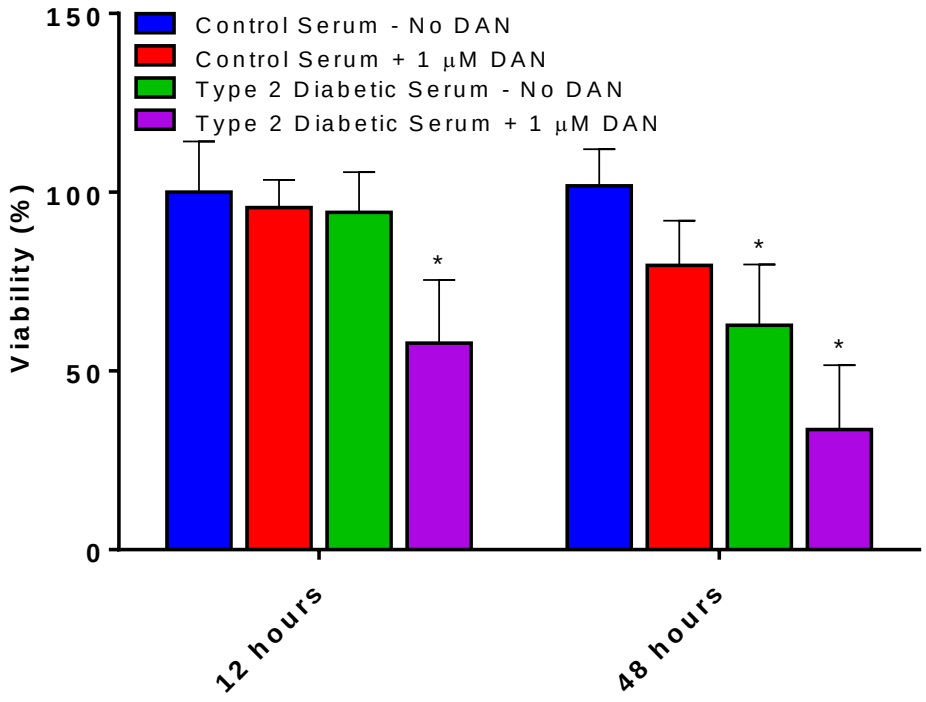

Figure 5.6. Cell viability of human cardiomyocytes cultured in human serum. At 12 hours, there are no significant changes in viability, except when cells were cultured in type 2 diabetic media and treated with DAN, reducing viability to 58%. After 48h, cells in healthy serum, treated with DAN were 80% viable and cells in type 2 diabetic serum were 63% and 34% viable, in the absence and presence of DAN, respectively. * $p < 0.05$.

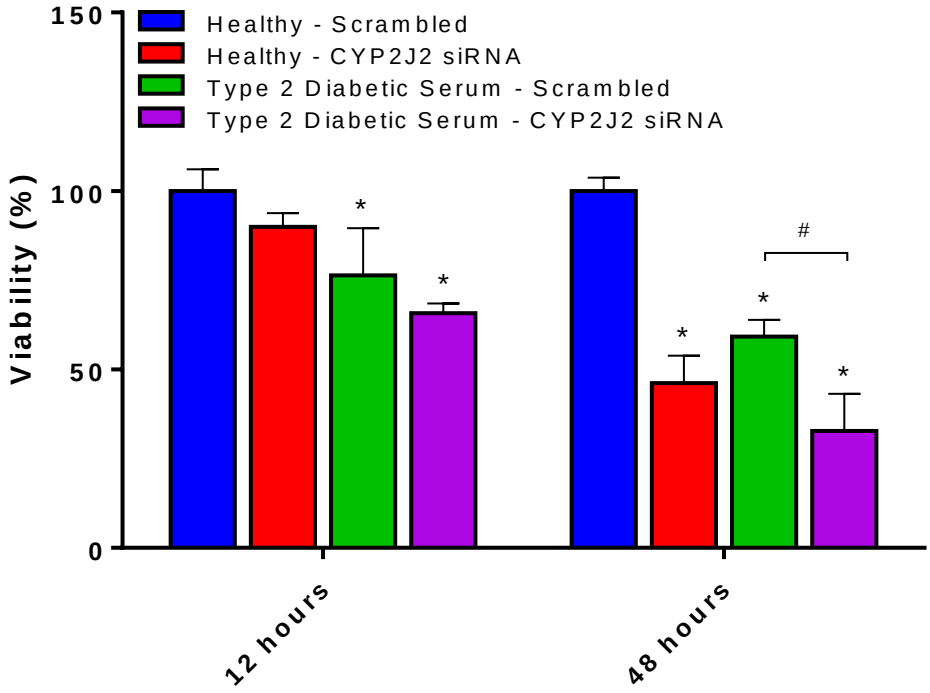

Figure 5.7. Ventricular myocytes cultured in human serum in the presence and absence of *CYP2J2* siRNA. Culturing in diabetic serum, but treated with scrambled siRNA, causes 25% cell death at 12 hours and about 40% cell death at 48 hours. Cells that have *CYP2J2* silenced are 90% and 46% viable at 12h and 48h, respectively when cultured in healthy human serum supplemented media. In the presence of type 2 diabetic serum supplemented media, cardiomyocyte viability is 66% and 30% at 12h and 48h, respectively, when *CYP2J2* is silenced. * $p < 0.05$, compared to cardiomyocytes cultured in healthy serum and treated with scrambled siRNA. # $p < 0.05$, comparing cells cultured in type 2 diabetic serum, with scrambled siRNA or *CYP2J2* siRNA.

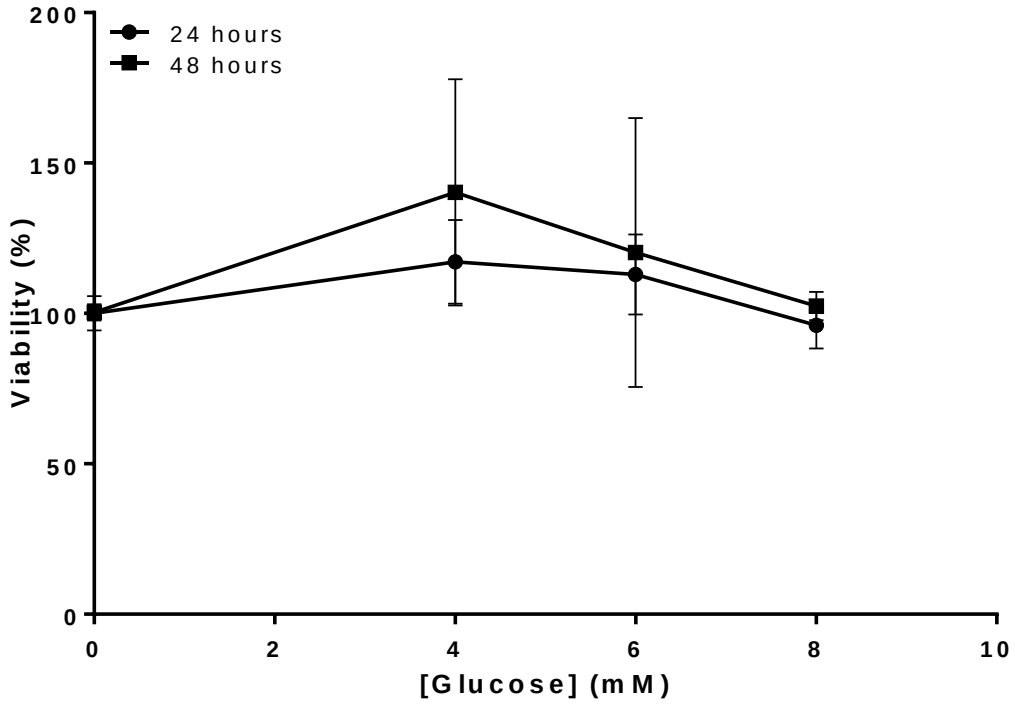

Figure 5.8. Cardiomyocyte viability at varying concentrations of glucose. At most, 4 mM glucose in cell media caused a 40% increase in viability. On the opposite end, 8 mM glucose at 24 hours caused a 4 % drop in viability.

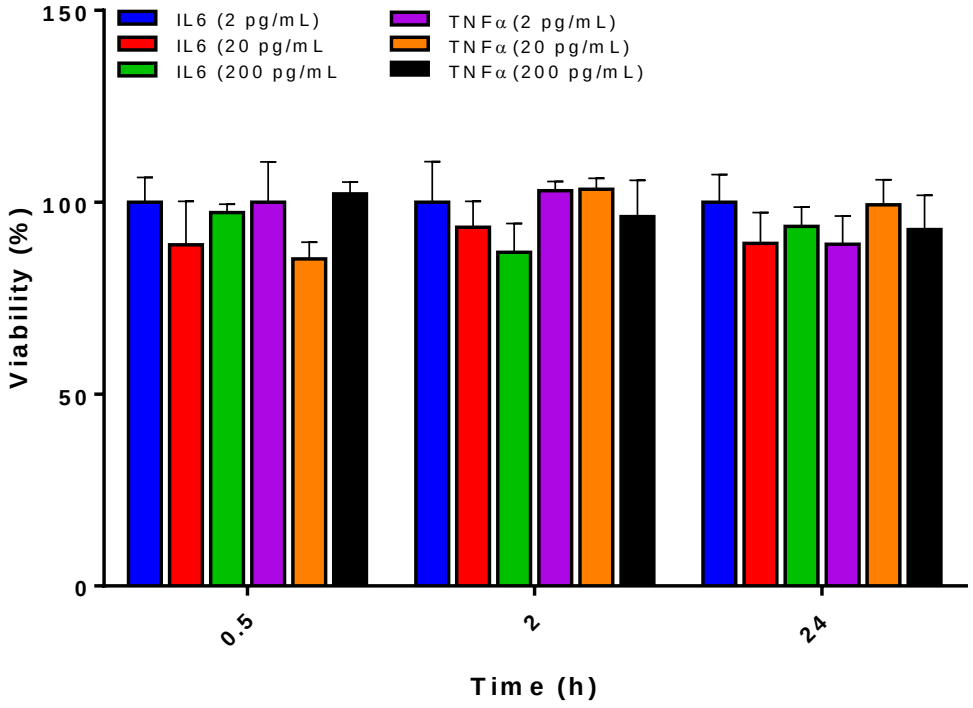

Figure 5.9. Cardiomyocyte viability when exposed to varying concentrations of IL6 and TNFα. There are no significant changes to cell viability when compared to untreated cells (set at 100 % viability).

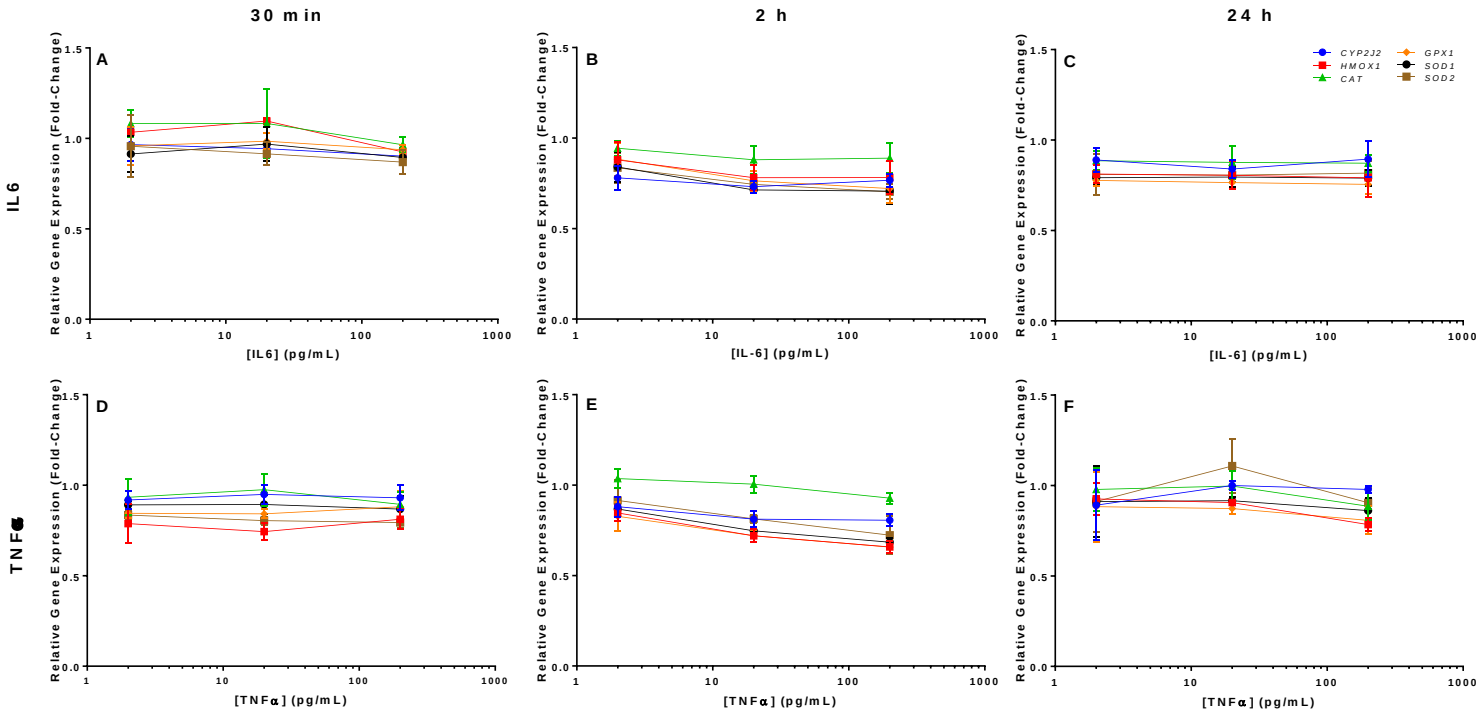

Figure 5.10. Gene expression for *CYP2J2*, *HMOX1*, *CAT*, *GPX1*, *SOD1* and *SOD2* in cardiomyocytes treated with IL6 (A-C) and TNFα (D-F) for 30 min (A, D), 2 h (B, E), and 24h (C, F). The greatest change in gene expression occurs at 2 hours. *CYP2J2* expression is downregulated approximately 20% in cells exposed to the cytokines IL6 and TNFα (200 pg/mL) for 2 hours. At 24 hours, these changes have either remained the same as what was observed at 2 hours or rebounded.

References

Abraham NG, Sodhi K, Silvis AM, Vanella L, Favero G, Rezzani R, Lee C, Zeldin DC, and Schwartzman ML (2014) CYP2J2 targeting to endothelial cells attenuates adiposity and vascular dysfunction in mice fed a high-fat diet by reprogramming adipocyte phenotype. *Hypertens (Dallas, Tex 1979)* **64**:1352–61, NIH Public Access.

Aitken AE, and Morgan ET (2007) Gene-specific effects of inflammatory cytokines on cytochrome P450 2C, 2B6 and 3A4 mRNA levels in human hepatocytes. *Drug Metab Dispos* **35**:1687–93.

Akash MSH, Rehman K, and Liaqat A (2018) Tumor Necrosis Factor-Alpha: Role in Development of Insulin Resistance and Pathogenesis of Type 2 Diabetes Mellitus. *J Cell Biochem* **119**:105–110.

Aliwarga T, Raccor BS, Lemaitre RN, Sotoodehnia N, Gharib SA, Xu L, and Totah RA (2017) Enzymatic and free radical formation of cis- and trans- epoxyeicosatrienoic acids in vitro and in vivo. *Free Radic Biol Med* **112**:131–140.

Asmat U, Abad K, and Ismail K (2016) Diabetes mellitus and oxidative stress-A concise review. *Saudi Pharm J SPJ Off Publ Saudi Pharm Soc* **24**:547–553.

Brownlee M, Aiello L, Cooper M, Vinik A, Plutzky J, and Boulton A (2016) Complications of diabetes mellitus, in *Williams Textbook of Endocrinology* (Melmed S, Polonsky K, Larsen P, and Kronenberg H eds) p, Elsevier, Philadelphia, PA.

Chen G, Wang P, Zhao G, Xu G, Gruzdev A, Zeldin DC, and Wang DW (2011) Cytochrome P450 epoxygenase CYP2J2 attenuates nephropathy in streptozotocin-induced diabetic mice.

Prostaglandins Other Lipid Mediat **96**:63–71.

Chen Y-L, Qiao Y-C, Xu Y, Ling W, Pan Y-H, Huang Y-C, Geng L-J, Zhao H-L, and Zhang X-X (2017) Serum TNF-α concentrations in type 2 diabetes mellitus patients and diabetic nephropathy patients: A systematic review and meta-analysis. *Immunol Lett* **186**:52–58.

Dai M, Wu L, Wang P, Wen Z, Xu X, and Wang DW (2017) CYP2J2 and Its Metabolites EETs Attenuate Insulin Resistance via Regulating Macrophage Polarization in Adipose Tissue. *Sci Rep* **7**:46743.

DeFronzo RA, Ferrannini E, Groop L, Henry RR, Herman WH, Holst JJ, Hu FB, Kahn CR, Raz I, Shulman GI, Simonson DC, Testa MA, and Weiss R (2015) Type 2 diabetes mellitus. *Nat Rev Dis Prim* **1**:15019.

Dostalek M, Court MH, Yan B, and Akhlaghi F (2011) Significantly reduced cytochrome P450 3A4 expression and activity in liver from humans with diabetes mellitus. *Br J Pharmacol* **163**:937–47.

Evangelista EA, Kaspera R, Mokadam NA, Jones III JP, and Totah RA (2013) Activity, inhibition, and induction of cytochrome P450 2J2 in adult human primary cardiomyocytes. *Drug Metab Dispos* **41**.

Evangelista EA, Lemaitre RN, Sotoodehnia N, Gharib SA, and Totah RA (2018) CYP2J2 expression in adult ventricular myocytes protects against reactive oxygen species toxicity. *Drug Metab Dispos* **46**.

Gravel S, Chiasson J-L, Turgeon J, Grangeon A, and Michaud V (2019) Modulation of CYP450 Activities in Patients With Type 2 Diabetes. *Clin Pharmacol Ther* **106**:1280–1289.

Hack CE, De Groot ER, Felt-Bersma RJ, Nuijens JH, Strack Van Schijndel RJ, Eerenberg-Belmer AJ, Thijs LG, and Aarden LA (1989) Increased plasma levels of interleukin-6 in sepsis. *Blood* **74**:1704–10.

Jarrar YB, Al-Essa L, Kilani A, Hasan M, and Al-Qerem W (2018) Alterations in the gene expression of drug and arachidonic acid-metabolizing Cyp450 in the livers of controlled and uncontrolled insulin-dependent diabetic mice. *Diabetes Metab Syndr Obes* **11**:483–492.

Kajbaf F, De Broe ME, and Lalau J-D (2016) Therapeutic Concentrations of Metformin: A Systematic Review. *Clin Pharmacokinet* **55**:439–59.

Kristiansen OP, and Mandrup-Poulsen T (2005) Interleukin-6 and diabetes: the good, the bad, or the indifferent? *Diabetes* **54 Suppl 2**:S114-24.

Li R, Xu X, Chen C, Wang Y, Gruzdev A, Zeldin DC, and Wang DW (2015) CYP2J2 attenuates metabolic dysfunction in diabetic mice by reducing hepatic inflammation via the PPARγ. *Am J Physiol Endocrinol Metab* **308**:E270-82.

Livak KJ, and Schmittgen TD (2001) Analysis of Relative Gene Expression Data Using Real-Time Quantitative PCR and the 2−ΔΔCT Method. *Methods* **25**:402–408, Academic Press.

Luo P, and Wang M-H (2011) Eicosanoids, β-cell function, and diabetes. *Prostaglandins Other Lipid Mediat* **95**:1–10, Elsevier Inc.

Ma B, Xiong X, Chen C, Li H, Xu X, Li X, Li R, Chen G, Dackor RT, Zeldin DC, and Wang DW (2013) Cardiac-specific overexpression of CYP2J2 attenuates diabetic cardiomyopathy in male streptozotocin-induced diabetic mice. *Endocrinology* **154**:2843–56.

Mirza S, Hossain M, Mathews C, Martinez P, Pino P, Gay JL, Rentfro A, McCormick JB, and

Fisher-Hoch SP (2012) Type 2-diabetes is associated with elevated levels of TNF-alpha, IL-6 and adiponectin and low levels of leptin in a population of Mexican Americans: a cross-sectional study. *Cytokine* **57**:136–42.

Nordquist L, Friederich-Persson M, Fasching A, Liss P, Shoji K, Nangaku M, Hansell P, and Palm F (2015) Activation of hypoxia-inducible factors prevents diabetic nephropathy. *J Am Soc Nephrol* **26**:328–38.

Rehman K, Akash MSH, Liaqat A, Kamal S, Qadir MI, and Rasul A (2017) Role of Interleukin-6 in Development of Insulin Resistance and Type 2 Diabetes Mellitus. *Crit Rev Eukaryot Gene Expr* **27**:229–236.

Rodrigues KF, Pietrani NT, Bosco AA, Campos FMF, Sandrim VC, and Gomes KB (2017) IL-6, TNF-α, and IL-10 levels/polymorphisms and their association with type 2 diabetes mellitus and obesity in Brazilian individuals. *Arch Endocrinol Metab* **61**:438–446.

Ruotsalainen E, Stancáková A, Vauhkonen I, Salmenniemi U, Pihlajamäki J, Punnonen K, and Laakso M (2010) Changes in cytokine levels during acute hyperinsulinemia in offspring of type 2 diabetic subjects. *Atherosclerosis* **210**:536–41.

Samuel SM, Ghosh S, Majeed Y, Arunachalam G, Emara MM, Ding H, and Triggle CR (2017) Metformin represses glucose starvation induced autophagic response in microvascular endothelial cells and promotes cell death. *Biochem Pharmacol* **132**:118–132.

Smith PK, Krohn RI, Hermanson GT, Mallia AK, Gartner FH, Provenzano MD, Fujimoto EK, Goeke NM, Olson BJ, and Klenk DC (1985) Measurement of protein using bicinchoninic acid. *Anal Biochem* **150**:76–85.

Swaroop JJ, Rajarajeswari D, and Naidu JN (2012) Association of TNF-α with insulin resistance in type 2 diabetes mellitus. *Indian J Med Res* **135**:127–30.

Waage A, Brandtzaeg P, Halstensen A, Kierulf P, and Espevik T (1989) The complex pattern of cytokines in serum from patients with meningococcal septic shock. Association between interleukin 6, interleukin 1, and fatal outcome. *J Exp Med* **169**:333–8.

Wang C-P, Hung W-C, Yu T-H, Chiu C-A, Lu L-F, Chung F-M, Hung C-H, Shin S-J, Chen H-J, and Lee Y-J (2010) Genetic variation in the G-50T polymorphism of the cytochrome P450 epoxygenase CYP2J2 gene and the risk of younger onset type 2 diabetes among Chinese population: potential interaction with body mass index and family history. *Exp Clin Endocrinol Diabetes* **118**:346–52.

Williams CC, Singleton BA, Llopis SD, and Skripnikova E V (2013) Metformin induces a senescence-associated gene signature in breast cancer cells. *J Health Care Poor Underserved* **24**:93–103.

Xu M, Bhatt DK, Yeung CK, Claw KG, Chaudhry AS, Gaedigk A, Pearce RE, Broeckel U, Gaedigk R, Nickerson DA, Schuetz E, Rettie AE, Leeder JS, Thummel KE, and Prasad B (2017) Genetic and nongenetic factors associated with protein abundance of flavin-containing monooxygenase 3 in human liver. *J Pharmacol Exp Ther* **363**:265–274, American Society for Pharmacology and Experimental Therapy.

Chapter 6: Conclusions & Future Directions

6.1 General Conclusions

The overarching goal of this dissertation was to investigate how CYP2J2 is regulated in the heart, and how decreases in *CYP2J2* expression would affect the cell's ability to respond to external stressors associated with cardiac disease and diabetes. To achieve this, we first examined the consequences of *CYP2J2* downregulation by siRNA using a commercially available human adult-derived ventricular myocyte cell line. This was followed up by determining how increased oxidative stress, hypoxia, and type 2 diabetes patient-derived serum affects *CYP2J2* expression in these cells. In addition to the effects that these stresses have on gene expression, their effects on cell viability were also examined with *CYP2J2* expression at basal levels or downregulated via siRNA or when the enzyme is being inhibited pharmacologically. In subjecting the cells to these external stressors, we also examined whether their effects on the cells could be mitigated by the addition of external EETs, the CYP2J2-mediated metabolites of arachidonic acid bioactivation. Finally, RNASeq and pathway analyses provided insight on the effects of these stresses to ventricular myocytes and identified unique pathways that may lead to new druggable targets.

Studies carried out in cardiomyocytes indicate that CYP2J2 plays an important role to support proper cellular functions. Significant decreases in *CYP2J2* expression resulted in almost complete loss of enzyme activity after 3 days, which then led to significant alterations to gene expression of enzymes and proteins involved in a wide variety of pathways, ranging from metabolism and extracellular matrix to ion channel function. These RNASeq-based discoveries were corroborated by further *in vitro* experiments. RT-PCR analyses of total RNA confirmed the

RNASeq findings using a select batch of genes. Electrophysiology experiments further solidified a link between ion channel signaling and CYP2J2 activity, where inhibition of CYP2J2 using chemical inhibitors negatively impacted cardiac electrophysiology in transgenic mice overexpressing human CYP2J2 in heart tissue. Finally, these detrimental effects are likely linked to CYP2J2 mediated AA metabolism. Previously, others have established links between ion channels and EETs, and our electrophysiology work confirmed that CYP2J2 is involved. MSPPOH is a specific epoxygenase inhibitor, supporting the link between CYP2J2, EETs and ion channels. Combined, these data support an essential function for CYP2J2 in cardiac homeostasis. Repressing expression of *CYP2J2* causes cardiomyocytes to compensate, resulting in alterations in many pathways.

Stressing cardiomyocytes by increasing reactive oxygen species (ROS) or hypoxia yielded opposing effects on *CYP2J2* expression. Elevated ROS levels increased gene expression levels, while hypoxia by reducing oxygen tension to 0.1% downregulated *CYP2J2*. The former finding suggests a protective role for CYP2J2 and studies with silenced *CYP2J2* expression support this. In contrast, low oxygen tension downregulates *CYP2J2*. Studies using $CoCl_2$, a hypoxia mimetic that also causes increases in internal ROS through mitochondrial damage, also causes a downregulation of *CYP2J2* despite rising ROS levels. This may indicate that there is a possible hierarchy in the regulation of this enzyme, where hypoxic regulation takes precedence over ROS regulation. This may be due to an effort to conserve O_2 levels for functions essential to survival, as CYP2J2 consumes O_2 as part of its catalytic cycle. Regardless, silenced gene expression leads to greater ROS toxicity or cell death due to low oxygen tension/exposure to $CoCl_2$ in ventricular myocytes, effects that can be mitigated with the addition of a small amount

of EETs. This agrees with a large body of evidence that CYP2J2 has a protective role in cardiomyocytes as an epoxygenase.

Finally, studies utilizing human derived serum from either healthy patients or type 2 diabetic patients modeled the effects of type 2 diabetes on cardiomyocytes. Type 2 diabetes is a multifactorial disease that subjects multiple organs to a wide range of stresses, including hypoxic conditions and elevated ROS. Human cardiac tissue of healthy patients and patients with cardiac health issues, with or without type 2 diabetes, revealed that individuals with diabetes had lower *CYP2J2* transcripts and protein levels than healthy or nondiabetic individuals. Treating primary ventricular myocytes confirmed that when cultured in the presence of type 2 diabetic serum, *CYP2J2* expression decreases. Potential causes for this downregulation were explored, including elevated glucose levels and the inflammatory factors TNFα and IL6, inflammatory factors that have long been associated with diabetes. Unfortunately, none of those conditions, examined separately, provide a conclusive explanation as to why *CYP2J2* downregulation occurres in the presence of type 2 diabetic serum, which may require the combination of these effects present in the diabetic serum to manifest this effect.

6.2 Future Directions

Future studies are needed to further outline how *CYP2J2* expression is affected by cellular stresses. RNASeq data obtained from cells cultured in hypoxia and diabetic serum would provide better insight on the global effects of these stresses in ventricular myocytes. Pathway analysis would reveal potential CYP2J2-dependent pathways and may provide novel potential druggable targets. In addition, further studies should also focus on individual aspects of type 2 diabetes as we had attempted in Chapter 5. There are many more cytokines that should be investigated individually to determine effects on ventricular myocyte health and its link with CYP2J2 expression and activity. Once key cytokines have been identified, determining how they might affect *CYP2J2* regulation and cardiomyocyte health together would provide further insight on how diabetes results in the biological alterations in the heart and the role of CYP2J2 in preventing and protecting against these alterations.

Finally, the functions of EETs, individually and together, need to be further delineated. Currently, an EET receptor remains elusive in cardiac cells and it is unclear whether individual isomers activate the same signaling cascades to exert their physiological functions. One or two receptors have been identified to respond to EET signaling, but it is unknown if these receptors are the EETs' true receptor in cardiac cells. Future work should focus on better understanding how CYP2J2 and EETs are cardioprotective, specifically in the context of various cell stresses. Better insight into the pathways that are altered in response to changes in CYP2J2 expression and activity may provide novel avenues for treating a wide range of diseases with adverse cardiac complications.